3-19-2018

Synthesis and Characterization of Covalent Adaptable Networks Comprised of Dynamic Imine and Aminal Covalent Bonds

Albert Chao
Louisiana State University and Agricultural and Mechanical College

SYNTHESIS AND CHARACTERIZATION OF COVALENT ADAPTABLE NETWORKS COMPRISED OF DYNAMIC IMINE AND AMINAL COVALENT BONDS

A Dissertation

Submitted to the Graduate Faculty of the
Louisiana State University and
Agricultural and Mechanical College
in partial fulfillment of the
requirements for the degree of
Doctor of Philosophy

in

The Department of Chemistry

by
Albert Chao
B.A., University of Cincinnati, 2010
May 2018

Acknowledgements

I would like to thank my advisor Prof. Donghui Zhang for her guidance, mentorship, and financial support on the projects I have worked on during the past 5 years in graduate school at Louisiana State University. Prof. Donghui Zhang allowed me to think independently and develop projects from the beginning to the end. When I lost interest on each project, her patience and encouragement always turned failure into success. Thanks to my advisory committee: Prof. David Spivak, Prof. Jayne Garno, and Prof. Philip Adams for their time and suggestions. Moreover, I would like to thank all my lab colleagues, Dr. Brandon Chan, Dr. Jinbao Cao, Dr. Ang Li, Jessica Simpson, Garrett Sternhagen, Zhaoyuan Liu, Dr. Xin Li, Tianyi Yu, David Slefker, Dr. Naisheng Jiang for their useful discussion and emotional support during my PhD years.

I would like to thank to Prof. Paul Russo, Prof. John Pojman, Prof. Doug Gilman, Prof. Louis Haber who have taught macromolecule, analytical and physical chemistry during my first and second year in graduate school. I would like to thank Dr. Rafeal Cueto for training with DSC, DLS, TGA and DMA in the polymer laboratory. I would like to thank Prof. Ioan Negulescu for allowing me to use his rheometer. Also, thanks to Prof. Gang-yu Liu from UC, Davis for her support on my graduate school application. Last but not least, I would like to thank my lovely parents and brother. Their faith and encouragement helped me to overcome difficulties from both school and personal life. I would not be able to finish a PhD degree without their support.

Thanks everyone for the discussions, emotional and moral support.

Table of Contents

List of Tables

List of Schemes

List of Figures

Abstract

The dissertation is about the design, synthesis and characterization of materials comprised of covalent adaptable networks (CANs). There are three chapters within this dissertation.

Chapter 1 contains a short overview of conventional thermosets and thermoplastics. A new strategy of combining advantages from thermosets and thermoplastics is utilizing dynamic covalent chemistry (DCC) for material design. Dynamic covalent bonds are able to undergo dynamic exchange which allow the material to adapt to a new state when under stimuli such as stress or strain. Material comprised of such reversible networks is called covalent adaptable networks (CANs). These types of reversible covalent bonds followed two types of exchange mechanisms: dissociation and association. A review of dissociative-pathway-based materials includes retro-Diels-Alder, [2+2] and [4+4] cycloaddition, boronate ester, and alkoxyamines. CANs followed associative mechanism including radical addition fragmentation chain transfer reaction, anionic disulfide exchange, and transesterification are also reviewed. Lastly, a general consideration in designing CANs includes the importance of each experiment, the information obtained from the experiments, and general experimental procedures.

Chapter 2 is about the design, synthesis and characterization of solvent-swelled polyimine networks. The presence of reversible imine bond exchange was found to influence the dynamical properties of the polymer networks. Investigation of the imine bond exchange kinetics and characterization of the creep and stress relaxation properties of the polyimine networks have been conducted. A correlation was found between the relative imine bond exchange rate in different solvents and the relative stress relaxation rate of the solvent-swelled networks. The polyimine networks can also be re-mended and recycled by hydrolysis.

Chapter 3 is focused on CANs based on aminal linkage. The thermodynamics and kinetics of the aminal dissociation as well as transaminalation reaction have been investigated using model compounds. Temperature-dependent stress relaxation behavior of the polyamine networks have also been characterized by dynamic mechanical analysis (DMA) method, allowing for an assessment of the activation energy of the transaminalation in the network. Aminal exchange was found to occur by a dissociative mechanism that requires the presence of catalytic protic sources to facilitate the formation of iminium intermediates. The polyaminal networks can be reprocessed as a viscoelastic solid (above the gel point) rather than a viscoelastic liquid. These materials were shown to be elastomers and can be thermally reprocessed and re-mended.

Chapter 1 : Introduction of Conventional Thermosets, Thermoplastics and Thermosets based on CANs

1.1 Introduction of conventional thermosets

Traditional thermoset plastics are crosslinked by permanent covalent bonds. The permanent crosslinking significantly increases the strength, stiffness and dimensional stability of thermosets along with increasing glass transition and melting point temperature. These advantages have led to many applications. They have been used for electrical insulating, packaging, and coating. One of the earliest thermosets is cross-linked phenol-formaldehyde used as an adhesive during World War II. Other examples are epoxies, acrylic, or thermally cured polymers which are all traditional thermosets. Alternatively, many modern thermosets such as dental materials,[1] contact lenses,[2] and coatings[3] are cured by a light-driven process, with fast curing at room temperature and are energy efficient.[4]

As traditional thermosets are polymer networks connected by permanent covalent bonds, they cannot be reshaped, processed or recycled after curing. As a result, these materials tend to be elastic (no creep behavior) with high mechanical strength and modulus when under strain deformations. In recent developments, there are various stimuli responsive thermosets like shape memory materials where polymers are frozen at a non-equilibrium state below their glass transition temperature. Upon heating above its critical switching temperature, a polymeric network relaxes to its equilibrium states. Despite this unique behavior conventional thermosets have been used in numerous applications such as mechanical actuators, sensors, and self-deployable structure;[5] these permanently crosslinked networks cannot be further modified or re-molded once cured. In 2012, millions of tons of rubbers were produced to accommodate the need of human lives. Around 800

million tire wastes were produced each year. In order to minimize the rubber waste problem, one of the strategies is to develop thermosets that are reprocessable and recyclable.

1.2 Introduction of thermoplastics

In contrast to thermosets, thermoplastics can be reprocessed by extrusion and recycling in many different ways. Thermoplastics are comprised of many polymer chains with potentially different architectures (e.g., linear or branch polymers) that are held together by non-covalent interactions in contrast to the conventional thermosets. The noncovalent interactions can include hydrogen bonds, π-π stacking, ionic interactions or van der Waals interactions. Thermoplastics are capable of macroscopic flow or plastic deformation because these noncovalent interactions can be easily perturbed by environmental triggers (e.g., heating). Above the glass transition or melting transition temperature (T_g or T_m), linear polymer chains can freely move past one another. Thermoplastics can be remolded thermally due to the noncovalent interactions that hold the polymer chains together and thus is considered healable. The physical properties of thermoplastics are highly tunable and strongly dependent on both the macromolecular structure and non-covalent intermolecular interactions.

Various types of thermoplastics are made for specific applications. High performance thermoplastics have been developed such as polyphenylene sulfide (PPS), polyetherimide (PEI) for applications that require a high degree of thermal stability. More sophisticated thermoplastics including thermoplastic elastomers (TPEs) provide materials with elastomeric properties.[6] Thermoplastic elastomers are flexible and low modulus that can be used in a wide range of applications, from automotive interiors and heat resistant tubing to soft touch grips. Biodegradable thermoplastics utilize renewable sources such as amino acids[7] and starch[8] as a building block and are made to solve issues from traditional non-degradable petro-based thermosets and non-

environmentally friendly thermoplastics. Furthermore, thermoplastic composites use fibers such as glass, Kevlar, carbon, or polyethylene to reinforce the mechanical properties and possess a high degree of durability.[9] Their mechanical properties are often stronger than steel but the weights are much lighter.

1.3 Introduction of thermosets based on CANs

1.3.1 Dynamic covalent chemistry

A new approach of designing materials that combines advantages from both thermosets and thermoplastics is by introducing dynamic covalent chemistry (DCC) in the design of polymeric networks. The bonds involve reversible formation and breaking of covalent bonds and produce products that are a result of thermodynamic equilibration under the experimental conditions defined by Lehn[10]. Dynamic covalent chemistry deals with stronger covalent bonds as compared to noncovalent interactions, e.g. hydrogen bonds. Some key requirements for DCC to be used in the design of polymer networks are that the lifetime of a given covalent bond cannot be too short ($t < 1$ ms) or too long ($t > 1$ min) so that the network structure can be maintained while still undergoing topological rearrangement by dynamic bond exchange.[11] In addition to the kinetic aspects, the exchange reaction is desired to occur under mild conditions so that the structural integrity of the material will not be compromised under the conditions. Lastly, for different applications, it is also beneficial to have an exchange reaction that can be mediated by pH or by different catalysts.[12] Recent polymer networks based on DCC including transesterification,[13] Diels-Alder reaction,[14] photodimerization,[15] radical reaction,[16] and boronate ester,[17] all have been shown to exhibit dynamic behavior. Among the known reversible covalent bonds, imine, hydrazones, and oximes are widely used due to the various monomers that are readily available

from commercial sources or obtainable by facile synthesis. These exchange reactions occur under mild conditions without the need of external catalysts.

Polymer networks comprised of dynamic covalent bonds are called covalent adaptable networks (CANs).[18] Networks are capable of topological rearrangement via covalent bond exchange under certain stimuli. The characteristics of CANs was first observed in the 1940s, by polysulfide networks that exhibit creep behavior under stress. The continuous deformation behavior is caused by disulfide exchange.[19] The major difference between CANs and the previously mentioned polymers is the dynamic covalent bonds provide rearrangement at the molecular level to achieve flow in the macroscopic level, resulting in stress relaxation. During the stress relaxation, the rate of deformation is associated with the rate of the exchange reaction which can be tuned by external or environmental stimulus (e.g., heat). This creep characteristic was impossible from the conventional thermosets.

The unique chemistry and material properties of CANs have formed a bridge between conventional thermosets and thermoplastics. Covalent adaptable networks can be made through different types of reversible covalent bonds, and often exhibit different stress relaxation and bond exchange mechanisms. They are used in healable materials,[20] imprinting,[21] shape changing polymers,[22] and remoldable or recyclable materials.[23] Covalent adaptable networks can be classified into two sub-categories based on the mechanism of dynamic covalent bond exchange: (1) reversible addition, condensation reaction or (2) bond exchange reaction (Scheme 1.1). The former two involve a dissociative pathway, whereas the latter occurs by an associative mechanism. The dynamic properties of the polymer network are influenced by the type of bond exchange mechanism, as well as the equilibrium constant and exchange kinetics of the reversible reactions.

Some examples of dynamic covalent bonds utilized in CANs are shown in Table 1.1. Imine exchange and hemiaminalation will be discussed in Chapter 2 and 3, respectively.

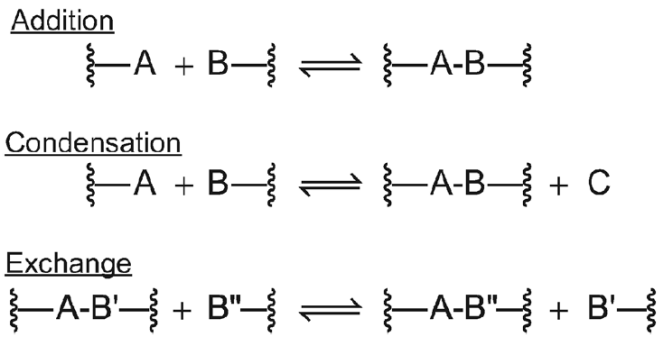

Scheme 1.1. A general reversible reaction diagram of addition, condensation and bond exchange reaction. Reproduced from Ref. 16 with permission from American Chemical Society.

Table 1.1 Examples of DCC that have been used in CANs.

Dissociative mechanism	**Associative mechanism**
r-Diels-Alder	Transesterification
[2+2] cycloaddition	Siloxane silanolate
Hemiaminalation (1,3,5-triazine)	Olefin metathesis
Boronate ester	Imine exchange

1.3.2 Dynamic covalent bond exchange by a dissociative mechanism

Dynamic covalent bond exchange can occur by a dissociative pathway, as shown by the addition and condensation reactions in Scheme 1.1. The bond-breaking reaction lowers the cross-

linking density that negatively impacts on the shear modulus of the polymer network. Depending on the equilibrium constant for the reaction, the extent of crosslinking and polymerization varies, which can affect the state of polymers (e.g., gel or sol). Polymeric networks comprised of linkages based on the Diels-Alder (DA) reaction is a classic example of CANs that undergo dynamic rearrangement by a dissociative pathway (Scheme 1.2, top). For example, the [4 + 2] cycloaddition reaction between furans and maleimides is only mildly exothermic (5-10 kcal mol^{-1}), indicating that bond dissociation equilibrium can be significantly perturbed by heating. A variety of polymer backbone bearing side chains of furans and maleimides are used for cross-linkers including linear polymer,[24] networks,[14a, 25] hydrogels,[26] and dendrimers.[27] When heating above the gel point temperature, the retro-DA reaction is accelerated more than the D-A reaction, shifting the equilibrium toward monomers and thus resulting in depolymerization of the polymer network. Upon cooling, the polymer network will reform. The dynamic equilibrium between the DA and retro-DA reaction confers the polymer network with remendability, recyclability, and healing ability. These properties are not accessible in conventional thermosets.

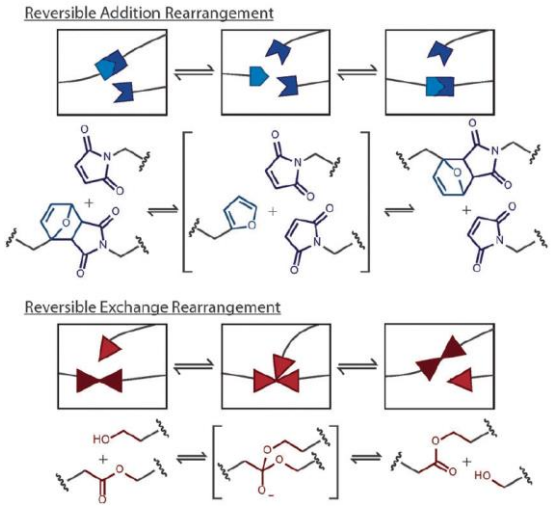

Scheme 1.2. Examples of dynamic covalent bond exchange that occurs by a dissociative (e.g., D-A reaction) or an associative mechanism (e.g., transesterification reaction). Reproduced from Ref. 16 with permission from American Chemical Society.

In addition to using heat to induce the bond dissociation in CANs (e.g., Diels-Alder networks), photo-irradiation has also been investigated to induce dissociative bond exchange in polymer networks. Covalent adaptable networks comprised of photo-reversible networks behave as conventional thermosets when light sources are not available. No creep behavior is observed in the absence of photoirradiation. Photo-reversible covalent bonds only become activated with exposure to irradiation. The bond breaking and reforming leads to stress-relaxation and creep behavior. There are two types of photo-reversible mechanisms. One type is bond cleavage with one wavelength and reforms with a different wavelength. This requires the sample to be irradiated with both wavelengths at the same time to achieve dynamic bond exchange. Several photo-triggered moieties follow this mechanism in polymers including coumines,[28] cinnamates,[29] anthracenes,[29c, 30] and thymines.[31] When irradiated at a certain wavelength, coumarin and anthracene undergo [2 +2] and [4 + 4] cycloaddition (Scheme 1.3).[18]

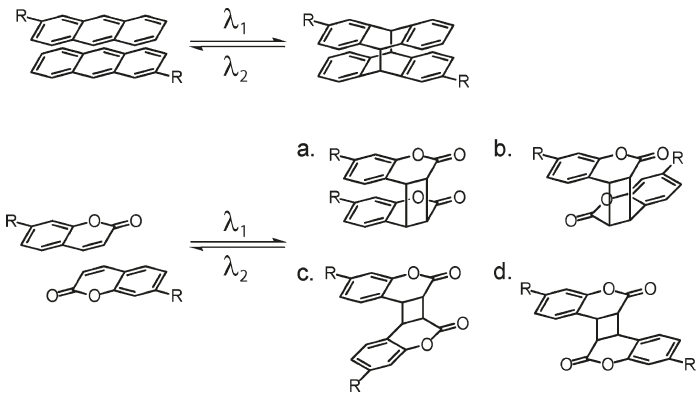

Scheme 1.3. Photoinduced dimerization of coumarin and anthracene within polymer network. Reproduced from Ref. 16 with permission from American Chemical Society.

Understanding dynamic behaviors at the molecular level (e.g., the thermodynamic and kinetics of the bond exchange reaction) can provide information of dynamic properties of polymer networks at the macroscopic level. This structure-property relationship is highly valuable for the rational design and development of smart polymeric materials for targeted applications. An

increased variety of dynamic covalent bonds have been investigated in the design and synthesis of polymer networks. Examples of selected DCC chemistry used in the design of CANs are highlighted below.

1.3.2.1 CANs based on boronate ester.

Boronic acid and diol produced a reversible boronate ester. One of the advantages is that the exchange reaction requires no catalyst. Various responsive hydrogels especially sugars have incorporated boronic acids as a way to create cross-linking sites. Tarus et al. demonstrates the synthesis of biocompatible polysaccharide hydrogels based on the boronate ester bond. Carboxylate containing polysaccharides are modified with phenylboronic acid and maltose. The hydrogels are able to adapt and self-heal in mild acidic conditions or simply by adding more glucose. Another benefit of this design is that soft hydrogels have potential applications for drug delivery.

1.3.2.2 CANs based on alkoxyamines.

Covalent N-O bonds in alkoxyamines can form a stable free radical when heating at high temperatures (Scheme 1.4). The thermally activated CANs are similar to a retro-Diels-Alder reaction except that alkoxyamines rearrange through radical intermediates. Polymer chains bearing 2,2,6,6-tetramethylpiperidine-1-oxy (TEMPO)-based alkoxyamine moiety can undergo dynamic grafting upon heating. The degree of grafting is dependent on the concentration of the molecules targeted for grafting.[32] Furthermore, Sato et al. have used this strategy to cross-link two polymer chains with different alkoxyamines.[33] The cross-linking density can be tuned by the amount of small molecule alkoxyamine present. By adding an excess of small molecule alkoxyamine and heating at 100 °C for 48 h, the equilibrium shifted to the initial polymers. This class of reversible

covalent bond is water stable and has been incorporated in water soluble polymers for making hydrogels.

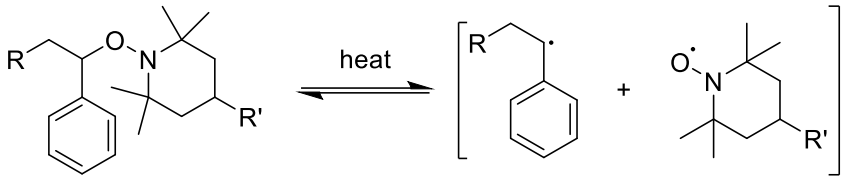

Scheme 1.4. Thermally reversible alkoxyamines produce radical intermediates upon heating.

1.3.3 Dynamic covalent bond exchange by an associative mechanism

The dynamic bond exchange in CANs can also occur by an associative pathway (Scheme 1.1). In this mechanism, the bond exchange is enabled by a sequence of first covalent bond-forming and then bond-breaking events (Scheme 1.2, bottom). The cross-linking density does not decrease during the topological rearrangement in the network via the bond exchange. The first associative CANs is based on the photo-mediated free radical addition fragmentation chain transfer reaction.[34] Allyl sulfides have been used as efficient RAFT agents, as shown in Scheme 1.5. The intermediate is transformed into an initial functionality and radical. Tsarevsky and Matyjaszewski have introduced a more sophisticated disulfide moiety in the design of a self-healing polyurethane (Figure 1.1a). The thiuram disulfide undergoes exchange in the presence of visible light, in air, and at room temperature.[35] Due to the nature of low T_g (-50 °C to -34 °C) materials, they are capable of self-healing even at room temperature in the absence of solvent (Figure 1.1b). The Young's modulus of the original polymer sample is 544 kPa, and the mended one is 612 kPa, comparable modulus indicating the disulfide exchange reaction regenerates polymer networks. Despite facile preparation of photo-induced CANs, the lifetime of radical exchange is limited due to unavoidable termination reactions. Non-radical dynamic covalent bonds by an associative mechanism are desired in the CAN design to avoid radical termination.

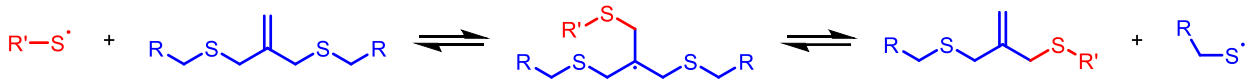

Scheme 1.5. Associative mechanism based on the photo-mediated RAFT.

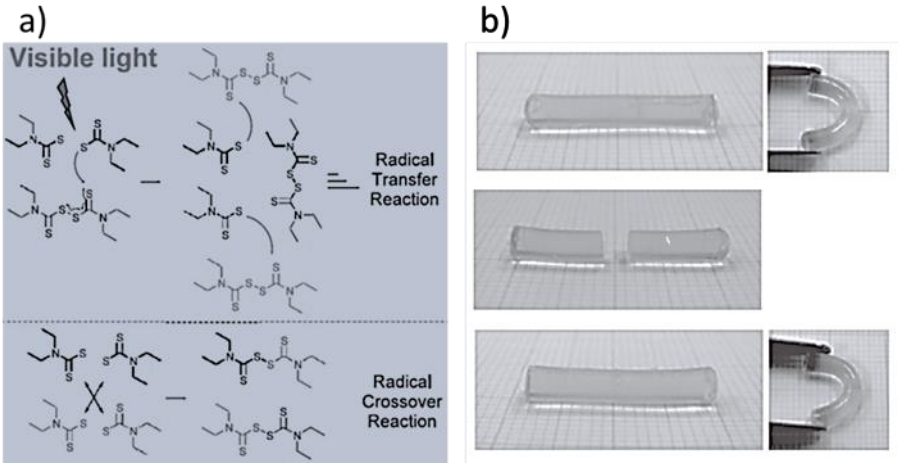

Figure 1.1. Visible light-induced thiuram disulfide exchange with (a) two possible mechanisms and (b) damaged polymers containing thiuram disulfide are healed over 24 h. Reproduced from Ref. 35 with permission from Advanced Materials.

Thermally activated associative CANs are called "vitrimers" which describes a polymer network that can undergo thermally stimulated bond exchange by an associative pathway. Leibler's group demonstrated the first polyester vitrimer that underwent the topological rearrangement in the network by a transesterification reaction.[36] Vitrimer networks show a gradual drop of viscosity upon heating above the vitrification temperature ($T_{v,}$ see below), following the Arrhenius law. This unique characteristic is similar to vitreous silica.[37] At temperatures above T_v, the vitrimer still exhibits a finite and constant storage modulus, indicative of the unperturbed crosslinking state of the network. This is in contrast to thermoplastics which undergo a more precipitous drop of viscosity with temperature following the Williams-Landel Ferry model (WLF) relationship and turn into viscous fluids above the glass transition temperature (T_g). The WLF viscosity behavior is dictated by the diffusion of polymer chains.[38] Covalent adaptable networks

that undergo dissociative bond exchange behave like thermoplastics once a ceiling temperature is reached. This distinctive feature of vitrimers sets them apart from the CANs that undergo dissociative bond exchange. Vitrimers behave like conventional thermosets below T_v and become thermally mendable above T_v, making them attractive as a replacement for conventional thermosets.

The detailed viscosity dependence of vitrimers on temperature is dictated by two thermal transitions in the network. The first transition is the glass transition temperature, T_g. The movement of polymer chains is limited below T_g, which significantly slows down or inhibits any bond exchange to occur within the network. The network behaves as a conventional thermoset and shows no creep or stress relaxation. The second transition, as introduced by Leibler et al., is the topology freezing transition temperature T_v. At this temperature, the rate of bond exchange is fast enough for the material to be processed efficiently. This is when the material changes from a viscoelastic solid to a viscoelastic liquid with the viscosity dropping to 10^{12} Pa s, commonly used to define the glass-liquid transition in silicates.[36, 39]

The order of the two thermal transitions, i.e., T_g and T_v, play an important role for designing CANs. When T_g is lower than T_v, the material will change from a glassy state to a rubber state first before any bond exchange takes place (Figure 1.2a).[40] This transition is also dependent on the gap between T_g and T_v. For example, material will exhibit deformation at T_g if T_v is relatively close to T_g; however, when T_v is much higher than T_g, the network will maintain its topology due to a slow exchange reaction. Material is simply an elastomer, and it showed no or limited creep behavior within this temperature range. After heating above the T_v, the flow behavior is fully dependent on the rate of bond exchange. In contrast, materials that have T_g higher than T_v will behave differently than the previous scenario (Figure 1.2b).[40] This means the bond exchange can occur below the T_g,

but it is rendered impossible due to freezing of the long-range polymer motion. As a result, materials still behaved as thermosets even if the temperature has reached T_v. The most intriguing finding is that after heating to T_g, the WLF viscosity is observed in the beginning. That is, the bond exchange reactions are too fast at T_g when the polymer chains motion is initiated. The rate of the exchange reaction will start to take over and follow an Arrhenius law with a further increase in temperature.

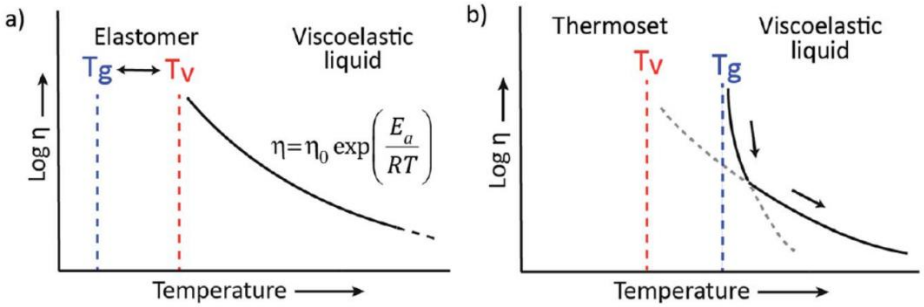

Figure 1.2. Viscosity dependence on temperature for vitrimers having either (a) $T_g < T_v$ and (b) $T_g > T_v$. Reproduced from Ref. 40 with permission from Chemical Science.

The order of two transitions T_g and T_v are important for designing CANs, as described previously. The cross-linking density, rigidity of monomers, and the rate of the exchange reaction can all be manipulated in order to control T_g and T_v. Ideal vitrimers will behave as thermosets within a temperature window for specific applications. The exchange process can be easily triggered by external stimuli (heat) when needed for reprocessing, recycling and repairing.

1.3.3.1 Vitrimer based on disulfide.

Disulfide exchange is one of the earliest reactions used in DCC. The chemistry has been well studied. Disulfide bonds can be found in biological systems such as in protein folding.[41] Disulfide chemistry can have both dissociative and associative mechanisms. Disulfides can form two thiols and then oxidize again.[42] Alternatively, disulfides can be photolytically cleaved under UV irradiation.[43] Both reactions are a dissociation process. Associative disulfide exchange can be

achieved by a thiolate anion nucleophilic attack on another disulfide bond and reformed to make a new thiolate anion (Scheme 1.6).[44] This reversible reaction is pH sensitive and can undergo dynamic exchange under a basic condition. Canadell et al. have demonstrated self-healing materials based on disulfide bonds.[44a] They incorporated a disulfide moiety in the network. Base catalyzed disulfide exchange is responsible for the self-healing properties. From tensile testing, mechanical properties of pristine and mended polymers are fully restored. Materials can be fractured and then healed multiple times when heating above T_g with only a minor decrease of modulus.

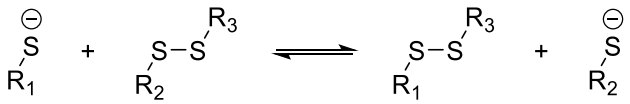

Scheme 1.6. Associative disulfide bond exchange reaction.

1.3.3.2 Vitrimer based on transesterification.

Transesterification is one of the reversible reactions that are commonly categorized in a thermally activated associative mechanism. The exchange reaction occurs between an ester bond and an alcohol (Table 1.1). Ring-opening polymerizations such as lactide and caprolactone are polymerized by alcohol initiators.[45] Furthermore, vegetable oil such as sunflower oil transesterification with alcohol species produces fatty acids that can be used in foods, textiles, cosmetics, and rubber.[46] The reaction is generally conducted under acid or base catalyzed conditions; other catalysts such as Sn and Zn have also been used for transesterification.[47] Leibler et al. have used metal-catalyzed transesterification for healing and assembling highly cross-linked polyester thermosets. The rate of healing is controlled by the rate of transesterification. Elevated temperature increased the rate of the exchange reaction which leads to a faster healing process. Other parameters like changing the amount and nature of the catalyst will affect the activation

energy and T_v. For example, activation energies for 1,5,7-triazabicyclo[4.4.0]dec-5-ene (TBD), zinc(II)acetate ($Zn(OAc)_2$), and triphenylphosphine (PPh_3) are 106, 86 and 43 kJ mol^{-1} respectively. Transesterification vitrimers are relatively straightforward to make due to the availability of monomers and facile reactions. The kinetics of the exchange reaction are also easy to control by catalysts.

1.4 Considerations in designing CANs

1.4.1 Choice of monomer

Manipulation of the monomer structure is the most common strategy to control the material properties such as the glass transition temperature and mechanical properties. Glass transition temperature is the most important transition in CANs design. Topological rearrangement in CANs can only occur when the exchange reaction is activated and unrestricted by the segmental motions associated with T_g in the entire network. In general, crosslinking density is proportional to T_g, which means materials that have a higher cross-linking density will have higher T_g. There are many strategies to tune the cross-linking density such as changing the number of functional groups per monomer. For example, step-growth polymerization of tetra-aldehyde and diamine will result in a higher cross-linking material than tri-aldehyde and diamine, assuming that all functional groups have equal reactivity. Further consideration is necessary when the polymerization reaction contains monomer A and B or more, and the reactivity of monomer A toward monomer B is important. Low reactivity will influence the polymerization conversion, which will affect the overall cross-linking density. Mono-functional model compounds can be used to determine the relative reactivity of monomers toward each other. Monomer A and B produce high K_{eq} and high yield with less side product and are most suited for synthesizing vitrimers. In addition, changing the molecular weight, stiffness and steric hindrance of monomers are all useful parameters to

control the T_g. It is often difficult to precisely predict a priori the properties of a given polymer having a particular monomer structure. A systematic investigation of the structure-property relationship is therefore important to guide the search of monomers and polymers having a specific property profile for targeted applications.

1.4.2 Dissociation constant (exchange reaction follows a dissociative pathway)

For CANs that undergo dissociative covalent bond exchange, understanding the dependence of the dissociation constant (K_d) on temperature is important to fully assess the efficiency of bond exchange. Some reversible covalent bonds have a K_d that is strongly dependent on the temperature, such as a retro Diels-Elder (rDA) reaction. This reaction of a model compound has a K_d value of 1.7 M at 120 °C. With such a high dissociation constant at this temperature (greater than gel point temperature), the polymer network changed from a viscoelastic solid to a viscoelastic liquid.[48] In comparison, oxime exchange showed less dependence on temperature with a K_d of 3.2×10^{-3} M at 120 °C.[49] A reversible reaction with small dissociation constant means the rate of bond reforming is faster than the bond breaking. Thus, the oxime-based CANs can be remolded, reprocessed and recycled with a fairly wide temperature window without going through the gel-to-sol transition. Figure 1.3. shows a simulation of equilibrium constants derived with low enthalpy and high enthalpy values as a function of temperature. The K_{eq} is less dependent on the temperature when ΔH is less negative, whereas temperature has a greater influence on the K_{eq} when ΔH is more negative. The case of oxime exchange reaction is shown as a blue curve, and the red curve is a simulation rDA reaction for its thermally dependent K_d, resulting in an abrupt gel-to-sol transition.

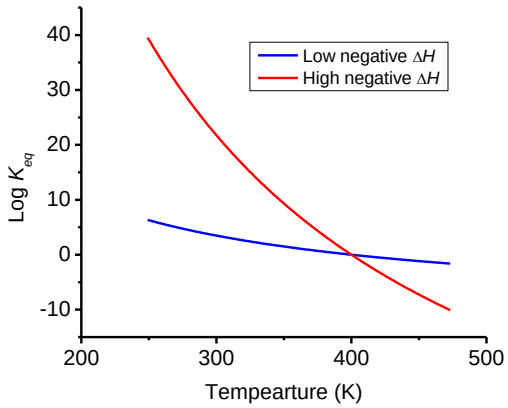

Figure 1.3. Simulation of the effect of temperature on the equilibrium constant with low and high ΔH values.

The K_d can be measured using a model compound by NMR analysis of the reaction equilibrium at different temperatures. The equilibrium constant is temperature dependent. For an exothermic reaction ($\Delta H°<0$), the equilibrium constant decreases with increasing temperature, whereas the opposite is true for an endothermic reaction ($\Delta H°>0$). Analysis of K_d at different temperatures using the Van't Hoff equation will afford the enthalpy (ΔH_d) and entropy (ΔS_d) of the bond dissociation.

1.4.3 Kinetic and activation energy study

Kinetic study of bond exchange from molecular studies can estimate how quickly the material can be deformed under a constant stress. Especially when comparing conditions, a reversible bond will behave differently under different parameters such as temperature effects, catalyst effects, and pH effects. Additives including acids, bases, or catalysts are added to investigate the reaction kinetics in organic media. Depending on the nature of the dynamic covalent bond, additives will indicate the conditions to either facilitate or hinder the exchange reaction. We can optimize the conditions for a specific application by studying the kinetics of bond exchange. Two model compounds should be chosen that have a similar chemical structure as the cross-linked

network. Their chemical shift should also be differentiated easily from ^{1}H-NMR. The kinetics of the exchange reaction is measured from a collection of ^{1}H-NMR spectra obtained over different times. The activation energy of the exchange reaction can be calculated by measuring the kinetics at different temperatures, and then an Arrhenius plot is made. Initial linear rates are normally used for preparing an Arrhenius plot. The rate can be obtained at a higher temperature if the exchange rate is too slow at a lower temperature. We can also measure the activation enthalpy ($\Delta H^{\ddagger}$) and entropy ($\Delta S^{\ddagger}$) from an Eyring plot.

1.4.4 Synthesis of linear polymerization

Molecular characterization of cross-linked polymers is challenging. To gain an understanding of the polymerization reaction, synthesis of linear polymers is often attempted. Characterization of the soluble linear polymers by spectroscopic methods (e.g., NMR and MS) will provide information regarding the molecular structure of the polymers. Nuclear magnetic resonance provides information of the degree of polymerization, from which K_{eq} and ΔG° of bond formation equilibrium can be determined based on certain assumptions. Mass spectrometry can further provide information regarding the polymer structure, end-group structure, average molecular weight and molecular weight distribution.

1.4.5 Synthesis of Cross-linked polymerization

Cross-linked polymer networks are prepared with monomers that contained an average functional group number (f) greater than two. For step-growth polymerization, the functional groups between monomers have to be equivalent in order to achieve high conversion. For example, the functional groups for 3 moles of monomer A ($f_A = 2$) and 2 moles of monomer B ($f_B = 3$) are stoichiometrically balanced.

Fourier-transform infrared spectroscopy is the most direct structural characterization tool of cross-linked polymers. Depending on the type of DCC, each covalent bond has a unique vibrational band associated to their functional group. For example, polyimine has a distinct C=N stretching band ($\nu_{C=N}$) at 1650 cm^{-1} for imine functionality. The extent of polymerization can be quantified by monitoring the disappearance of monomer over time. For example, the conversion of aldehyde can be tracked by the decreases of the C=O stretching band ($\nu_{C=O}$) at 1720 cm^{-1}. Thermal properties of the polymers can be analyzed by differential scanning calorimetry (DSC) to obtain the glass transition (T_g), melting temperature (T_m) and crystallization temperature (T_c), and by thermogravimetric analysis (TGA) to acquire the thermal decomposition temperature (T_d).

The theoretical gel point corresponds to the extent of reaction threshold for a step-growth polymerization system with a certain average functionality (f_{avg}) to reach infinite molecular weight. There are two theoretical descriptions commonly used to estimate the gel point: Carothers theory or Flory-Stockmayer statistical theory. Carothers theory followed equation 1 if stoichiometrically is in balance. The parameter of p_c is the theoretical gel-point conversion and f_{ave} is the average functionality of a mixture of monomers. The second way is a statistical approach by Flory-Stockmayer theory. From equation 2, r is the stoichiometric ratio of the functional groups (i.e., r = 1 for a stoichiometrically balanced composition), and the parameter of f_w is the weight-average functionalities of individual monomer. Gelation (sol-gel transition) occurs when the experimental conversion is above the estimated conversion, p_c. In a case when p_c is above 100 %, it means this monomer composition will never reach gelation. A gel is considered to be a giant molecule that is insoluble in all solvents before degradation. Therefore, insoluble gel content has been commonly interpreted as polymer molecules that are cross-linked to each other. Gel content can be quantified by a solvent extraction experiment. This involves the extraction and separation

of the soluble polymer portion and gravimetric quantification of the gel portion. The ratio of polymer sample mass before and after the extraction is referred to as gel content.

Equation 1: $$p_c = \frac{2}{f_{avg}}$$

Equation 2: Monomer A and B $$p_c = \frac{1}{\sqrt{r(f_{w,A}-1)(f_{w,B}-1)}}$$

1.4.6 Dynamical behavior of CANs

Dynamic mechanical thermal analysis (DMTA) of CANs measures the change in the storage (elastic) modulus (G') and loss (viscous) modulus (G") as a function of temperature. Storage modulus is a measure of the material's elasticity whereas loss modulus is a measure of the material's ability to dissipate energy. Tan delta is the ratio of loss modulus to the storage modulus. When Tan delta is less than 1, this indicates elastic dominance or solid behavior, whereas values greater than 1 indicate viscous dominance or liquid like behavior. The G"/G' = 1 is described as the sol-gel transition point. The temperature dependence of the storage modulus can determine various thermal transitions (e.g., T_g, T_m) that occur in a polymer. It is an alternative method to DSC thermal analysis. The experimental crosslinking density (ν_e) can be calculated from equation 3, where R is the universal gas constant, and T is the temperature.

Equation 3: $$G'(T) = 3RT\nu_e$$

Stress relaxation analysis (SRA) can be used to characterize the rate of dynamic bond exchange within the network, resulting in a controlled macroscopic relaxation under a constant strain. The relaxation behavior has a direct relationship with the kinetics of bond exchange. For dissociative CANs, relaxation happens when network connectivity is broken and reformed subsequently to restore the cross-linking network. The individual rate of bond breaking (k_b) and bond forming (k_f) dictate the viscoelastic properties. That means when the $K_{eq} < 1$, the polymer

network will stay as a viscoelastic solid. Alternatively, the polymer becomes fluid when $K_{eq} > 1$. As the rate of bond breaking dominates in the exchange process, the cross-linking density is insufficient to maintain gelation (below the gel point). By comparison, associative CANs do not have this issue. [Write a sentence to set up equations below]

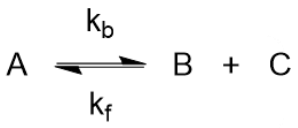

$$K_{eq} = \frac{k_b}{k_f} \qquad K_{eq} < 1 \qquad\qquad K_{eq} > 1$$

From stress relaxation analysis (SRA) of CANs, activation energy can be calculated from monitoring stress decay as a function of time at different temperatures. Based on the Maxwell model for viscoelastic fluids, the relaxation time (τ*) is defined as the time when the normalized stress decays to 37 % (1/e) of its original value. Analysis of τ* versus temperature using the Arrhenius relationship (Equation 4) will afford the activation energy barrier for the bond exchange in CANs. The τ* value is the stress relaxation time, τ_0 is the relaxation time at infinite (constant), E_a is the activation energy, R is the universal gas constant, and T is the temperature at which the SRA was performed.

Equation 4: $$\tau^*(T) = \tau_0 e^{E_a/RT}$$

Combining DMTA and SRA will provide further information about the topology of the freezing transition temperature, T_v, described by Leibler et al. The T_v is the temperature transition from a viscoelastic solid to a viscoelastic liquid as the viscosity (η) of the material drops to 10^{12} Pa s. The relaxation time (τ*) at this viscosity (10^{12} Pa s) that corresponds to T_v can be calculated

by equation 5, where parameter G' comes from the DMTA experiment. The relaxation time τ^* obtained from equation 4 can plug into equation 5 to determine T_v.

Equation 5: $$\eta = \frac{1}{3} G' * \tau^*$$

1.4.7 Mechanical properties of CANs

The definition of modulus (Pa) is stress (Pa) over strain %. Since strain is unitless, the unit of modulus and stress are identical. This value can be measured directly by a tensile test from a stress-strain curve. This curve is a representation of the behavior of a material under force. From this curve, we can classify the material in the following categories, based on their performance: elastomer, brittle material, or ductile materials. The initial linear region from the stress-strain curve is called the elastic region that is normally referred to as the Young's modulus. It describes tensile elasticity of an object to deform. The stress and strain at break is called the yield point, sometimes reported as yield modulus. Moreover, the stress-strain curve can demonstrate the healing properties of CANs when comparing tensile properties of pristine and thermally mended samples. Stress-strain curves with multiple healing cycles are conclusive evidence of self-healing behavior.

Chapter 2 : Dynamic Covalent Polymer Networks Based on Degenerative Imine Bond Exchange: Tuning the Malleability and Self-Healing Properties by Solvent

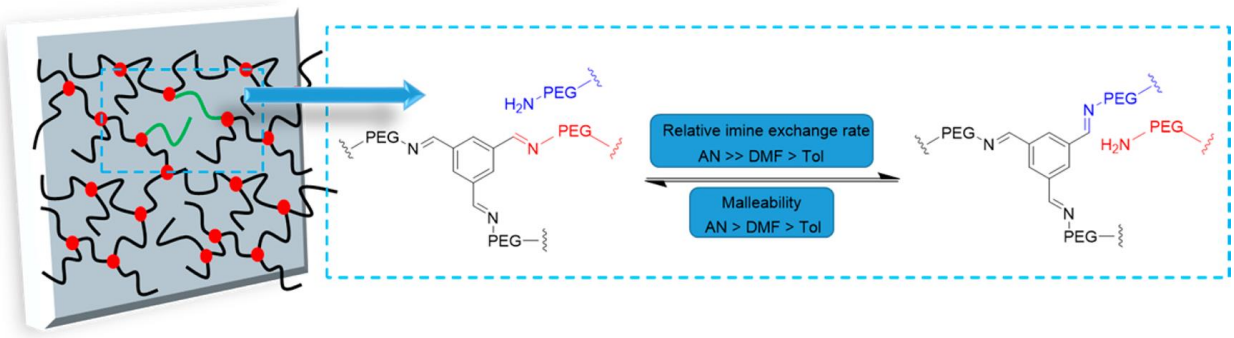

2.1. Introduction

Imine bond, often referred to as Schiff bases are synthesized from condensation of a ketone or aldehyde with a primary amine (Scheme 2.1).[50] The formation of imine bond can be catalyzed by acid but the pH should be controlled such that the amine is not protonated. Imine is a strong covalent bond with a bond dissociation energy of 147 kcal·mol^{-1}, can undergo rapid degenerative bond exchange (associative,[51] dissociative,[52] metathesis[53] pathway, Scheme 2.1) without any significant side reactions.[54,2-4,17,51] Reports on polymeric network comprised of imine linkages are surprisingly limited[55,53] in view of the diverse range of primary amines and aldehydes that are readily available.

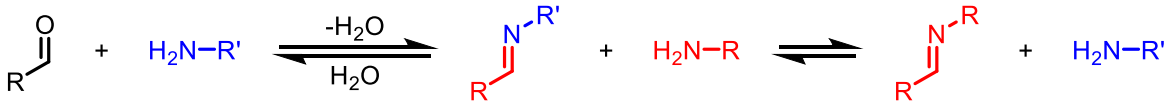

Scheme 2.1. Imine exchange by condensation reaction (dissociation) and exchange reaction with primary amine (association).

* Chapter 2 previously appeared as Chao, A.; Negulescu, I.; Zhang, D., Dynamic Covalent Polymer Networks Based on Degenerative Imine Bond Exchange: Tuning the Malleability and Self-Healing Properties by Solvent. Macromolecules **2016,** 49 (17), 6277-6284. It is reprinted by permission of ACS Publisher (see page 107).

One recent study by Zhang and coworkers[56,57,58] showcased the excellent mechanical and dynamical properties of the thermosets comprised of imine linkages. The nature of imine exchange allows thermosets to be malleable when temperature increases to 80 °C. Unlike thermoplastic, imine vitrimer maintained their mechanical strength during reprocessing and recycling. Stress-strain curves showed the mechanical properties are comparable before and after recycling. Furthermore, cross-linked polyimine are remoldable at room temperature by wetting the polymer in water. A recent published work by Chen et al. demonstrates designing multi-phase networks based on dynamic imine bonds. Condensation of peptides (H-Asn-Phe-CHO) provides oligomers including linear dimers, linear trimers, cyclic dimers and cyclic trimers.[46] Cyclic dimers were the most dominate structure of oligomers. Cyclic dimers were dynamically transformed into linear dimers by hydrolysis. This linear dimer reacted further with amine to give trimer followed by self-assembly into β-sheet fibre states. Oligomer slowly phase changes from solution, particles and to fibre stages at 96 h.

Recent studies of small model imine compounds in solution by Stefano et al. revealed that the imine bond exchange is catalyzed by the presence of primary amine.[59] The rate of exchange is dependent on the solvent, temperature and imine structure. We envisioned that the dynamical property of polymeric networks comprised of imine linkages can be controlled by these parameters. In this study, we reported the synthesis of dynamic covalent polymeric networks comprised of poly(ethylene oxide) (PEO) strands and imine cross-linkers (Scheme 1) and the investigation of the effect of imine bond exchange kinetics on the macroscopic dynamical properties of the polymeric networks.

2.2 Results and discussion

2.2.1 Synthesis and characterization of cross-linked polyimine gel

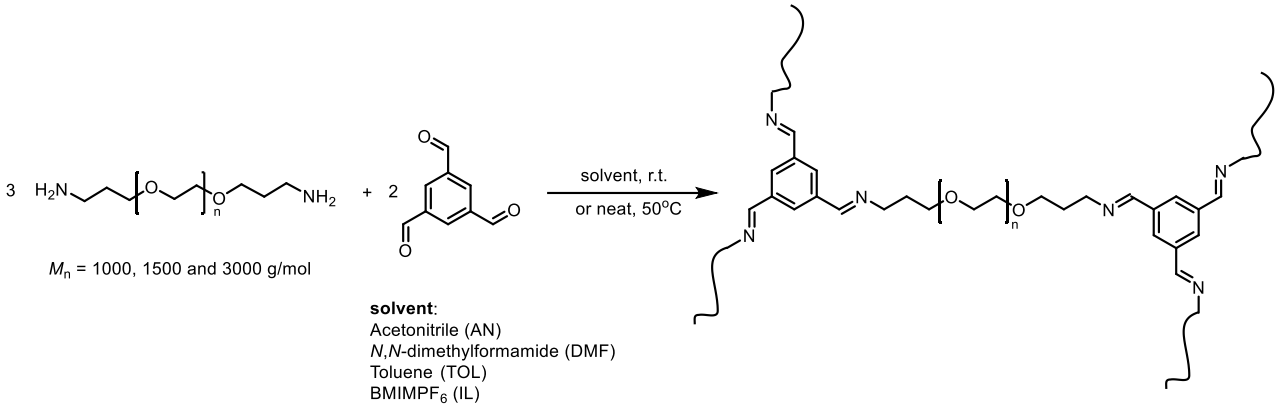

Scheme 2.2

The polymeric networks comprised of poly(ethylene oxide) (PEO) strands and imine cross-linkers have been prepared by condensation polymerization of poly(ethylene oxide) bis(3-aminopropyl) (PEO-diamine) having varying molecular weight (M_n = 1000, 1500 and 3000 g·mol^{-1}) and 1,3,5-triformylbenzene (trialdehyde) in solvents with varying polarity [i.e., acetonitrile (AN), N,N-dimethylformamide (DMF), benzyl alcohol (BnOH), toluene (TOL) and 1-Butyl-3-methylimidazolium hexafluorophosphate (BMIMPF$_6$ or IL)] at room temperature as well as in neat conditions at 50°C (Scheme 2.2). The initial stoichiometric ratios between the aldehyde and amine functional group were kept at unity for all reactions to ensure high functional group conversion. The initial concentrations of the functional groups (i.e., [amine]$_0$ and [aldehyde]$_0$) were both kept at 0.37 M. FTIR spectroscopy was used to monitor the progression of the condensation polymerizations, as both imine and aldehyde groups exhibit characteristic C=X (X=N or O) stretching bands at 1650 and 1700 cm^{-1} respectively (Figure 2.1). All reactions reach high conversion (86-99%) after 4 h at room temperature, as determined by the percentage reduction of the aldehyde C=O stretching band in the FTIR spectra of the reaction mixture. Prolonged reaction time or increasing initial reactant concentration did not result in significant increase of the

conversion (Table 2.1). The cross-linking density for an ideal network with a quantitative functional group conversion is estimated to be approximately 3.7×10^{-4} mol·mL^{-1}. If the actual crosslinking density is assumed to be proportional to the functional group conversion, all samples in Table 2.1 exhibited comparable crosslinking density in the $3.1\text{- }3.6 \times 10^{-4}$ mol·mL^{-1}range (Table 2.1).

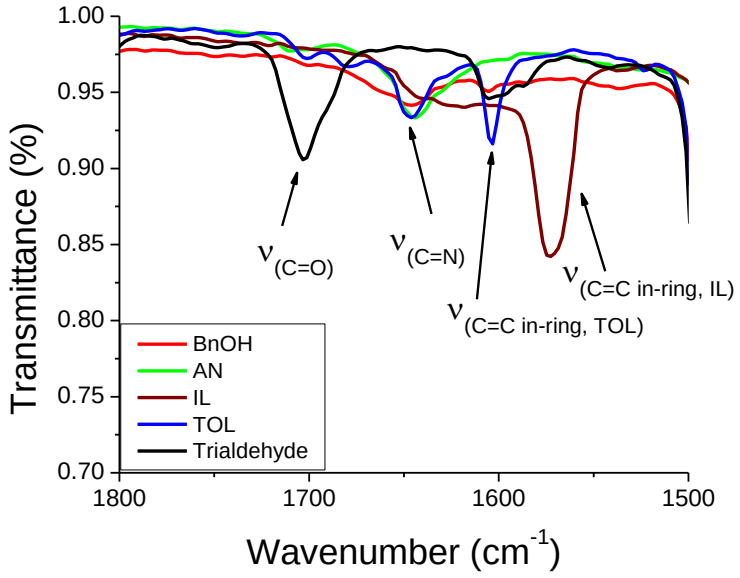

Figure 2.1. Representative FT-IR spectra of the polymerization mixtures of PEO-diamine and 1,3,5-triformylbenzene in various solvents (colored lines) in comparison to that of 1,3,5-triformylbenzene monomer (black line) to verify the formation of imine bonds for gels in various solvents.

2.2.2 Rheological characterization of the sol – gel transition

All reactions using low molecular weight PEG diamines (M_n= 1000 and 1500 g·mol^{-1}) result in the formation of free standing gels in organic solvents after 4 h at room temperature, whereas the networks consisting of long PEG chains (M_n= 3000 g·mol^{-1}) form soft and non-free-standing gel (Entry 12 and 13, Table 2.1). Time-dependent oscillatory rheological measurements of condensation polymerization mixtures under identical conditions (i.e., 20 °C, $[amine]_0=[aldehyde]_0$=0.37 M, DMF) revealed a gradual increase of storage modulus (G') and loss

modulus (G'') over time (Figure 2.2). The G' was smaller than G'' initially and became larger than G'' beyond a time point. The G' and G'' cross-over point was defined at the gelation point, indicating the formation of an elastic network. The moduli (G' and G'') at the gelation point are also dependent on the molecular weight of PEO diamines. As the M_n of the PEO diamines increases from 1000 to 1500 g·mol^{-1}, the moduli decrease from 104 to 15 Pa (Figure 2.2), in agreement with the formation of increasingly soft gels.

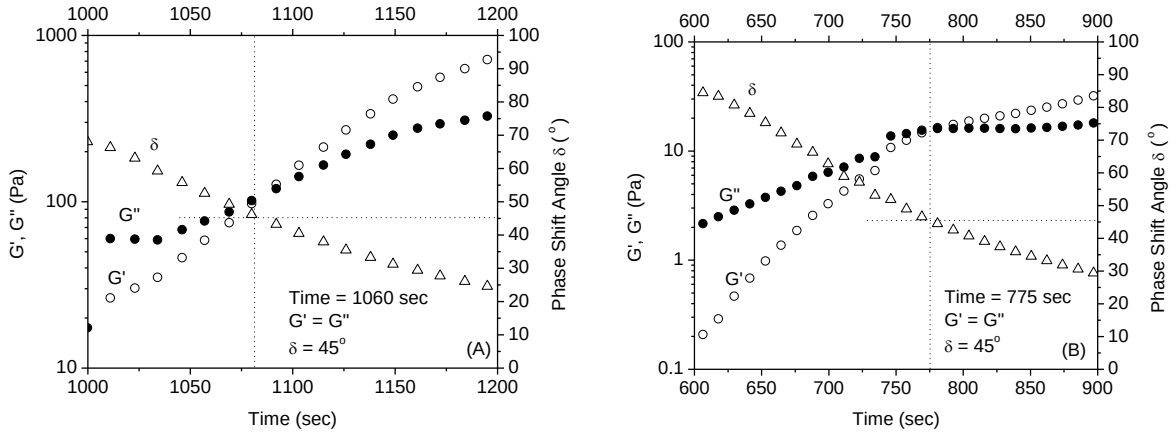

Figure 2.2. Plots of storage moduli (G',●), loss moduli (G'',○), and delta degree (Δ) versus time for the condensation polymerization mixtures of PEO diamines with varying molecular weight [Mn= 1000 (A) and 1500 g·mol-1(B)] and 1,3,5-triformylbenzene in a 1:1 molar ratio of the total amine to aldehyde functional groups in DMF at room temperature obtained by oscillatory rheological measurement at room temperature under a constant frequency (ω= 1 Hz). The initial concentrations of amine and aldehyde functional groups are both kept at 0.37 M.

Solvent has also been shown to influence the gelation time: increasing polarity of the solvent appears to be correlated with prolonged gelation time, as revealed by the in situ oscillatory rheological measurements of the PEO-diamine (M_n=1500 g·mol^{-1}) and 1,3,5-triformylbenzene mixture in various solvents (AN, DMF and TOL) at 20°C. For example, the reaction mixture undergoes a sol-to-gel transition at 2180 s in AN as compared to 775 s and 318 s in DMF and toluene respectively (Figure 2.3). The origin of the solvent dependence of gelation time will be further discussed later. In addition, the moduli at the respective gelation point are also solvent dependent with toluene gel having the highest moduli (40 Pa) followed by the DMF gel (15 Pa)

and AN gel (3.3 Pa). As the crosslinking density is approximately the same in all the gel samples regardless of the solvent (Table 2.1), the moduli are related to the specific interaction between the polymer and the respective solvent.[60]

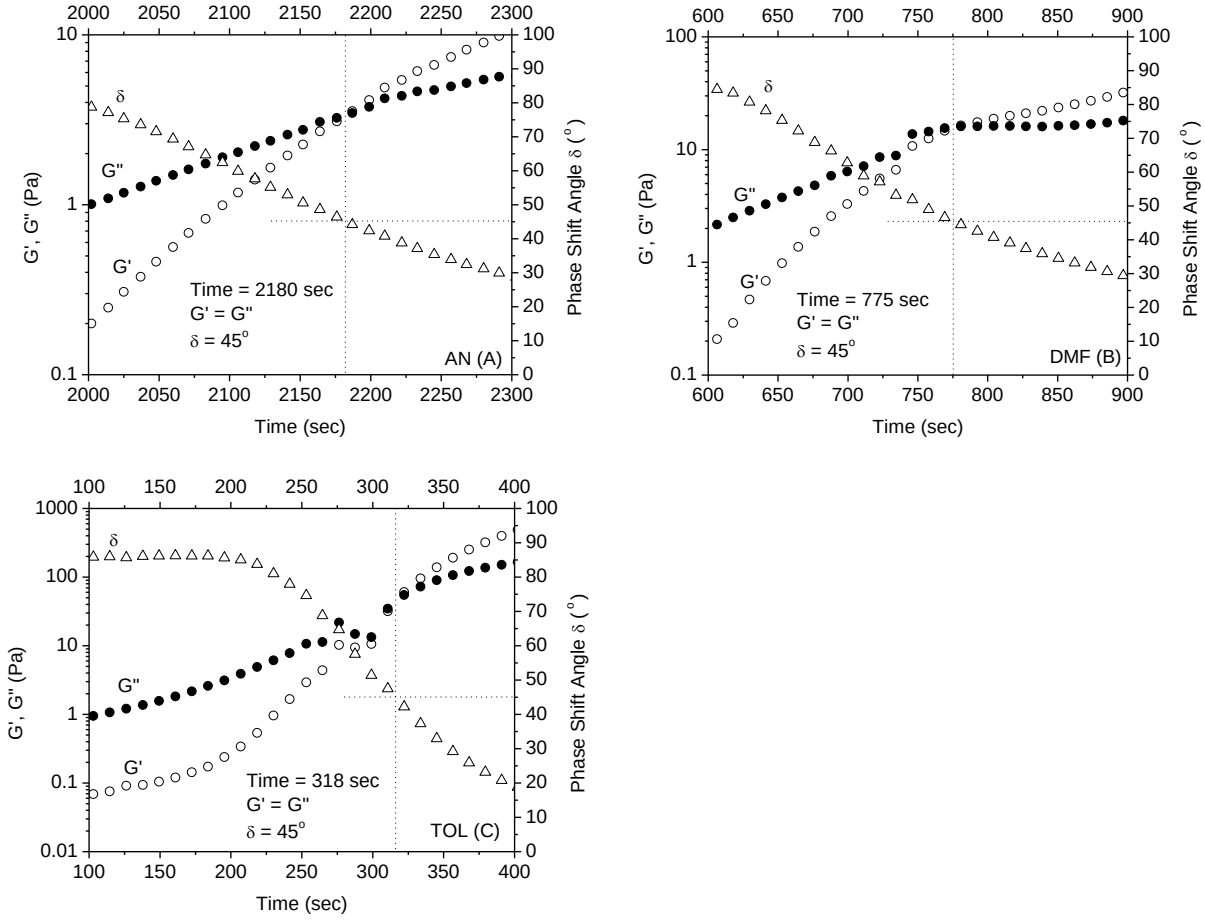

Figure 2.3. Plots of storage moduli (G',●), loss moduli (G'',○), and delta degree (Δ) versus time for the condensation polymerization mixtures of PEO diamine (Mn= 1500 g·mol-1) and 1,3,5-triformylbenzene in a 1:1 molar ratio of the total amine to aldehyde function groups in various solvents [i.e., AN (A), DMF (B) and TOL (C)] at room temperature obtained by oscillatory rheological measurement at room temperature under a constant frequency (ω= 1 Hz). The initial concentrations of the amine and aldehyde functional groups are both kept at 0.37 M.

Table 2.1. Characterization of polymeric networks comprised of PEG strands and imine cross-linkers by condensation polymerization of PEG-diamine and 1,3,5-triformylbenzene[a]

Entry number	M_n (PEG-diamine) ($g \cdot mol^{-1}$)	Solvent	Gel Appearance	Conv. [b,c] (%)	Actual cross-linking density ($mol \cdot mL^{-1}$)
1	1000	AN	clear & free-standing	87	3.2×10^{-4}
2		DMF		- [d]	
3	1500	AN	clear & free-standing	86	3.1×10^{-4}
4		DMF		- [d]	-
5		TOL		89	3.3×10^{-4}
6		THF		99	3.6×10^{-4}
7		EtOH		98	3.6×10^{-4}
8		BnOH		95	3.5×10^{-4}
9		H_2O [e]		- [d]	-
10		$BMIMPF_6$		98	3.6×10^{-4}
11		NEAT		97[f]	-
12	3000	AN	clear & non-free- standing	90	3.3×10^{-4}
13		DMF		- [d]	

[a.] All reactions were conducted at 1:1 initial molar ratios of the amine (0.37M) and aldehyde (0.37M) functional groups. [b.] The theoretical gel point of 83% is estimated based on the Carother's equation. [c.] The extent of imine formation or conversion was calculated by using the following equation: 1-(integrated area of aldehyde peak at time=4 h / integrated area of aldehyde peak at time=0). [d.] The conversion in DMF and H_2O cannot be determined by FTIR spectroscopy due to the overlap of the aldehyde peak with the DMF solvent peak; [e.] Free-standing hydrogels were obtained when the initial amine and aldehyde concentrations are 0.90 M respectively. [f.] FTIR spectrum of the aldehyde at time 0 was taken using a homogeneous mixture of PEO without diamine end groups (M_n=1500) and trialdehyde obtained by slight heating.

2.2.3 Creep and stress relaxation studies of organogel

The viscoelastic responses of the polymeric gels produced in three different solvents (i.e., AN, DMF, and TOL) have been investigated using dynamic mechanical analysis (DMA) methods under either constant stress (creep study) or constant strain (stress relaxation) conditions. Two free-standing gels having varying molecular weight PEO strands (M_n=1000 and 1500 $g \cdot mol^{-1}$) in

DMF have been subjected to a constant stress of 0.01 MPa for 5 min in compression mode. The associated strain response over the course of 10 min was monitored and is shown in Figure 2.4. Both gels exhibited an initial rapid strain increase followed by a more gradual deformation over the course of 5 min. Upon stress removal at the 5 min point, the gel sample exhibited various levels of strain reduction. The initial rapid increase of strain was attributed to the elastic deformation of the gel network. The gel network comprised of higher molecular weight (MW) PEG strands exhibited lower elastic modulus than the one having lower MW PEG strands, as evidenced by a 20% deformation for the former versus a 7% for the latter under a constant 0.01 MPa stress. This is consistent with the former gel network having a lower density of elastically effective PEO strands than the latter gel, since both gel networks have nearly identical cross-linking density and polymer concentration. During the gradual deformation stage, the gel with higher MW PEG strands deforms more slowly to a lesser extent than the gel comprised of lower MW PEGs, indicating that the former gel is less malleable than the latter. As the cross-linking density is identical in both gel networks, we attribute the difference of the creep (or strain relaxation) behavior to the slower diffusion of high MW PEG strands than the low MW PEG strands in the networks,[61] resulting in slower imine bond exchange in the former gel network than the latter. In addition, upon stress removal, the gel network comprised of high MW PEGs (M_n= 1500 g·mol^{-1}) afforded a higher percentage strain recovery (26%) relative to the gel having low MW PEGs (M_n= 1000 g·mol^{-1}) (strain recovery=2%), consistent with a faster dynamic bond exchange taking place in the latter gel than the former. It was also found that the gel samples that were allowed to age for various durations (4-140 h) at room temperature prior to the creep study did not result in significant change of the percentage strain recovery (Figure 2.5), indicating that the gel networks have already equilibrated at 4 h after preparation.

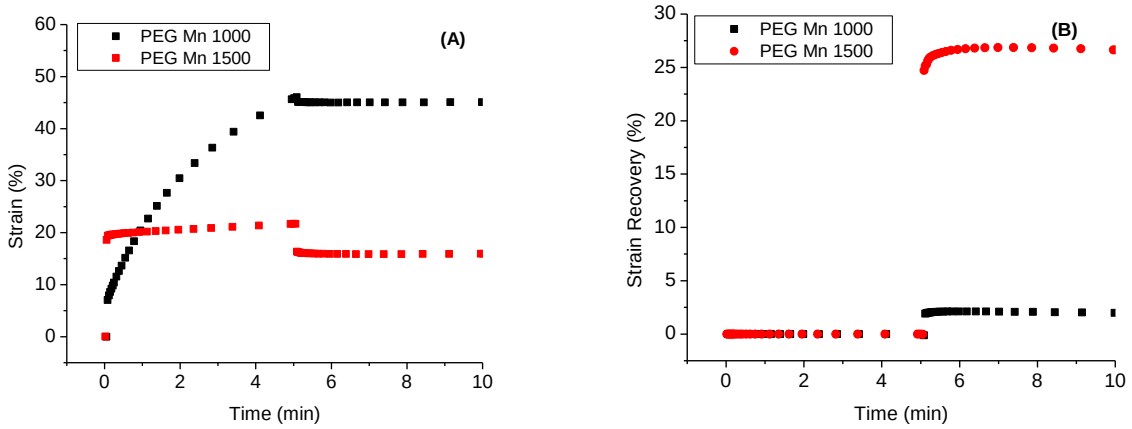

Figure 2.4. (A) Plot of percentage strain and (B) percentage strain recovery versus time for the dynamic covalent polymeric networks comprised of low molecular weight PEG strands (Mn= 1000 and 1500 g·mol^{-1}) and imine cross-linkers in DMF (Entry 2 and 4, Table 2.1). The experiments were conducted in compression mode with a constant stress (σ=0.01 MPa).

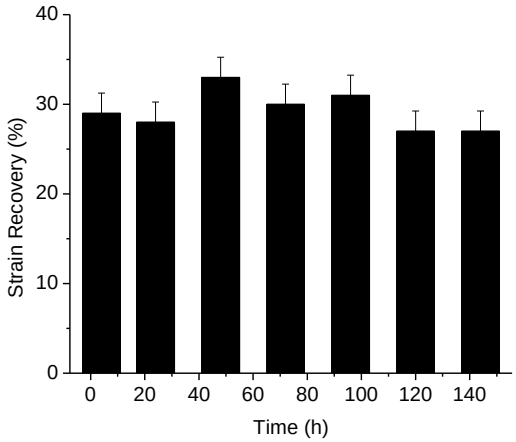

Figure 2.5. The plot of percentage strain recovery versus aging time for the dynamic covalent polymeric network comprised of low molecular weight PEG strands (Mn= 1500 g·mol^{-1}) and imine cross-linkers in DMF (Entry 4, Table 2.1). The experiments were conducted in compression mode with a constant stress (σ=0.01 MPa). The mean percentage recovery is 29± 2%.

The solvent effect on the creep behavior of polymeric gels comprised of PEGs (M_n=1500 g·mol^{-1}) has been studied under the identical conditions as that for the gels in DMF (i.e., σ=0.01 MPa for 5 min, compression mode). The gels in different solvents exhibited varying degrees of initial elastic deformation (Figure 2.6A) owing to the difference in their respective compression modulus. As the crosslinking density is approximately the same in all the gel networks, the

modulus is determined by the interaction between the polymer and the specific solvent.[24] The toluene gel exhibited the lowest degree of initial elastic deformation followed by the DMF gel and then the AN gel (Figure 2.4). This is consistent with the relative strength of the moduli of organic gels in various solvents at the gelation point: TOL > DMF > AN (Figure 2.3). Upon removal of the stress at the 5 min time point, all gels exhibited varying levels of permanent deformation, as evidenced by the non-quantitative percentage strain recovery, in contrast to an elastic polymer network showing quantitative strain recovery (Figure 2.6). The extent of percentage permanent deformation is solvent-dependent and appears to increase with increasing solvent polarity in the following order: TOL < DMF < AN (Figure 2.6B). To further characterize the effect of dynamic imine bond exchange on the network viscoelastic properties, the gels were also subjected to a constant 10% strain with a preload force of 0.0010 N over a period of 5 min. The stress was shown to decrease over time to adapt to the external strain, in contrast to an elastic polymer network which maintains a constant stress during deformation. The rate of stress relaxation was also shown to decrease with time in a solvent-dependent manner (Figure 2.7). The initial rate of stress relaxation was determined using the data where the stress decays linearly with the time. The more polar the solvent is, the higher is the rate of stress relaxation [i.e., AN (0.59 min^{-1}) >> DMF (0.12 min^{-1}) > TOL (0.088 min^{-1})] (Figure 2.8). These results are consistent with the occurrence of rapid dynamic bond exchange in the network that allows for the permanent deformation of the gel or stress relaxation through topological change of the network structures.

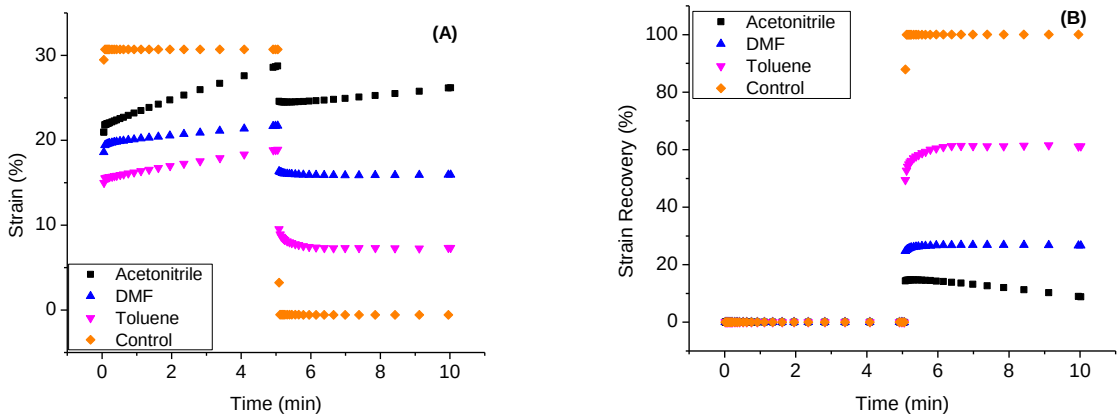

Figure 2.6. (A) The plot of strain and (B) percentage strain recovery versus time for the dynamic covalent polymeric network comprised of low molecular weight PEG strands (Mn= 1500 g·mol-1) and imine cross-linkers in the AN solvent (Entry 3, 4 and 5, Table 2.1). The strain recovery experiments were conducted by applying an initial constant stress (σ=0.01 MP) to the gel sample in compression mode for 5 min and allowing the sample to recover for 5 min at room temperature. The control sample is a polymeric thermoset without dynamic covalent bonds.

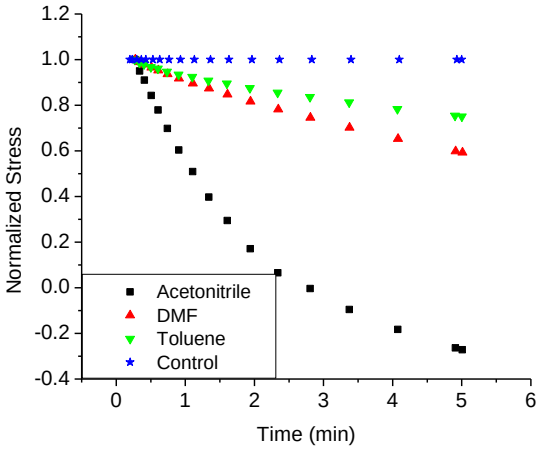

Figure 2.7. The plot of normalized stress versus time for the dynamic covalent polymeric network comprised of low molecular weight PEG strands (Mn= 1500 g·mol^{-1}) and imine cross-linkers in the various solvents (AN, DMF and TOL) (Entry 3, 4, and 5, Table 2.1). The stress relaxation studies were conducted by inducing a constant initial strain (ε=10 %) of the gel sample in compression mode for 5 min at room temperature. (Note: the negative normalized stress value for the AN gel at the later stage of the measurement was attributed to the slow evaporation of the solvent, resulting in slight shrinkage of the gel.) The control sample is a polymeric thermoset without dynamic covalent bonds.

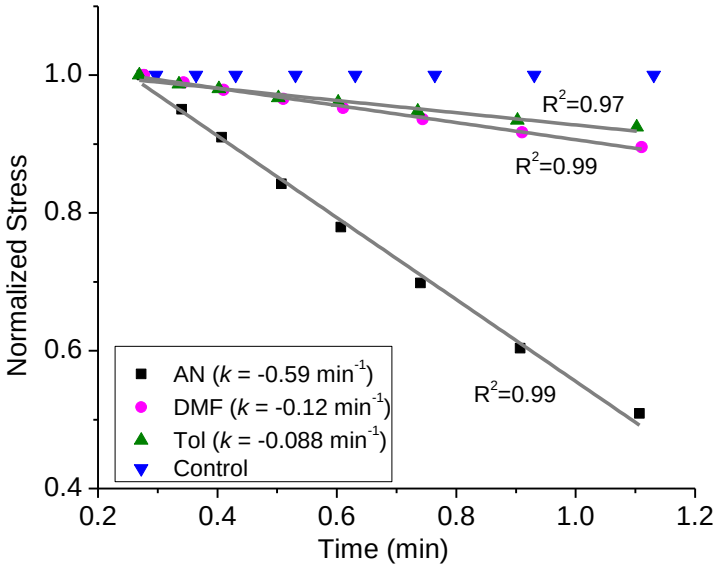

Figure 2.8. The plot of normalized stress versus time for the dynamic covalent polymeric network comprised of low molecular weight PEG strands (Mn= 1500 g·mol^{-1}) and imine cross-linkers in various solvents (An, DMF and TOL) (Entry 3-5, Table 2.1) in the initial stage where the stress decays linearly with the time. The data was linearly fitted and the slope corresponds to the relative rate of the stress relaxation (k shown in the inset).

2.2.4 Kinetic study of model compound

To understand the molecular origin for the solvent-dependent viscoelastic behavior of the polymeric gels, ^{1}H NMR experiments were conducted to gain insights regarding the relative rate for imine exchange using small molecular model compounds (Scheme 2.3). We have shown that the imine exchange does not occur at room temperature on its own regardless of the solvent. It is clear that catalytic species is required to effect the imine exchange[62]. As the water byproduct from the aldehyde and amine condensation reaction remains in the gel and the residual amino groups on the PEG chain ends also present in the gel due to the non-quantitative conversion, we envision that imine exchange can occur through two different pathways. The first involves the primary amine-promoted imine exchange reaction by an associated mechanism; the second involves the water-promoted imine exchange reaction via the reversible formation of aldehyde and amine (i.e., a dissociative mechanism) or activation of imine through hydrogen bonding interaction. To

understand their relative contribution to the imine exchange reaction, kinetic studies of the imine exchange were conducted in the presence of a catalytic amount of primary amine (Scheme 2.3A), water (Scheme 2.3B) or a combination of both (Scheme 2.3C) under identical initial imine concentration ([imine]= 0.136 M, room temperature) (Figure 2.9). We have found that the imine exchange reaches equilibrium rapidly in the presence of propylamine (0.001 eqv. relative to the imine) with a second-order observed rate constant $k_{obs}= 3.18 \times 10^{-3}\ M^{-1}min^{-1}$ in the solvent of AN-d_3 (Figure 2.9A). By contrast, the reaction is much slower in the presence of same equivalence of water. A comparable second-order observed rate constant ($k_{obs}= 5.09 \times 10^{-3}\ M^{-1}min^{-1}$) in AN-$d_3$ was only observed when a significantly larger equivalence of water is present (i.e., 1.2 eqv. of water relative to the imine compound) (Figure 2.9C). This suggests that imine exchange in the AN organic gel is primarily catalyzed by residual unreacted primary amino groups on the PEG chain-ends via an associated mechanism. While water can also mediate the imine exchange equilibrium, the effect of residual water on imine exchange rate is significantly less pronounced in AN under the standard condition (room temperature, $[aldehyde]_0=[amine]_0= 0.37$ M). When water content is high, its effect on the imine network formation becomes more pronounced. For example, no free-standing gel was formed when water was used as the solvent under the standard condition. This is due to the amine-imine equilibrium lying to the side of the starting materials (i.e., amine and aldehyde) when water is the solvent. Consistently, increasing the initial total aldehyde and amine group concentration to 0.90 M has resulted in free-standing hydrogels by shifting the amine-imine equilibrium toward imine formation.

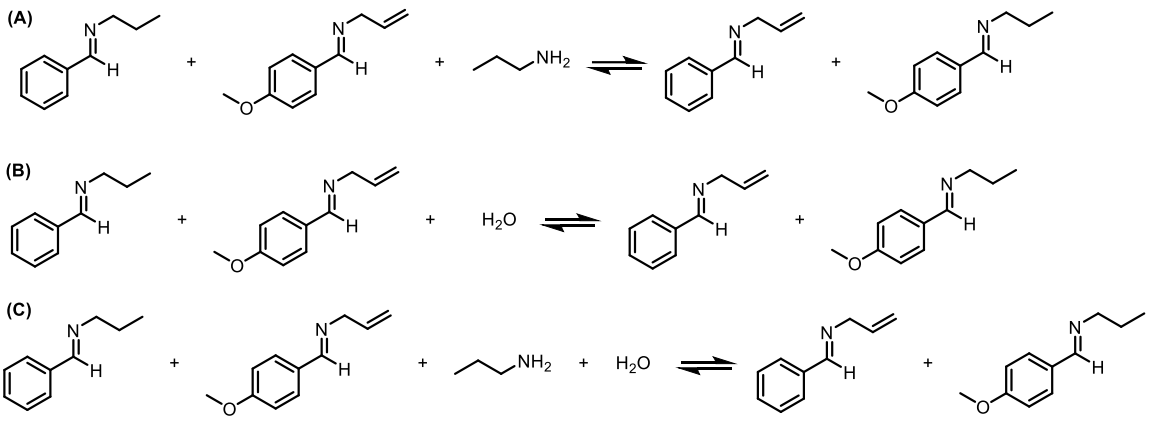

Scheme 2.3. Imine exchange reactions using model imine compounds in the presence of a catalytic amount of primary amine, water or a combination of both in various organic solvents (AN-d_3, DMF-d_7 and TOL-d_8).

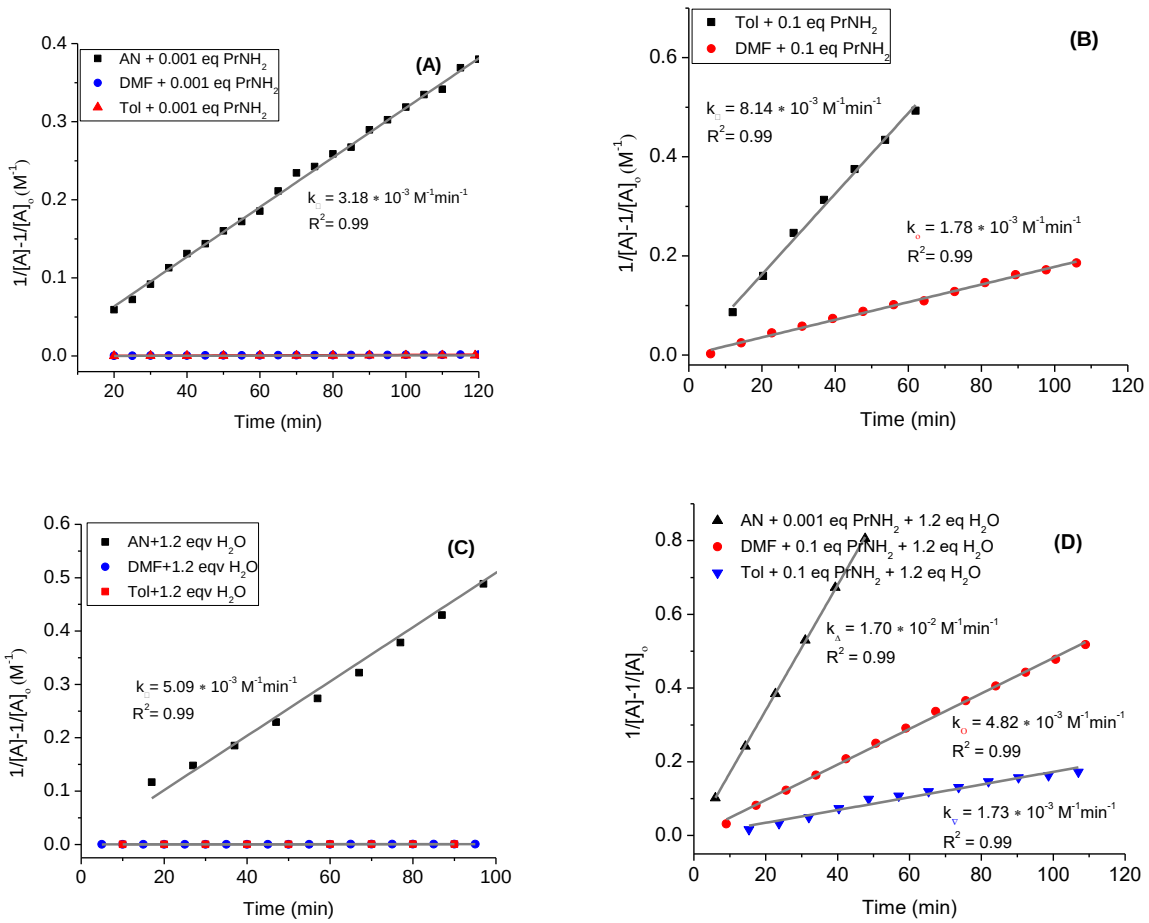

Figure 2.9. Kinetic studies of imine-imine exchange reactions using model imine compounds (Scheme 2.3) in the presence of a catalytic amount of $PrNH_2$, H_2O or a combination of both in various deuterated solvents (AN-d_3, DMF-d_7 and TOL-d_8).

The primary amine-promoted imine exchange rate is also strongly dependent on the solvent. The imine exchange rates in TOL-d_8 and DMF-d_7 are significantly slower than that in AN-d_3 with no appreciable imine exchange observed in the former solvents in the same time frame as the reaction in AN-d_3 in the presence of 0.001 eqv. propylamine relative to the imine (Figure 2.9A). Increasing the primary amine content by a 100-fold accelerates the imine exchange, allowing the relative exchange rate to be determined in TOL-d_8 and DMF-d_7. For example, the second order observed rate constant of imine exchange (k_{obs}) are 8.14×10^{-3} $M^{-1}min^{-1}$ and 1.78×10^{-3} $M^{-1}min^{-1}$ respectively in TOL-d_8 and DMF-d_7 in the presence of 0.1 eqv. propylamine relative to imines under identical experimental conditions (i.e., [imine]= 0.136 M, room temperature) (Figure 2.9B). This indicates that primary amine promoted imine exchange is faster in TOL-d_8 than in DMF-d_7. Considering that water is formed during the condensation polymerization and is expected to accelerate the imine exchange reaction, we further assessed the imine exchange rate using the model compounds in TOL-d_8 and DMF-d_7 in the presence of both primary amine (0.1 eqv. relative to imine) and water (1.2 eqv. relative to imines) (Figure 2.9D). The equivalence of water used in the study was chosen to account for the relative amount of water formed in the condensation polymerization at a quantitative conversion and the water already present in the non-anhydrous DMF solvent (determined by Fisher titration). Indeed, the imine exchange ($k_{obs}= 4.82 \times 10^{-3}$ $M^{-1}min^{-1}$) in DMF-d_7 in the presence of both propylamine and water is faster than that with only propylamine present ($k_{obs}= 1.78 \times 10^{-3}$ $M^{-1}min^{-1}$). Surprisingly, a reverse trend of relative rate was observed for the reactions in TOL-d_8. The reaction with primary amine and water ($k_{obs}= 1.73 \times 10^{-3}$ $M^{-1}min^{-1}$) is slower than that with propylamine alone in TOL-d_8 ($k_{obs}= 8.14 \times 10^{-3}$ $M^{-1}min^{-1}$). This unexpected result is presumably due to the poor miscibility of water with toluene and partial partition of the propylamine into the water phase, thus reducing the effective amount of

propylamine that catalyzes the imine exchange reaction in toluene. These kinetic studies suggest that the imine exchange is the fastest in AN followed by DMF and then TOL in the presence of catalytic primary amine and water. As such, the relative rate of imine exchange in various solvents parallels the solvent dependency of the strain recovery and the stress relaxation characteristics of the polymeric gels, suggesting that the primary amine-promoted imine exchange is the most likely molecular basis for the observed viscoelastic behavior of the polymer gels.

2.2.5 Solvent-promoted self-healing behavior for organogel

Polymer networks containing dynamic covalent linkages are expected to exhibit self-healing characteristics. We assessed the self-healing properties of the polymeric gels comprised of PEG strands and imine cross-linkages by preparing two disc-shaped gels in DMF (Entry 2, Table 2.1) containing 5 wt% fluorescein and rhodamine B dye respectively. The two gel discs were subsequently fractured using a razor blade and put together along the fractured interface using a tweezer (Figure 2.10A). Within 5 min, the gel interface became re-attached so that the resulting gel could sustain its own weight (Figure 2.10B). Within 24 h at room temperature, the gel interface became fully recovered and could be bent and twisted without breaking apart (Figure 2.10C). Notable diffusion of the dyes across the interface (Figure 2.10D) was also observed to occur in 48 h, suggesting the molecular level recovery of the interface. To quantitatively assess the self-healing characteristics of the gel, the re-attached gel disc was subjected to stress-strain measurements in compressive mode at different healing time intervals and compared to the pristine and undamaged gel disc (Figure 2.11A). The stress-strain curve of the re-attached gel became comparable to that of the pristine gel within 30 min. Prolonged healing time to 48 h did not result in any significant change of the compressive stress-strain profile. These results indicate that the fractured gel interface can heal rapidly through dynamic imine bond exchange to fully restore the compressive

properties. By contrast, a control sample of an elastic network without dynamic bonds failed to restore its compressive strength upon being damaged in a similar manner (Figure 2.11B).

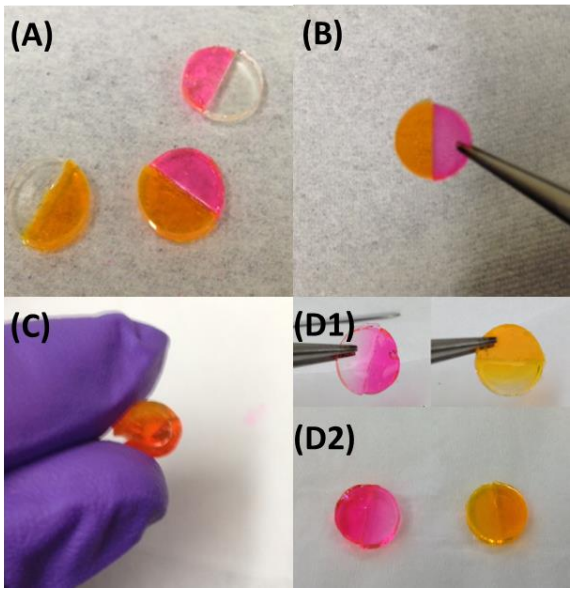

Figure 2.10. (A) Images showing the DMF gels (Entry 4, Table 2.1) containing fluorescein and rhodamine B dyes respectively. (B) The cut interface was healed rapidly by putting the two fracture gel discs together along the interface with a tweezer. (C) The gel could be bent on the healed interface without fracturing after one day. (D1, D2) The fluorescein and rhodamine B dyes were shown to diffuse across the healed interface after one and two days.

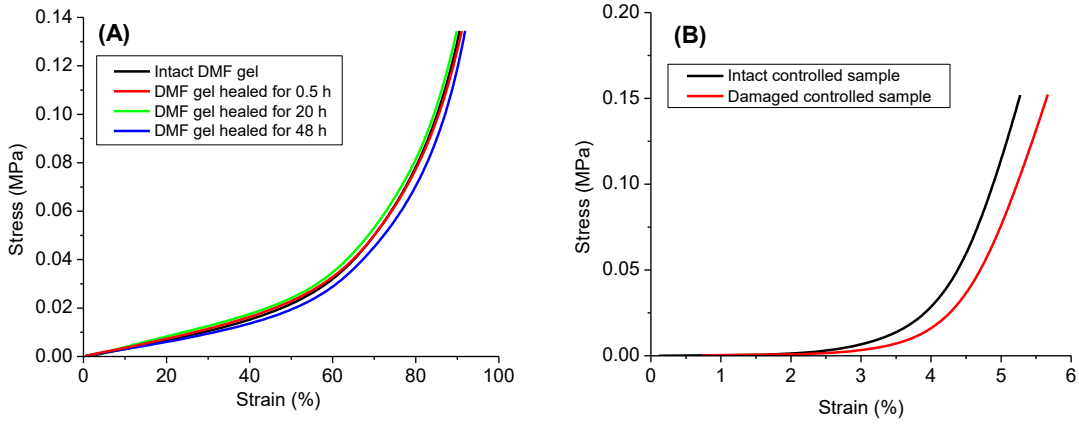

Figure 2.11. (A) The plot of compressive stress versus strain for the intact DMF gel (Entry 4, Table 2.1) and the DMF gels that were cut and allowed to heal for different durations (0.5, 24 and 48 h) by putting the two cut pieces together at the interface with a tweezer. (B) The plot of compressive stress versus strain for the intact control sample which is a polymeric thermoset and the damaged controlled sample after being cut and put together at the cut interface with a tweezer.

2.2.6 Adhesion study

We envision the potential use of the polymer gels as adhesives that can establish chemical bonds with surfaces bearing amine or aldehyde functional groups. For application as adhesives, polymer gels with low volatility and stable composition is important. This prompted us to synthesize a polymer gel comprised of PEG strands (M_n= 1500 g·mol^{-1}) and imine cross-linkers using an ionic liquid ($BMIMPF_6$) (Entry 10, Table 2.1) as the solvent. Two IL gel discs were separately put in contact for one minute with a glass slide where one end bears primary amine functional group on the surface and the other end is pristine glass without any modification (Figure 2.12A). Removal of the polymer gels with a razor blade resulted in the cohesive fracture of the gel attached to the amine-functionalized glass slide, in contrast to a clean removal of the gel attached to the pristine glass slide (Figure 2.12B). This supports the chemical adhesion between the gel and the amine-functionalized glass surface through dynamic imine bond exchange in the former and the physical adhesion in the latter. The remaining materials on modified glass can be easily removed through hydrolysis by soaking in water (Figure 2.13). This study demonstrates the potential use of the IL gels comprised of dynamic imine cross-linkages as adhesives.

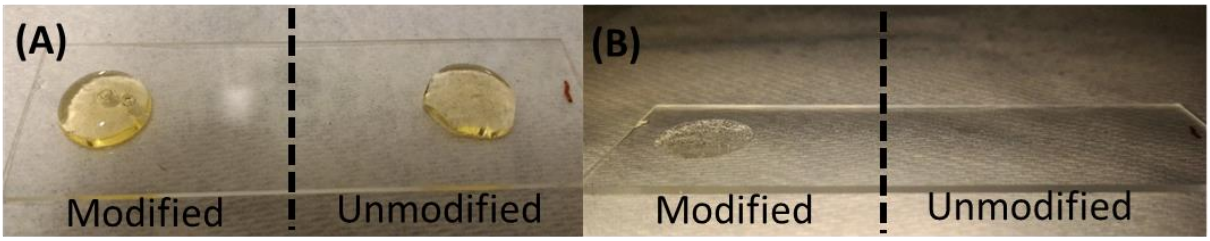

Figure 2.12. Optical images showing that IL gels (Entry 10, Table 2.1) pressed to the glass slide (A. left) using a spatula for 1 min and then detached from the glass (B, left). IL gel on the primary amine-modified glass surface in a cohesive manner upon removal with a spatula, leaving behind residual gel materials that remain covalently attached to the glass surface. This is in contrast to adhesive detachment of the IL gel from the unmodified glass surface (A, right), resulting in a clean removal of the gel from the glass surface (B, right).

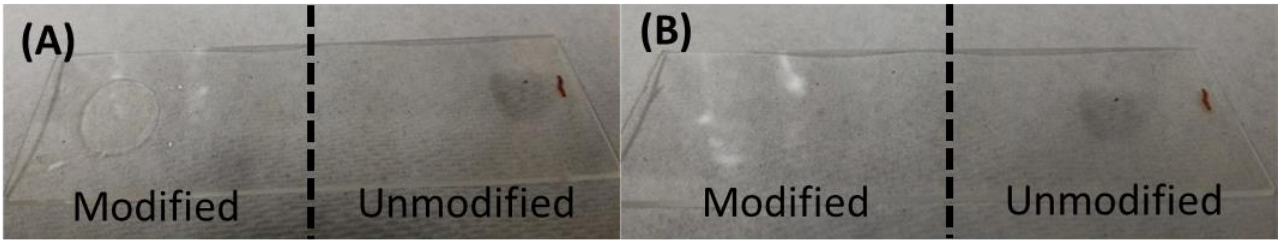

Figure 2.13. Optical images showing that the cohesively fractured IL gel that remains on the glass slide (Entry 10, Table 2.1) can be readily removed by first soaking in water for 10 min (A) and then wiping with a Kimwipe tissue paper (B).

2.2.7 Self-healing behavior for bulk material

A neat polymer network without solvent (Entry 11, Table 2.1) was also prepared by mixing PEG-diamine (M_n=1500 g·mol^{-1}) and aldehyde in the mold at 50 °C and characterized for the self-healing characteristic. As the neat polymer network is semi-crystalline with a melting point at ~40 °C (Figure 2.14), the damaged interface cannot be healed by simply attaching the two fractured interfaces together at room temperature. This is due to the low chain mobility at room temperature, which inhibits the imine bond exchange and hence the network recovery at the molecular level. Heating the fractured interface at 50 °C (above the T_m) for 5 min (Figure 2.15A) while holding them together by tweezer enables the recovery of the interface. The sample retains its dimension during the heating, in contrast to the non-crosslinked PEG-diamine sample which melted into a fluid (Figure 2.16). Furthermore, as we have demonstrated that polar solvents can effectively promote the imine bond exchange, the two fractured neat polymer discs can be reattached by rubbing a small amount of AN solvent at the cut surface (Figure 2.15B), attesting to the self-healing capability of the polymer network. The dynamic covalent polymeric network is also degradable, as evidenced by disappearance of the polymer disc upon being submerged in 50°C water for 4 h due to the hydrolysis of imine linkages (Figure 2.15C). This underscore the environmental appeal of covalent polymeric networks comprised of imine-linkages.

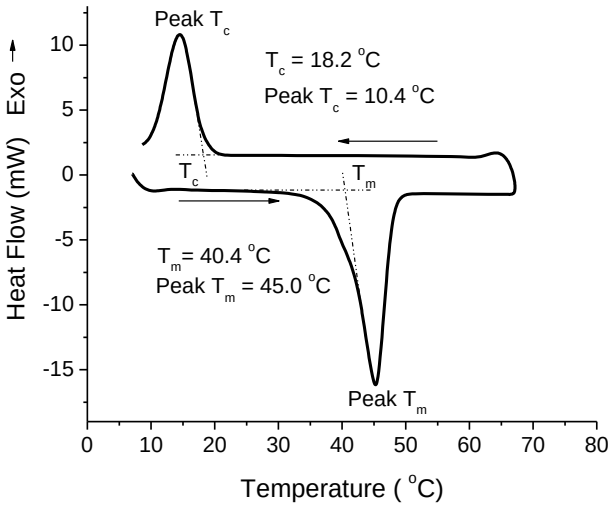

Figure 2.14. DSC analysis of the neat polymeric network comprised of low molecular weight PEG strands (Mn= 1500 g·mol-1) and imine cross-linkers (Entry 11, Table 2.1) showing a broad melting point (Tm) at ~40°C.

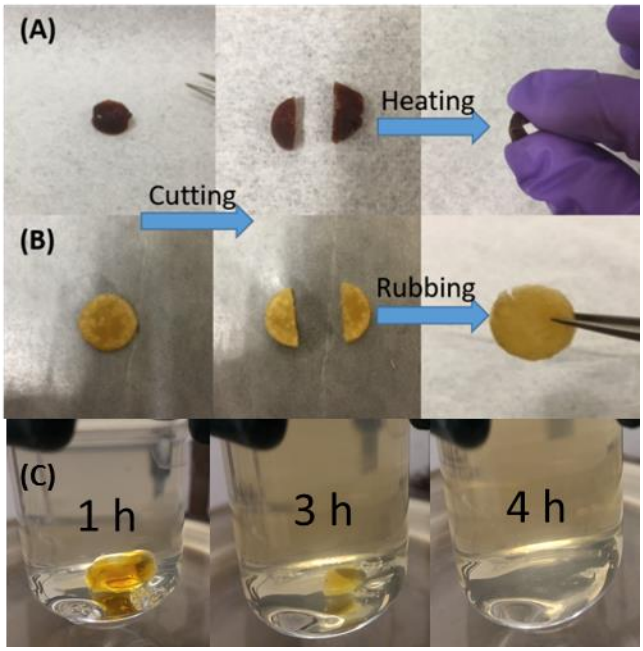

Figure 2.15. (A) Optical images showing that the neat dynamic covalent polymer network comprised of the low molecular PEG strands (Mn= 1500 g·mol-1) and imine cross-linkers can be cut and then healed by attaching two polymer pieces at the freshly cut interface with a tweezer and heating at 50 °C or (B) by rubbing organic solvents (e.g., AN) at the interface at room temperature. (C) The polymer can also be degraded by being submerged in distilled water for 4 h at 50 °C.

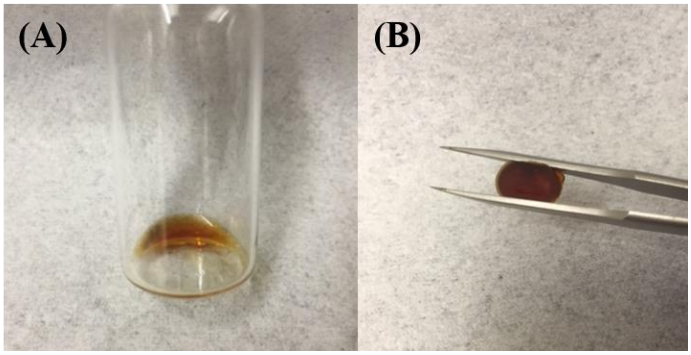

Figure 2.16. Optical images showing the low molecular PEO diamine (Mn= 1500 g·mol^{-1}) itself and the neat polymeric network comprised of the low molecular weight PEG strands (Mn= 1500 g·mol^{-1}) and imine cross-linkers at 50 °C. The former became a free-flowing liquid as expected for a thermoplastic and the latter became rubbery due to the dynamic covalent crosslinking.

2.3. Conclusions

A simple method to access dynamic covalent polymeric networks comprised of imine cross-linkages either in gel form or as bulk material has been demonstrated. The polymer network is malleable and is capable of self-healing without the need of any catalyst present. The malleability depends on the relative rate of dynamic imine bond exchange. It was found that the imine bond exchange is mainly catalyzed by residual dangling primary amine chain ends present in the network. Solvent can modulate the imine bond exchange rate and thus the dynamical properties of the polymer gel networks. For example, the polymeric gel in acetonitrile proves to be more malleable than the analogous toluene gel due to the faster imine bond exchange in the former solvent than the latter. This study provided fundamental insights regarding the molecular and kinetic basis for the macroscopically observed dynamical properties of the polymeric network comprised of imine linkages. The polymeric gel in non-volatile solvents such as ionic liquid has potential uses as adhesives to covalently bond to surfaces bearing primary amine or aldehyde functional groups. Due to the reversibility of imine bond formation, the polymer network can also be degraded in water, enhancing its environmental appeal.

2.4. Experimental information

2.4.1 General considerations

All chemicals used in the study were purchased from Sigma-Aldrich except for the PEG diamine (Mn=1,000 g·mol-1) which was purchased from Laysan Bio Inc. Model imine compounds (i.e., (E)-N-benzylidenepropan-1-amine and (E)-N-benzylideneprop-2-en-1-amine) were prepared by literature procedures[63] and distilled and stored under nitrogen before being used in the kinetic studies. The control sample is a thiolacrylate thermoset derived from trimethylolpropane tris(3-mercaptopropianate) and trimethylolpropane triacrylate in the presence of a catalytic amount of tertiary amine by a literature procedure.[64] The aluminum molding plate (each mold is d= 10 mm, h= 3 mm) was made by LSU mechanical shop. Deuterated acetonitrile and toluene were dried with calcium hydride and freeze pump thawed (3x) followed by vacuum transfer. Deuterated DMF was dried with sodium hydride for 1 h in the glove box and filtered before use.

2.4.2 Preparation of monomer and organogels

1,3,5-Triformylbenzene (trialdehyde, Scheme 2.4) was synthesized following a published procedure.[65] ^{1}H-NMR spectra of trialdehyde monomer were shown in Figure 2.17-2.18. Cross-linked polymeric gels were prepared by dissolving the PEO diamine (M_n= 1,000, 1,500, 3,000 g·mol^{-1}) in various solvents with slight heating and then allowing the solution to cool down to room temperature before addition of the trialdehyde. A representative procedure is given as follows. PEO diamine (100 mg, 0.067 mmol, M_n=1,500 g·mol^{-1}) was dissolved in DMF (370 μL) followed by adding trialdehyde (7.2 mg, 0.044 mmol) to make $[amine]_0=[aldehyde]_0$= 0.37 M solution. After the solution became homogeneous, it was transferred to an aluminium mold slowly using a pipette to minimize air bubble formation. The mold was covered with two microscope slides at the top and

bottom. The mixtures were allowed to stand in the mold at room temperature for 4 h. Dyed organogels were prepared under the same conditions except that a DMF solution containing 5 wt % fluorescein or rhodamine B was used as the solvent. Neat polymer network samples were also made in a similar manner except that the monomers were mixed in an aluminium mold that was preheated at 50 °C.

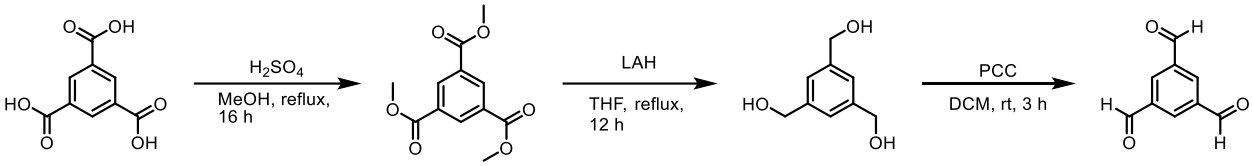

Scheme 2.4. Synthesis of trialdehyde

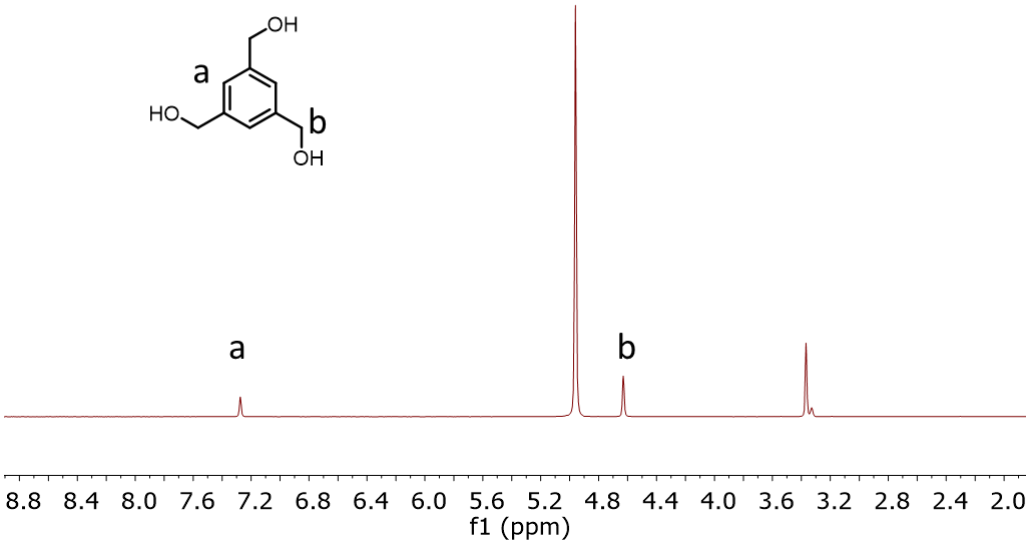

Figure 2.17. ^{1}H-NMR spectrum of triol in CD_3OD

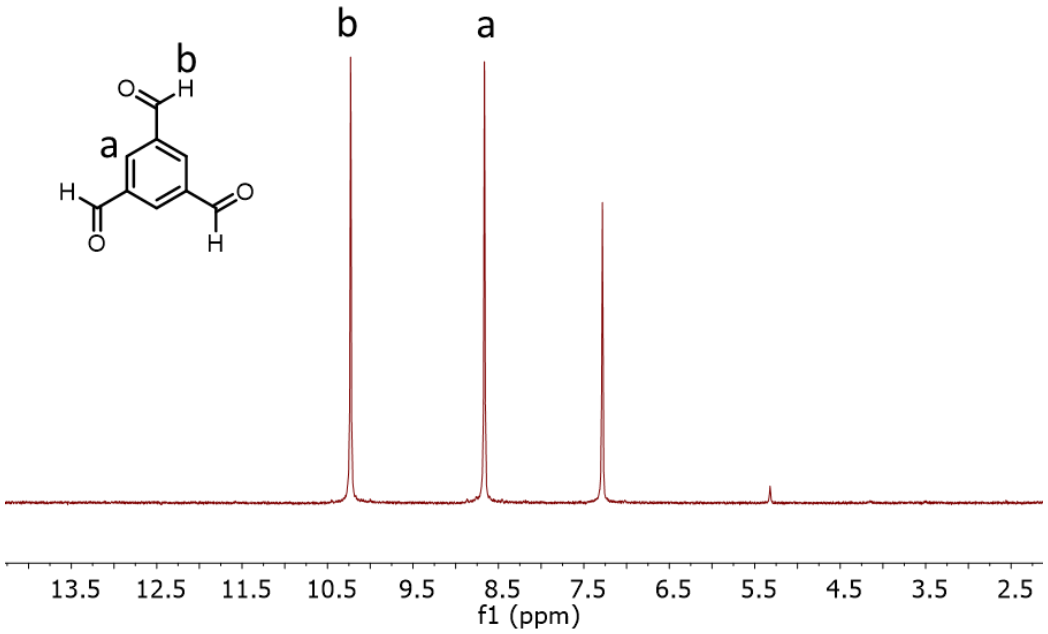

Figure 2.18. ^{1}H-NMR spectrum of trialdehyde in $CDCl_3$.

2.4.3 IR spectroscopy measurement

Imine conversion was measured by monitoring the disappearance of the aldehyde over time using ATR-FTIR spectrometer (Bruker Alpha). FTIR spectrum of the trialdehyde solution (0.12 M) without PEO diamine was measured as reference. After 4 h, FTIR spectrum of the organogel was measured again. The imine conversion was determined by the ratio of unreacted aldehyde to the initial aldehyde peak intensity.

2.4.4 Rheological measurements

In situ sol-to-gel transitions for the condensation polymerization was monitored using a TA instrument AR 1000 Rheometer with a parallel-plate geometry (50 mm diameter and a fixed 300 µm gap) at 1 Hz frequency at 20 °C. From oscillatory shear measurements the storage modulus G', the loss modulus G'' and delta degree can be determined. The condensation polymerization mixture (1 mL) was loaded into the rheometer and covered

with a round plastic lid to minimize solvent evaporation. Each experiment was stopped until delta degree reached to 40°.

2.4.5 Dynamic mechanical analysis (DMA)

Strain relaxation (creep) and stress relaxation experiments were performed using TA instruments DMA Q800 under uniaxial compression mode. A couple drops of tetradecane were added onto the compressive parallel plates to reduce friction and adhesion between the plate and the gel disc. Strain relaxation measurements of the polymer gels were conducted at a constant stress 0.01 MPa with a preload force 0.001 N for 5 min followed by load-free strain recovery for 5 min. Stress relaxation experiments were conducted with a 10% strain in compression mode with a preload force 0.001 N for 5 min. Deformation of the gels is described in terms of percentage strain recovery that was calculated by ($\sigma_{initial}$ - σ_{final})/ $\sigma_{initial}$. A triplicate of each polymeric gel was subjected to the same measurement for both strain and stress relaxation tests to get the mean result.

2.4.6 Kinetics studies of imine bond exchange

^{1}H NMR spectra were recorded on a Bruker AV-400 spectrometer, and the chemical shifts in parts per million (ppm) were referenced relative to AN-d_3, DMF-d_7, or TOL-d_8. 1,3,5-Trimethoxybenzene was used as internal standard for the kinetic study. A representative procedure for the kinetic study is given as follows. Inside the glovebox, (E)-N-benzylidenepropan-1-amine (10 mg, 0.07 mmol), (E)-N-(4-methoxybenzylidene)prop-2-en-1-amine (12 mg, 0.07 mmol) and 1,3,5-trimethoxybenzene (11.4 mg, 0.07 mmol) were dissolved in deuterated acetonitrile (AN-d_3, 0.49 mL) in a dried vial. The mixture was then transferred into a J. Young NMR tube followed by the addition of the AN-d_3 stock solution of $PrNH_2$ (10 μL, 6.8 mM, 0.001 eqv. relative to the total imine content) at room

temperature. ^{1}H NMR spectra were collected immediately after the preparation of the reaction mixture. Each spectrum was collected with 8 scans and 2 s relaxation time at room temperature. All kinetic experiments were repeated twice to get the mean reaction rate.

2.4.7 Differential scanning calorimetry (DSC)

DSC analysis of the neat polymer network was conducted using a TA DSC 2920 instrument. The polymer (8.2 mg) was hermetically sealed in a standard aluminium pan. An empty pan was used as reference. The sample was kept at 10 °C for 2 min and then heated to 65 °C at 5 °C·min^{-1}. It was held at 65°C for another 2 min before being cooled back down to 10 °C at the same rate. The heating and cooling cycles were repeated 3 times. Heat flow was recorded during the heating and cooling cycles and normalized by the sample mass.

2.4.8 Characterization of self-healing properties

Gel disc samples were cut with a razor blade and the half discs were re-attached at the cut-interface using a tweezer for 0.5, 20 and 48 h respectively at room temperature. These samples were then subjected to compressive strain-stress measurement using TA instruments DMA Q800 with the compressive force increasing in the 3 N - 18 N range. A triplicate of the healed gel sample, the intact gel sample and the control sample were measured.

2.4.9 Adhesion study

A microscope glass slide was modified with amino functional groups by submerging one end of the glass slide in a toluene solution of (3-Aminopropyl)-triethoxysilane (0.1 %, v/v) at room temperature for 5 h followed by rinsing with toluene and drying in air. Two IL gels (Entry 10, Table 2.1) were individually placed for one minute on each end of a glass

slide that has been either functionalized with primary amine group or unmodified, and then the gels were scraped with a spatula to reveal whether adhesive or cohesive damage would occur.

Chapter 3 : Investigation of the Dynamic Aminal Bond Exchange towards the Design and Synthesis of Polyaminal Networks

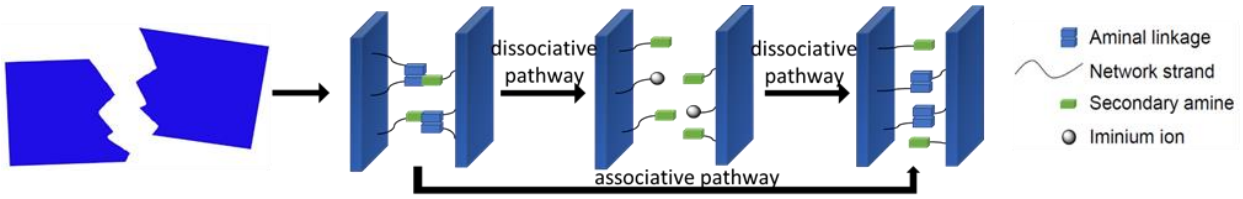

3.1. Introduction

Previously our group has synthesized polyimine organogels that had variable malleabilities in different solvents.[1] We had demonstrated that the rate of imine exchange is dependent on the solvent polarity, which in turn dictates the macroscopic stress-relaxation behavior of the gel networks. While a transimination reaction has been exploited in the design of CANs,[2-5] only limited research has been reported on transaminalation.[66] Aminal exchange facilitated by hydrolysis and condensation reactions have been previously reported.[67] The aminal exchange can also proceed in organic media presumably by forming iminium ions in the presence of a trace amount of protic impurities.[68] Several papers have documented the use of hemiaminal as cross linkers in the design of CANs.[66] In 2014, Garcia et al. developed recyclable poly(hexahydrotriazine) (PHT) through the condensation of paraformaldehyde and diamines.[66a] Triazine can promptly undergo an exchange reaction with water to form hemiaminal (Table 1.1). Modulus can be tuned by the equivalence of paraformaldehyde used in the polymerization. For example, 5 equiv. of paraformaldehyde exhibited a T_g of 125 °C and modulus of 6.3 GPa while 2.5 equiv. of paraformaldehyde exhibited a T_g of 193 °C and modulus 14 GPa. Moreover, the PEGylated diamine was used to make organogels. These aminal materials have high moduli and are resistant to bases, oxidants and solvent. Moreover, they are recyclable via depolymerization in acidic conditions (pH < 2) or neutral water after 24 h. Fox et al. have developed CANs organogels

by a similar chemistry, using PEG diamine and paraformaldehyde to synthesize 1,3,5-triazine polymers. The healing process of organogels was characterized by compression testing over time.

Both exchange mechanisms from the previous studies are based on hydrolysis and condensation. There is an obvious research gap on CANs based on aminal exchange especially with no water present. Considering the wide range of aldehydes and amines that are readily available, investigation of CANs that are comprised of aminal linkages is warranted and will lead to new thermoset materials with tunable molecular characteristics, mechanical and dynamical behaviors. In this chapter, I investigate the synthesis and characterization of polymer networks comprised of dynamic aminal bonds. The network was synthesized by simple condensation reactions of multifunctional aldehydes and secondary amines. The thermal, mechanical and stress-relaxation properties of the polyaminal network were characterized. The elastomeric polyaminal networks can be recycled and reprocessed with heating without compromising the mechanical properties. The thermodynamics of the aminal formation and transaminalation reactions have been investigated using model compounds. The transaminalation was shown to occur by a dissociative mechanism.

3.2. Preliminary design and results

To gain more knowledge of the mechanism of transaminalation, it is important to understand the relationship within the dynamical properties of molecular compounds and structural effect on the exchange process. The reversibility and structural tunability of the secondary amine-derived aminal bonds (Scheme 3.1) are highly attractive for the design and synthesis of CANs. We can manipulate the material properties by changing the electronic properties of an aldehyde through different substituents on benzene.

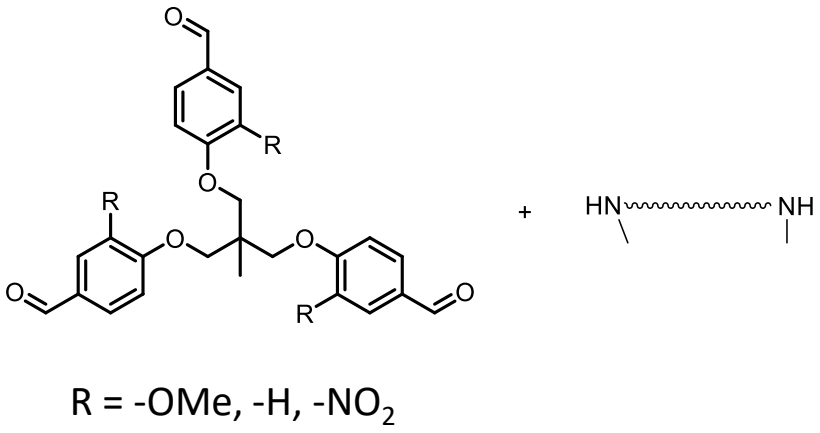

Scheme 3.1. General design and synthesis of cross-linked polyaminals: trialdehyde containing different R groups and a difunctional secondary amine.

The mechanism of aminal exchange will affect the overall properties (i.e., creep and stress relaxation) of a material. Hence, I investigated the molecular mechanism of dynamic aminal bond exchange in organic media without water and under conditions that are pertinent to the environment in the polymer solid. Understanding whether the aminal bond exchange in organic media occurs by an associative or dissociative mechanism without water and the role of water affects the exchange process, as it has significant bearing on the macroscopic dynamical behaviors (i.e., stress-relaxation behavior) of the polyaminal thermosets. The aminal model compound was synthesized from the condensation of benzaldehyde with two equiv. of secondary amines (Figure 3.1, left). During aminal formation, the solution became increasingly opaque as the reaction progressed due to the water phase separated out from the reaction. The consumption of benzaldehyde was monitored by FT-IR spectroscopy over the course of the reaction (Figure 3.1, right).

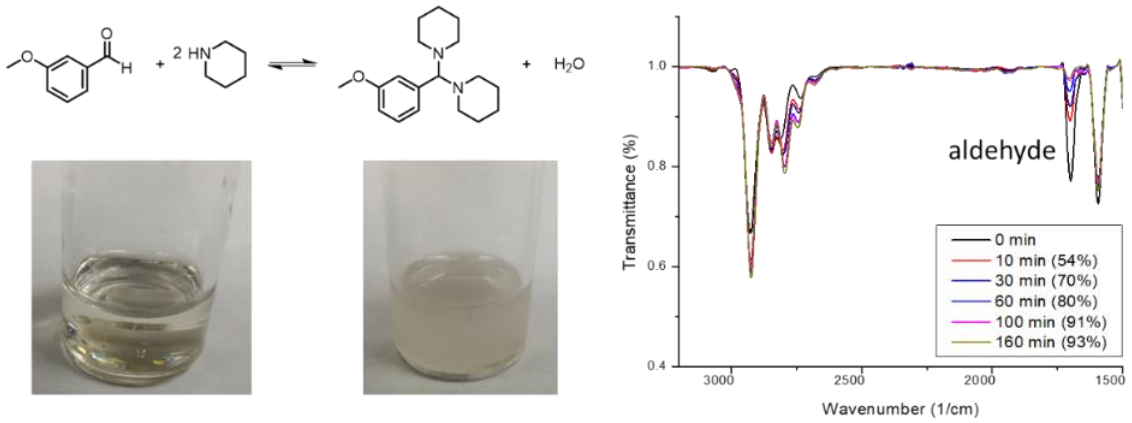

Figure 3.1. Synthesis of an aminal model compound by a condensation reaction (left). FT-IR spectroscopy monitored from time 0 to 160 min (right).

To further understand the molecular electron density effect on the formation of aminals, I compared the kinetic of aminal formation with two different aldehydes containing a nitro or hydrogen group with piperidine (Figure 3.2, left). As expected, nitro-benzaldehyde reacted much faster than the benzaldehyde with a non-electron withdrawing group. The result can be explained by the inductive effect on the aromatic ring. This means we expect to observe shorter gelation time when electron deficient trialdehydes are used to react with difunctional secondary amines. Moreover, exchange reactions with morpholine were slower for an aminal model compound containing nitro rather than a hydrogen group (Figure 3.2, right). The result of slower exchange will produce a higher T_v material.

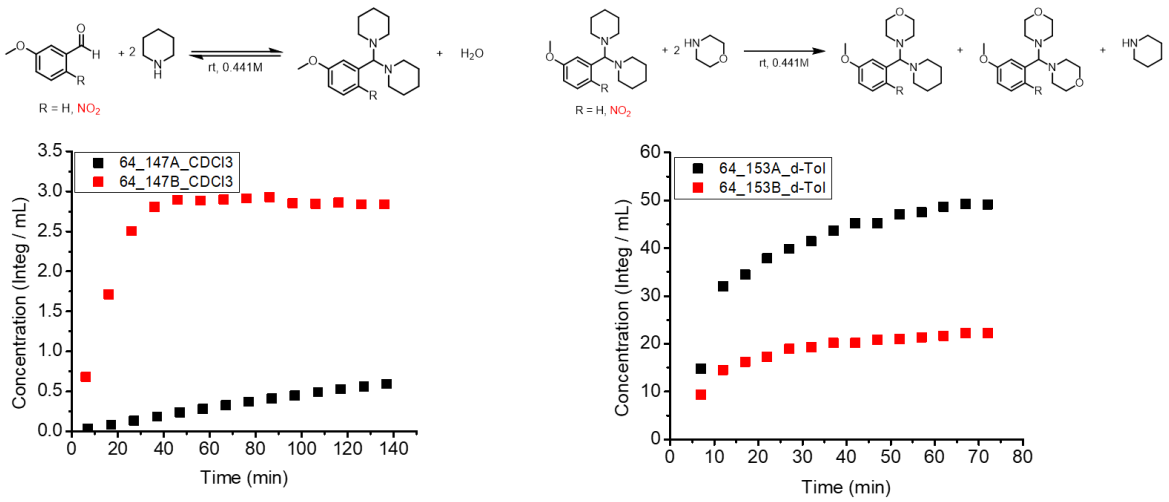

Figure 3.2. The formation of aminals was monitored using ^{1}H-NMR spectroscopies with two types of aldehydes with inherent different electronic properties (left) and an exchange reaction with morpholine (right).

Next, we mixed the two animal model compounds under the following four controlled conditions (Figure 3.3): (1) in anhydrous toluene-D_8; (2) in anhydrous toluene-D_8 with controlled piperidine concentration (0.1 molar equiv. relative to $[aminal]_0$); (3) in anhydrous toluene-D_8 with controlled piperidine concentration (2 molar equiv. relative to $[aminal]_0$); (4) in anhydrous toluene-D_8 with controlled TFA (0.1 molar equiv. relative to $[aminal]_0$). The progression of the transaminalation was monitored by ^{1}H-NMR spectroscopy at room temperature. It is clear from the plots of conversion versus reaction time that acid dramatically accelerates the aminal exchange reaction, while the base decelerates the exchange reaction rate. In the presence of a higher equiv. of base, the exchange reaction was completely suppressed (Figure 3.3). These results are consistent with the aminal exchange reaction occurring by a dissociative pathway where iminium ion is produced as an intermediate followed by the addition of another secondary amine to yield new aminal linkages.

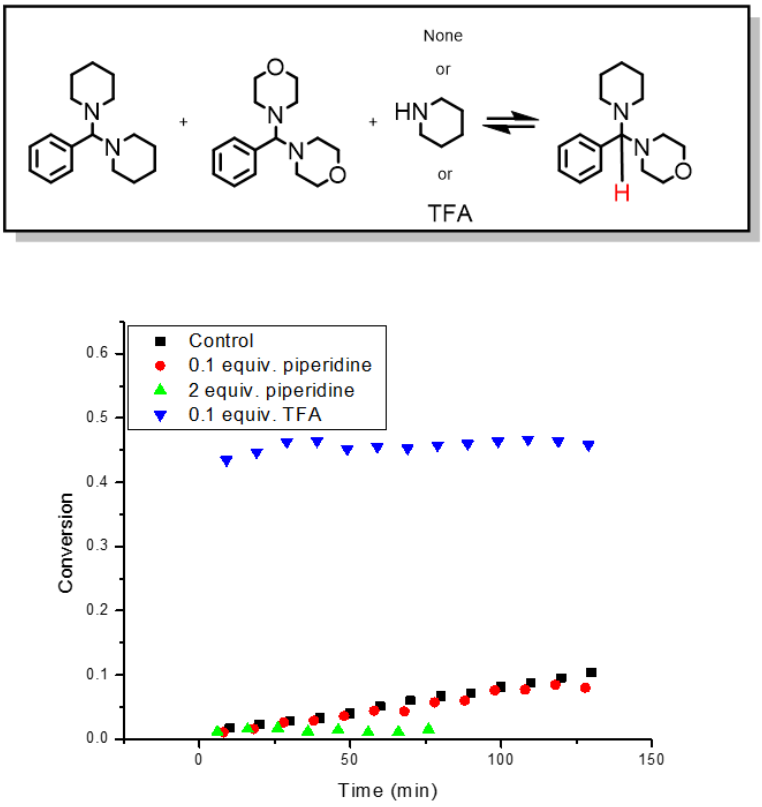

Figure 3.3. Plots of conversion versus reaction time for the aminal exchange reactions under different conditions. ^{1}H-NMR showed compound 3 formation at room temperature in TOL-d_8. The initial concentrations of compound 1 and 2 are both kept at 0.16 M.

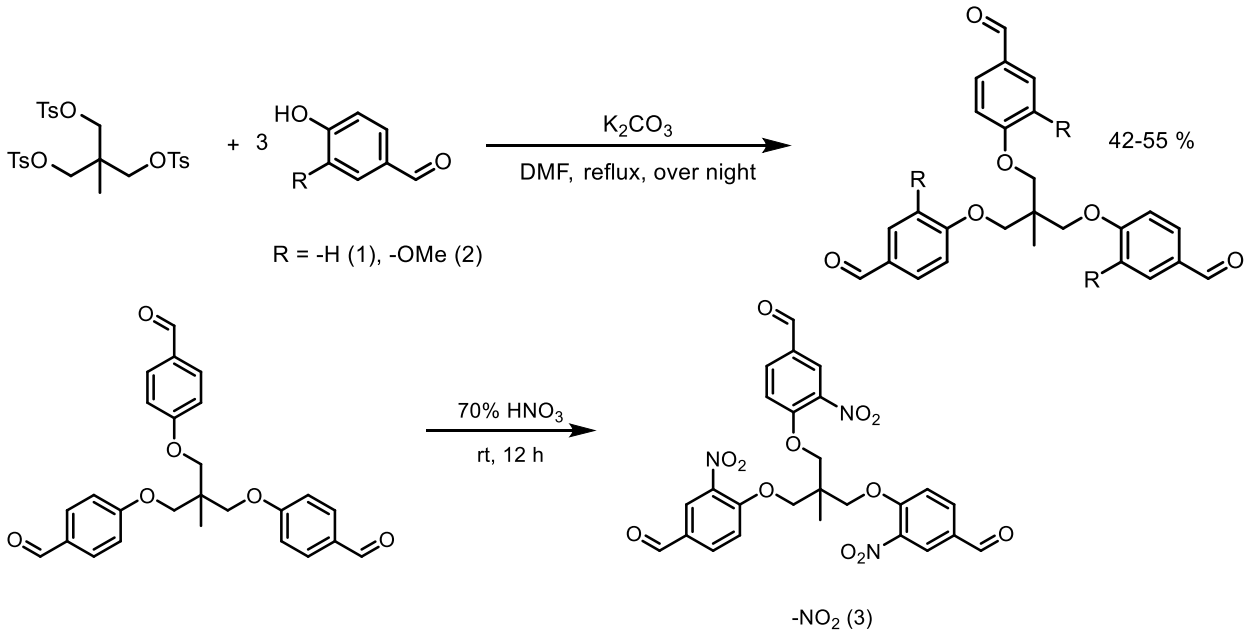

Scheme 3.2. Synthetic route to prepare trialdehyde.

Monomer 4 and 5 in Scheme 3.2 were made from tritosylate to react with 4-hydroxybenzaldehyde containing different R groups.[52b] Monomer 5 was synthesized directly from monomer 4 in 70 % HNO_3 (Scheme 3.2). I initially attempted condensation polymerization of trialdehyde (**4**) and piperazine in 1:3 molar ratio in neat monomer melts. The melting point of trialdehyde (**4**) is 105-109 °C. Piperazine starts to sublime at ~70 °C, thus, polymerization at 105°C in monomer melts resulted in a change of monomer stoichiometry, as piperazine crystals are evident on the top of the reaction flask. This method was discarded due to the difficulty in controlling the proper stoichiometry of the reaction mixture.

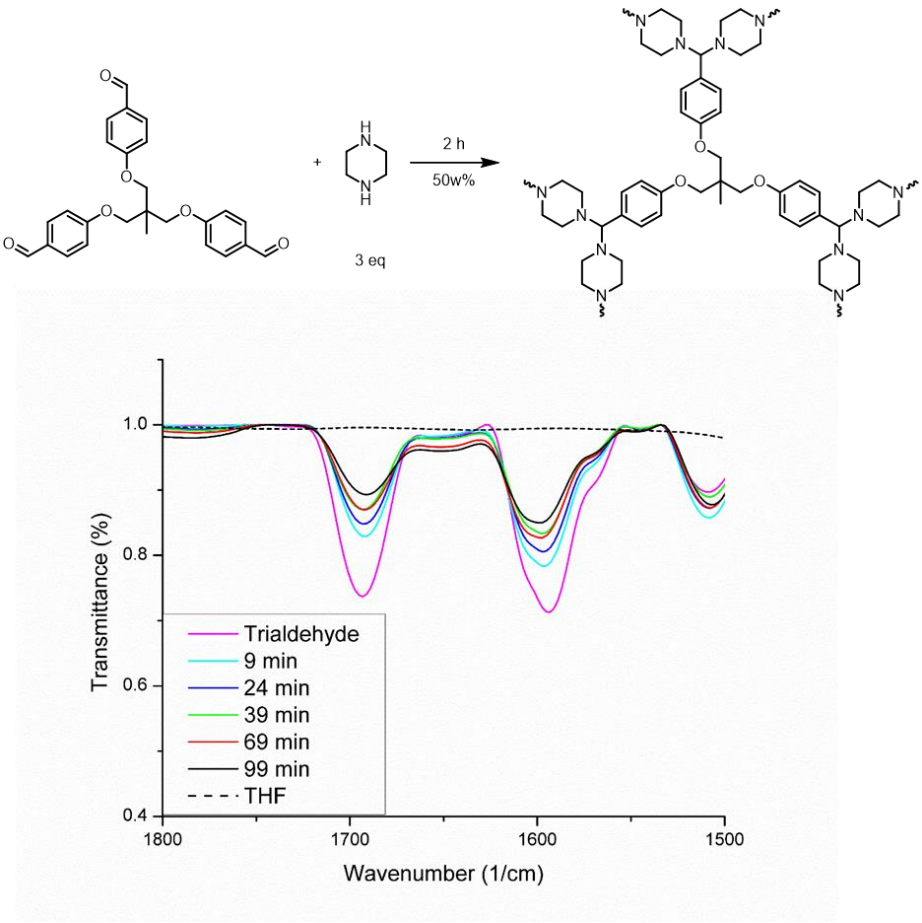

Figure 3.4. Synthesis of cross-linked polyaminal with trialdehyde (1) and piperazine (top); and FT-IR spectra of the polymerization mixture during the course of the reaction at room temperature.

I then investigated the polymerization in solution phase, i.e., THF (50 wt %) at room temperature using trialdehyde (**4**) and piperazine at a 1:3 molar ratio. Polymerization progression was monitored by FT-IR spectroscopy (Figure 3.4), and the reduction of aldehyde peak intensity was evident over time. Spectra collected after ~99 min were incompatible for systematic comparison with the previous measurement, mainly because polymer precipitated out from the THF, resulting in a baseline off the chart and a change of concentration. The material was very stiff and difficult to be removed from the vial. In order to facilitate the characterization of the resulting polyaminal network, an efficient recovery of the resulting polymers is important. So, I attempted to make a softer polyaminal network by using an oligomeric ethylene glycol derived dipiperazine (Scheme 3.3) in the condensation reaction.

The polymerization was conducted by mixing trialdehyde (**4**) and the oligomeric ethylene glycol derived dipiperazine in a 1:3 molar ratio in toluene (Note: Do not heat the reaction, this will give incomplete gelation; sonicate the solution if necessary, Figure 3.5). The aminal conversion was monitored by the decrease of the aldehyde peak over time by FT-IR spectroscopy. In ~2 h, the toluene solution became a standing gel (Figure 3.6, left). The volatile (toluene, H_2O) was subsequently removed at 60 °C under vacuum. The resulting polymer can swell when submerged in toluene for 10 min, evidenced by an increase of sample length from 6 to 7 cm (Figure 3.6, right). However, prolonged soaking in toluene resulted in the disappearance of the gel network, suggesting the depolymerization of the network occurred in diluted toluene solution.

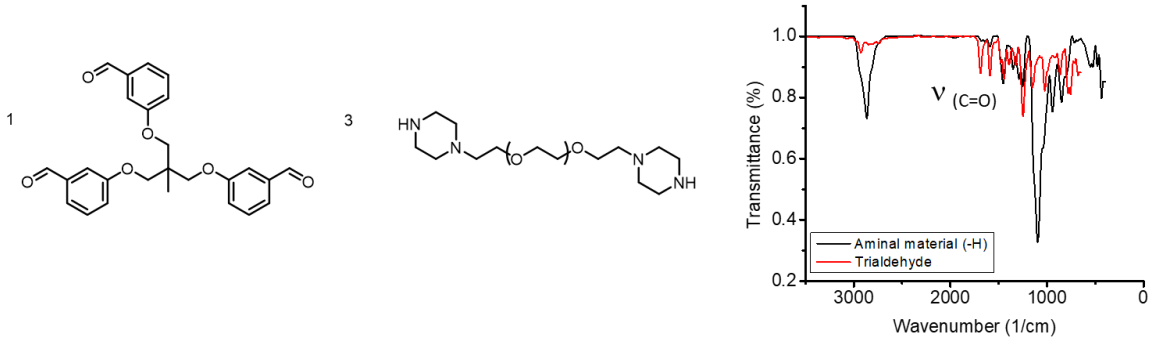

Figure 3.5. Synthesis of cross-linked polyaminal based on trialdehyde (**4**) and PEG dipiperazine (left). FT-IR showed the consumption of the aldehyde peak (right).

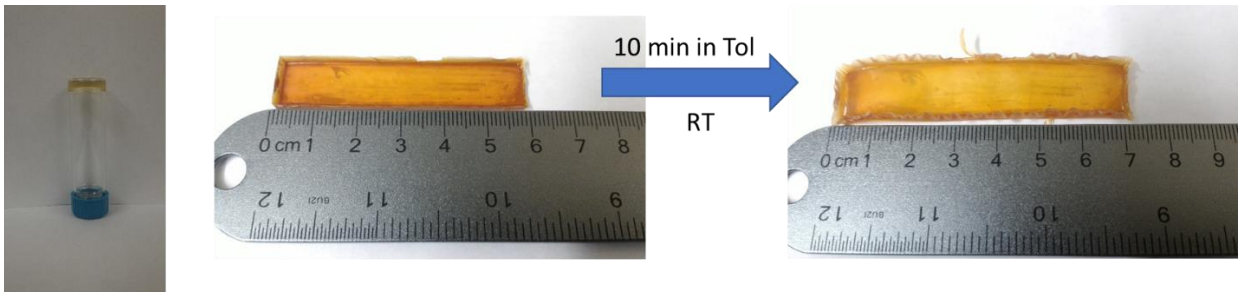

Figure 3.6. Photo of cross-linked gel, after 2 h of polymerization (left). Swelling experiment in toluene at room temperature (right).

These preliminary studies have shown the possibility of synthesizing cross-linked polyaminal by condensation of trialdehyde and a difunctional secondary amine. Aminal exchange reaction appears to occur by a dissociative mechanism with/without H_2O rather than an associative mechanism according to the kinetic study using model compounds. The relative rate of aminal exchange can also be adjusted by changing the electronic properties of the aldehyde. To enable the large-scale synthesis of polyaminals for different applications, I decided to focus my effort on polyaminal synthesis using commercially available and inexpensive monomers. Thus, I set out to investigate the synthesis of polyaminal polymers using formaldehyde and secondary amines.

3.3. Results and discussion

3.3.1 Choice of monomers to synthesize polyaminal polymers

In order to form cross-linked polyaminals, there should be sufficient thermodynamic driving force for aminal bond formation under mild conditions using appropriate monomers with few side reactions. Therefore, I initially screened various secondary amines for their reactivity toward condensation with formaldehyde. Aminal model compounds were obtained by the condensation of 2 equiv. of monofunctional secondary amine with 1 equiv. of formaldehyde as shown in Figure 3.7a. According to ^{1}H-NMR spectral analysis (Figure 3.7b), a mixture of aminal and ether linkages were observed. The N-butylmethylamine aminal compound had an equilibrium constant of 1.7×10^{4} M^{-1} (K_{eq}, a representative experiment shown in Figure S3.9) at room temperature and is comparable with previously reported ($1 \times 10^{3} - 1 \times 10^{4}$) for the cyclic aminal compounds obtained from the condensation of benzyladehyde and primary diamine.[67d] The side chains of secondary amine affected the ratio of aminal to ether linkage as shown in Table 3.1. The most sterically hindered secondary amine, diisopropylamine failed to react with formaldehyde under the experimental conditions. The reactivity of these secondary amines suggests that the steric effect plays a key role in aminal formation. Amines with less steric hinderance are ideal building blocks for making aminal linkages.

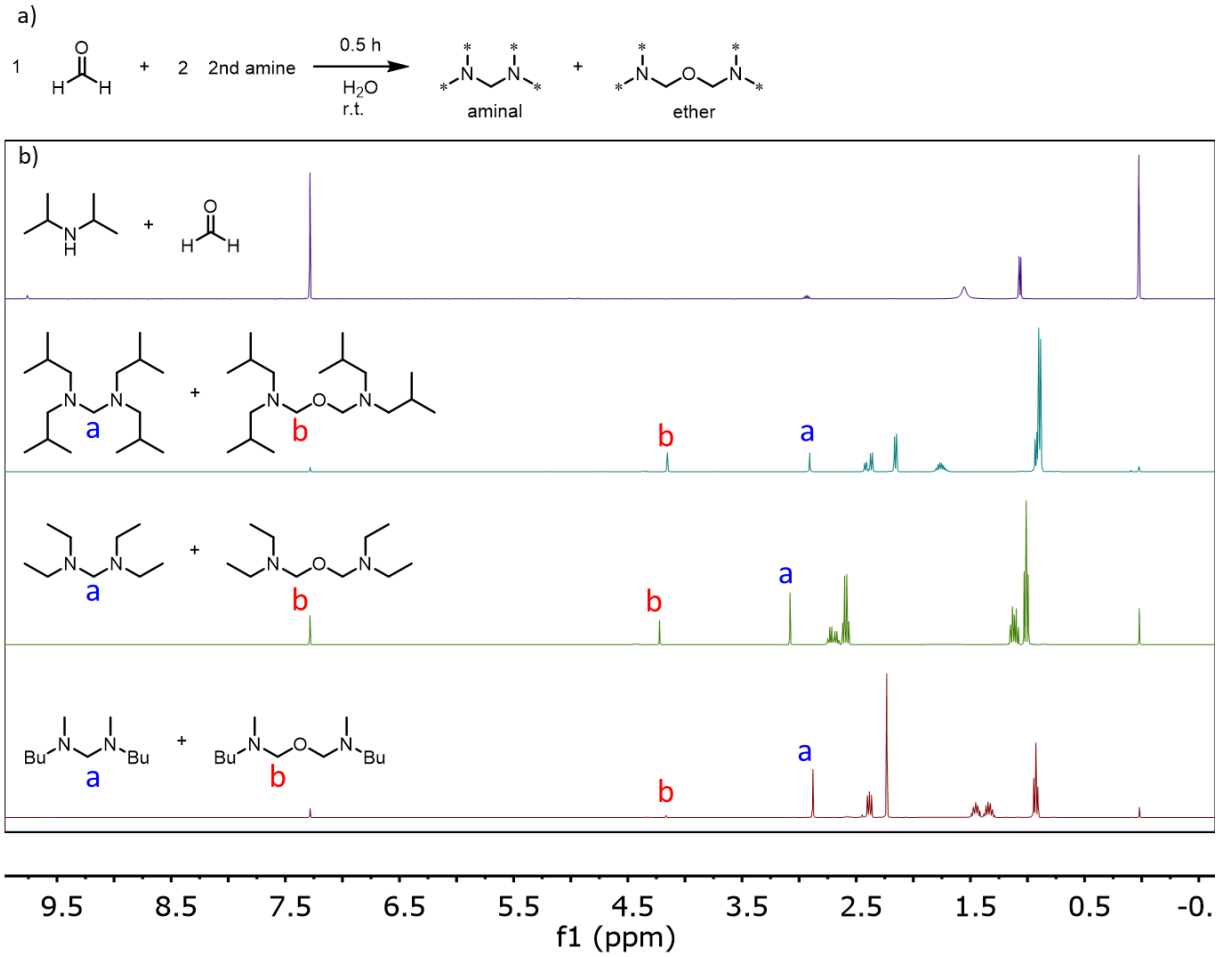

Figure 3.7. (a) Reaction of mono-functional secondary amines with formaldehyde. (b) ^{1}H-NMR spectra showing products contained aminal and ether linkages except purple spectrum (no reaction). All ^{1}H-NMR spectra were collected in chloroform-d_1.

Table 3.1. Comparison of different secondary amine reactivity toward formaldehyde and the ratio of aminal to ether linkage according to ^{1}H-NMR analysis.

2nd Amine	Aminal to ether ratio	Total yield
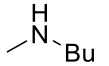	47.5/1	71 %
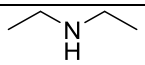	4/1	76 %
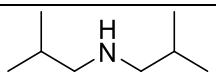	2/1	74 %
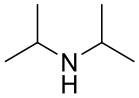	n/a	no reaction

3.3.2 Synthesis of polyaminal

Linear polyaminal was synthesized by a condensation reaction of N,N′-Dimethyl-1,6-hexanediamine (DA) and paraformaldehyde (Scheme 3.3). According to ^{1}H-NMR (Figure 3.8a) and MALDI-TOF Mass Spectrometry (Figure 3.8b), both linear and cyclic polyaminals were present. The chemical shift of d and c from DA shifted upfield after polymerization. Moreover, a new CH_2 group was formed between two nitrogens in polyaminals as shown at peak e. A side reaction produced a small amount of ether linkages (peak f). Every ether linkage produced 20 aminal linkages determined by the ratio of peaks e and f. The molecular weight of the polymer was about 1,500 g/mol with an average degree of polymerization 10 according to end-group (d') analysis. This low molecular weight could be due to the polymerizations conducted without removing water.

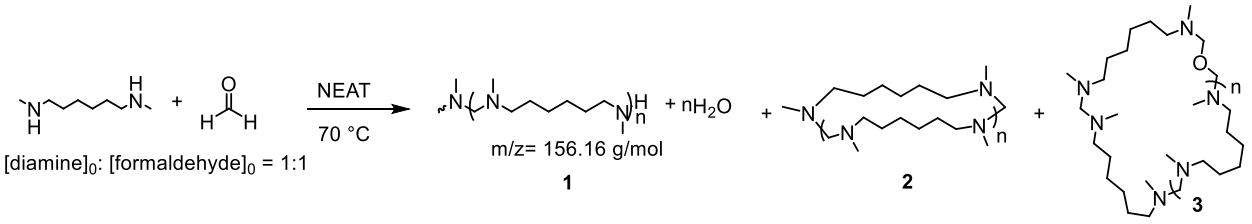

Scheme 3.3. Synthesis of non-crosslinked polyaminals using formaldehyde and N,N′-Dimethyl-1,6-hexanediamine in a 1:1 molar ratio.

In addition to ^{1}H-NMR analysis, the MALDI-TOF mass spectrum indicated the repeating unit of polyaminal was 156.198 g/mol. This value matches with the theoretical value of 156.16 g/mol for the expected aminal linkage. Both linear and cyclic polyaminals (**1**, **2**) with different cations (H^+, Na^+, K^+) were observed. In addition, minor species corresponding to the cyclic polyaminals with an occasional ether linkage (**3**) were also seen in the MS spectrum. These experiments are direct evidence for the formation of an aminal linkage using multifunctional reactants and set the stage for the synthesis of cross-linked polyaminals.

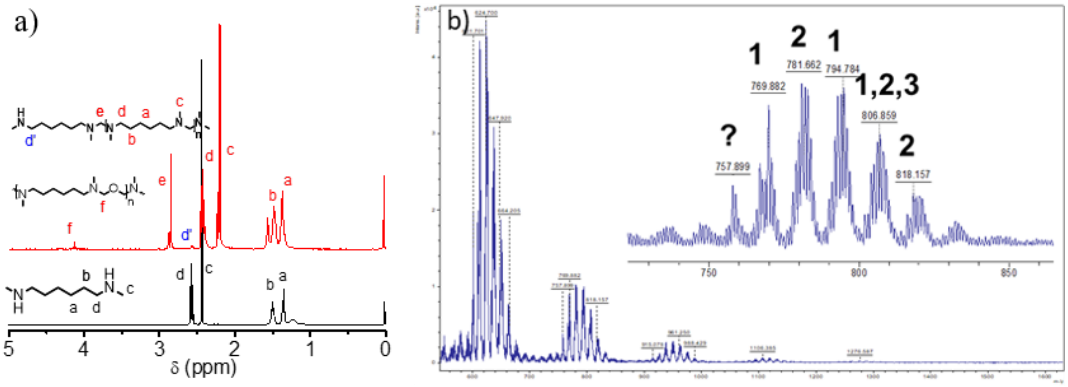

Figure 3.8. (a) Stacked ^{1}H-NMR spectra of monomer (black) and non-crosslinked polyaminal (red) (b) MALDI-TOF MS spectrum of non-crosslinked polyaminal. Note, linear polyaminal: 769.8 m/z (H^+), 791.8 m/z (Na^+), 807.7 m/z (K^+); Cyclic polyaminal: 781.8 m/z (H+), 803.8 m/z (Na^+), 819.8 m/z (K^+).

By mixing varying amounts of tri-functional monomer, triamine (TA) into the mixture of paraformaldehyde and DA, cross-linked polyaminal polymers were obtained (Scheme 3.4). Triamine was synthesized as previously reported with minor modification.[69] The molar ratio of functional groups, i.e., amine and aldehyde, were kept equivalent in all reactions in order to reach high conversion. The cross-linking density in the network can be tuned by changing the molar ratio of TA and DA (Table 3.2).[70] Formulation of 20 to 100 mol % of TA relative to DA varied the theoretical cross-linking density from 0.40×10^{-5} to 2.2×10^{-5} mol mL^{-1}. This systematic variation of the cross-linker content will allow for adjustment of glass transition and mechanical properties of the polymer network.

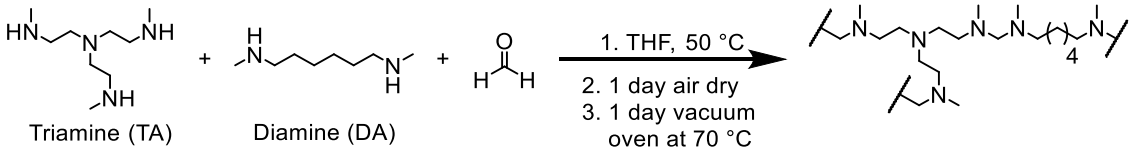

Scheme 3.4. Synthesis of cross-linked polyaminal of varied cross-linking density via triamine (TA), diamine (DA) and formaldehyde.

Condensation of amines and paraformaldehyde in THF was relatively slow at room temperature. After one day, the solution stayed heterogeneous as shown by a large amount of

unreactive paraformaldehyde. Therefore, the reaction was heated to 50 °C in THF (45 weight %) until the solution become homogeneous (~2 h). Aminal formation was monitored by ATR FT-IR spectroscopy. Absorbance corresponding to N-H bending (720-800 cm^{-1}) was used to determine the conversion of polymerization as shown in Fig 3.9. The N-H bending absorbance almost completely disappeared after 2 h. Upon cooling to room temperature, the conversions of entries 1 to 5 were calculated to be 95 to 99 %, which are higher than the Carothers' theoretical gel points, 83 to 97 %. As expected, entries 1 to 3 became standing gels within a minute after solutions reached room temperature. Entries 4 and 5 stayed as viscous fluids for a period of time before becoming standing gels.

Table 3.2. Material properties of cross-linked polyaminal.

Entry no.	TA initial molar fraction (%)	Cross-linking density (mol mL^{-1}) [a]	Conversion (%) [b]	Gel point (%) [c]	T_d (°C) [d]	T_g (°C)	$\Delta E_a^{\neq}$ (kJ/mol) [e]
1	100	2.2×10^{-5}	95	83	164	-51	52
2	50	1.0×10^{-5}	99	91	156	-67	51±0.17
3	39	0.78×10^{-5}	99	93	179	-70	67±3.82
4	28	0.53×10^{-5}	98	96	155	-72	81±1.26
5	20	0.40×10^{-5}	98	97	195	-76	76±0.64

[a]Theoretical cross-linking density, assuming 100 % conversion and no defect. [b]The extent of aminal formation or conversions were calculated by using the following equation: 1 – (integrated area of fingerprint region at time = 5 min / integrated area of peak at time = 0). [c]The theoretical gel point was estimated based on the Carother's equation. [d]T_d was defined as the temperature with 5 weight % loss by TGA analysis. [e]ΔE_a values were average of three repeated experiments and standard deviations.

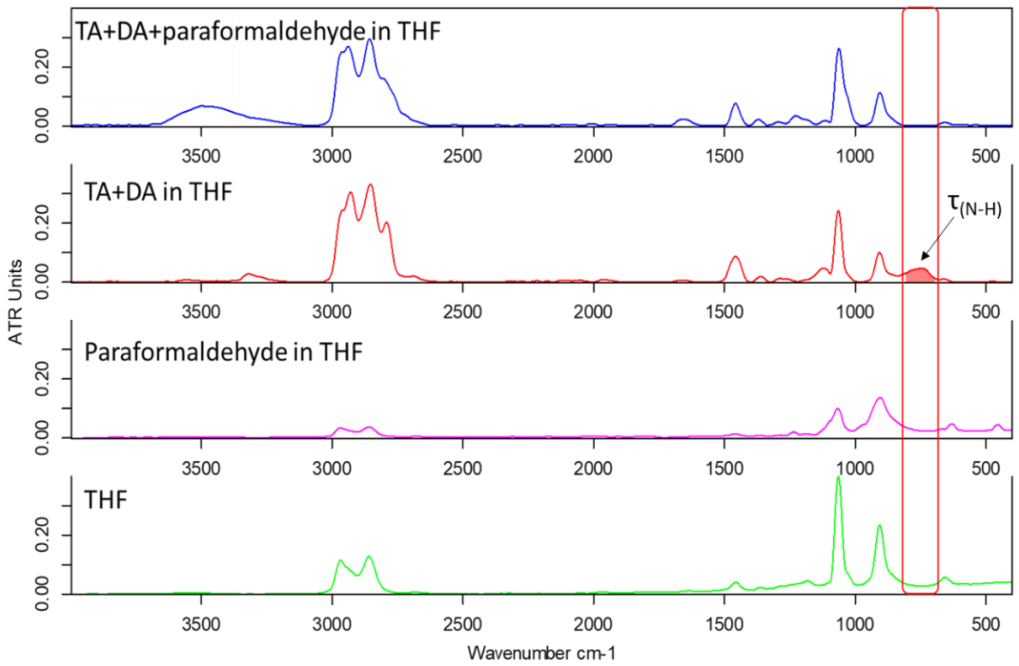

Figure 3.9. Representative FT-IR spectra of THF (green), 8 wt % of paraformaldehyde in THF (purple), the two monomers in THF (red), after reaction of two monomers and paraformaldehyde in THF (blue). Blue and red spectra prepared in 45 wt % in THF. The conversions were calculated from the disappearance of fingerprint absorbance at 720-800 cm^{-1}.

To ensure full conversion to aminals and the dryness of polymer samples, the condensation product was air dried under nitrogen for one day to remove most of the THF, followed by heating at 70 °C under vacuum (lower than 30 mmHg) for one more day to remove water and residual THF. Polyaminal polymers were found to be susceptible to oxidation when dried in air at high temperature, resulting in samples with darker color (Figure 3.10a) and the appearance of carbonyl absorbance associated with carbamate species (1650 cm^{-1}) in the FTIR spectrum (Figure 3.10b).

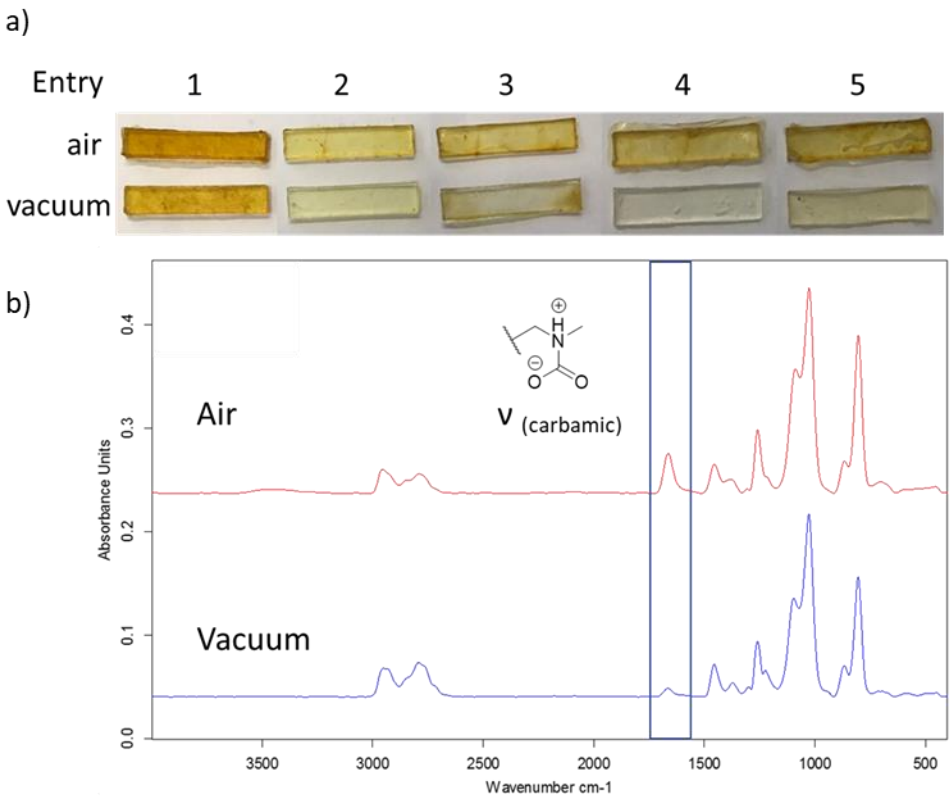

Figure 3.10. (a) Cross-linked polymer films synthesized in air (top row) or under vacuum (bottom row). (b) Stacked FT-IR spectra of films made in air (red) or vacuum (blue).

3.3.3 Thermal Analysis

All bulk cross-linked materials had rubbery-like mechanical properties at room temperature. Their glass-transition temperatures (T_g) were determined to be -76 °C to -51 °C via differential scanning calorimetry (DSC) analysis (Figure 3.11a). As expected, a general trend showing lower T_g with lower cross-linking content was observed (Table 3.2). Thermal stability was tested by thermogravimetric analysis (TGA) ranging from 155 °C to 195 °C (Figure 3.11b). These T_d were defined as temperature with 5 % mass loss by TGA analysis. Materials were also stable at 75 °C for at least 2 h as shown in Figure 3.12.

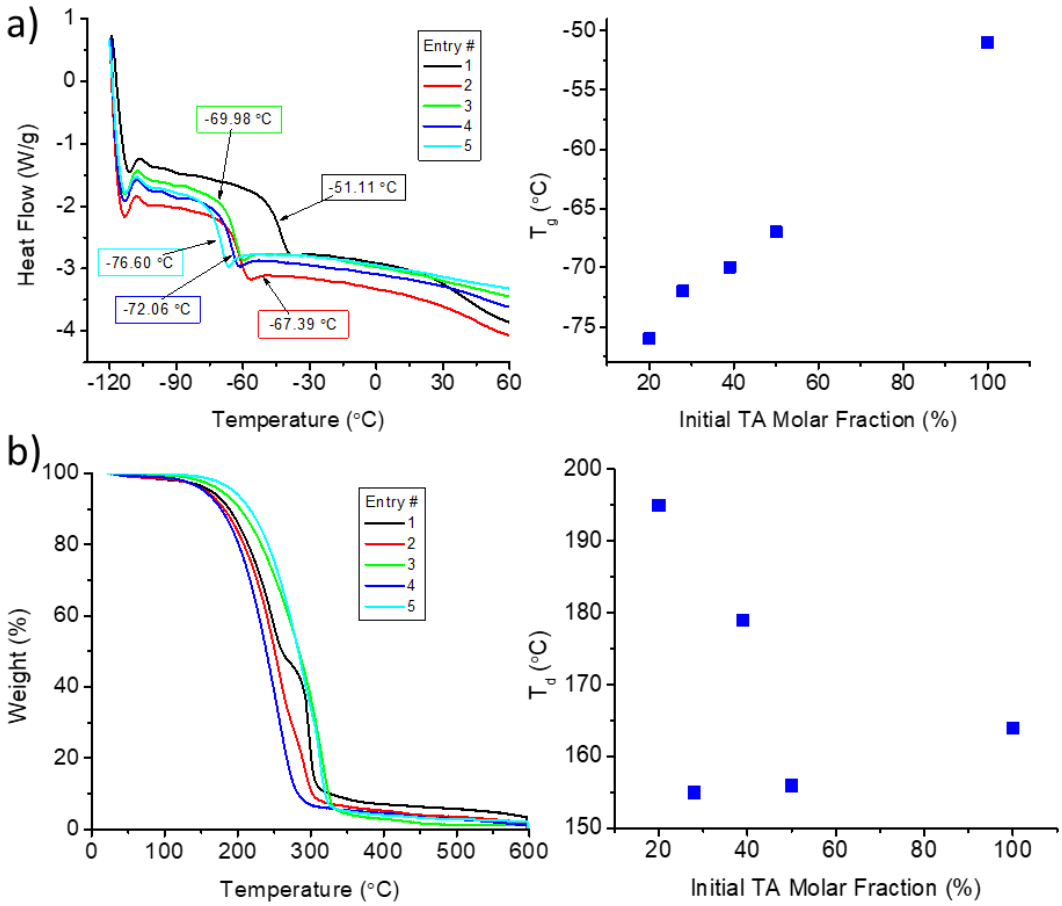

Figure 3.11. (a) DSC analysis of the polyaminal films (Entry 1-5). (b) TGA of the polyaminal films (Entry 1-5) under air atmosphere.

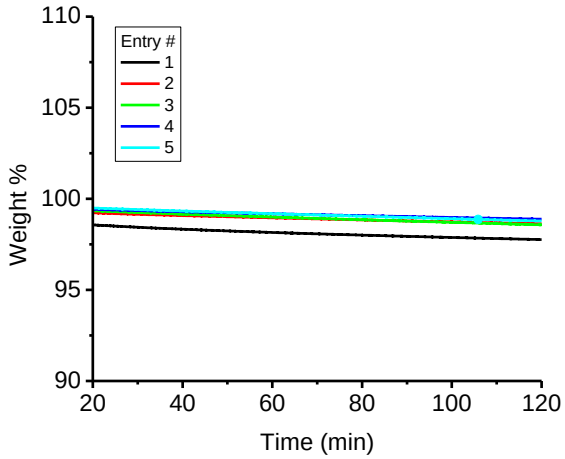

Figure 3.12. Isothermal TGA of cross-linked polyaminal films at 75 °C.

3.3.4 Rheology

Stress relaxation analysis (SRA) from entries 1-5 was performed until the sample relaxed to at least 37 % (1/e) based on the Maxwell model for viscoelastic fluids. Dog bone shape materials applied 1 % tensile strain under different temperatures. The normalized log stress relaxations of entries 1 to 5 were monitored as a function of time from 50 °C to 75 °C (Figure 3.13). Stress was shown to decrease over time, as a result of aminal bond exchange. The relaxation time is defined as the characteristic time at which the modulus decreases to 37 % of its original value at time=0. Materials that undergo topological rearrangement exhibited faster stress relaxation when the temperature increased. For example, entry 1 had a relaxation time of 40.1 min at 40 °C and 6.3 min at 70 °C when the modulus decreased to 37 %. In general, SRA showed a constant modulus in the beginning for the polymer materials that had inherently high T_g.[56, 71] However, modulus decreased in the beginning of our SRA study. It is likely the exchange reaction already occurred in the early stage of measurements in such low T_g materials.

The relaxation time at different temperatures was found to follow the Arrhenius relationship (Figure 3.14) with activation energies in the range of 51 – 81 kJ/mol for polyaminal networks with different cross-linker content. It seems that networks with higher cross-linker content tend to have lower activation energies than those with lower crosslinker content. For example, Entry 4 (28 % TA) has the highest activation energy of 81 kJ/mol, whereas entry 2 (50 % TA) has the lowest activation energy of 51 kJ/mol. The disparity in activation energy may be attributed to the difference in local environment around the functionalities involved in the bond exchange reaction. Activation energies obtained from SRA analysis were lower than the molecular model compounds (109±5 kJ/mol) (Figure 3.29d). One possible explanation is that model

compounds were not identical to the aminal structure in the networks. The activation barrier could change when the substituent bonded to the secondary amines are different.

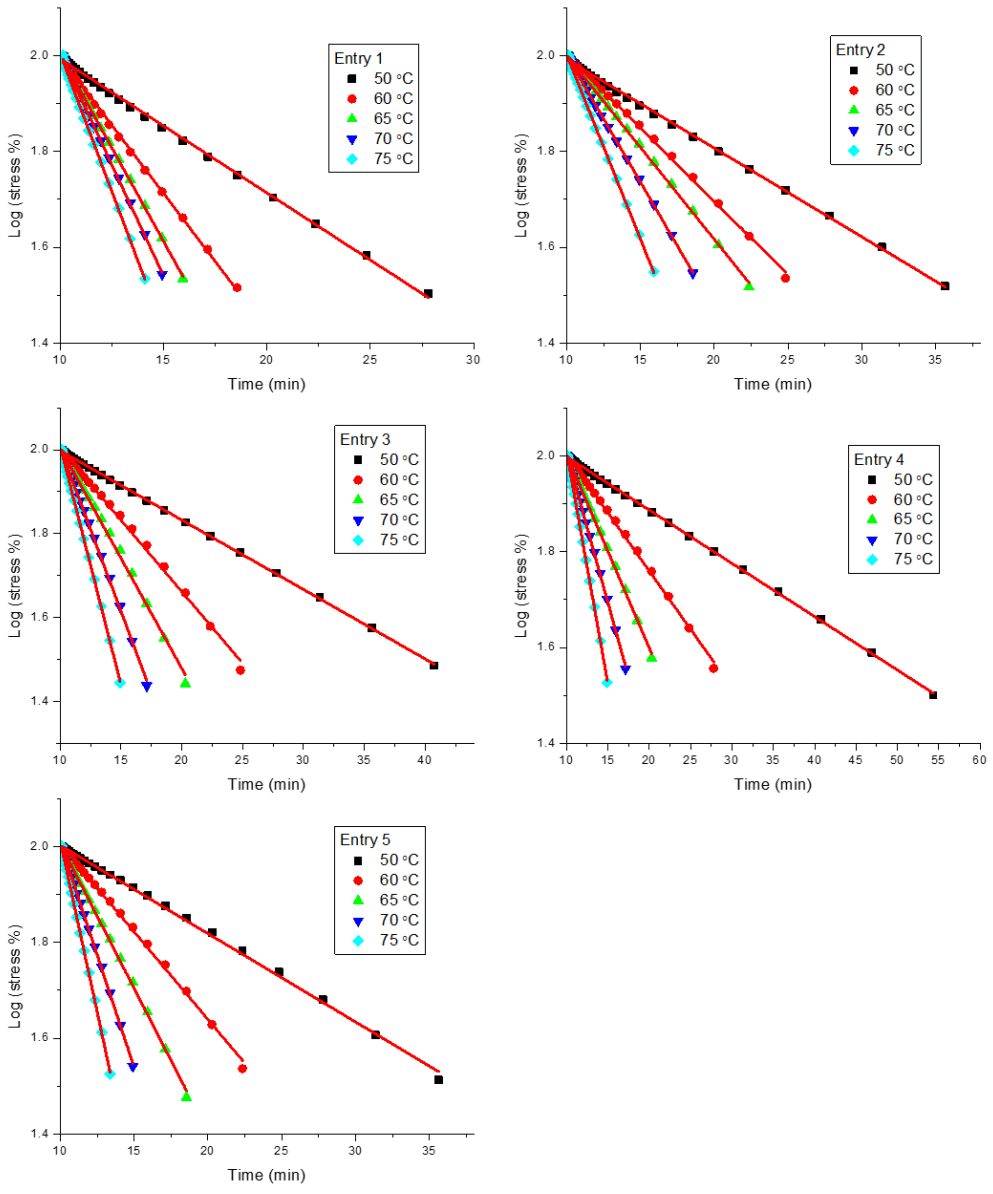

Figure 3.13. Representative normalized log stress relaxation curves for polyaminal networks with different cross-linker content (Entry 1-5, Table 3.2) at different temperatures (50 °C, 60 °C, 65 °C, 70 °C, and 75 °C).

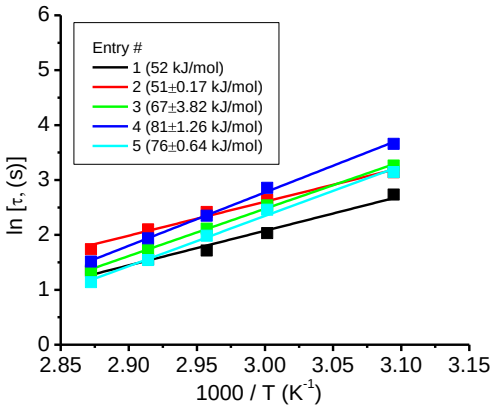

Figure 3.14. Arrhenius plot analysis of the characteristic relaxation time obtained from the SRA studies versus temperature for different polyaminal networks (Entry 1-5, Table 3.2).

The exchange reaction was relatively slow at room temperature compared to 50 °C and above. Based on the SRA experiment at 30 °C, normalized stress was still 83 % after 2 h for entry 1. To ensure a reasonable reprocessing time, recycling of polyaminal networks were heated at 80 °C in air. In Fig. 3.15, pieces of materials were able to remold into a triangular shape (a), as well as dyed material was able to reattach and become merged with non-dyed material (b) at the fractured interface. Moreover, material can merge from two materials with different cross-linking densities.

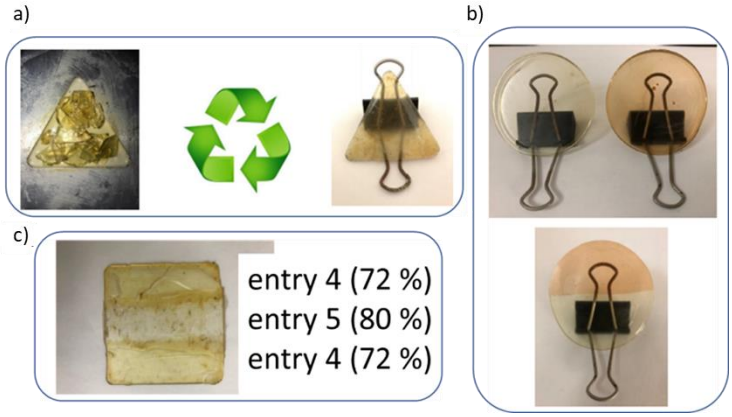

Figure 3.15. (a) fragments of cross-linked polyaminal remolded into a triangular shaped material at 80 °C. (b) virgin material and material containing 0.05 wt % rhodamine B merged bicolor material at 80 °C. The cracked line between the two halves is clear and healed. (c) Entry 4 and 5 merged bimodulus material.

3.3.5 Tensile tests

Five samples made with different cross-linker content were subjected to uniaxial tension at a constant rate using a dynamic mechanical analyzer. The Young's modulus (E') of polyaminal networks with varying crosslinker content are in the 31 –230 kPa range, whereas the strain-at-break is in the 4 – 20 % range (Table 3.3). Polyaminal networks with higher crosslinker content exhibit increased tensile modulus and reduced ductility relative to the ones with lower crosslinker content (Figure 3.16). The fractured samples from the initial tensile test were reprocessed by heating in a mold at 70 °C overnight. These thermally mended materials were subjected to tensile tests and exhibited comparable stress-strain curves as pristine polymers (Figure 3.16a). The Young's moduli of the thermally mended polyaminal networks are nearly identical to that of the pristine samples. The ductility of some thermally mended polymers is enhanced relative to the pristine samples. It is thus concluded that thermal mending can effectively restore the tensile properties of a polyaminal network.

Table 3.3. Tensile properties of cross-linked polyaminal films.

	Pristine films			Thermally mended films		
Entry no.	σ (MPa)	ε (%)	E'(kPa)	σ (MPa)	ε (%)	E'(kPa)
1	0.80±0.06	4.0±0.5	230±9	0.95±0.1	4.9±0.8	230±4
2	0.68±0.16	11±4.1	74±2	0.60±0.07	8.7±1.5	82±2
3	0.45±0.007	10±0.5	53±2	0.52±0.09	11±2.2	55±2
4	0.47±0.03	15±1.5	39±1	0.69±0.07	25±3.9	35±1
5	0.49±0.03	20±0.9	31±0.6	0.47±0.07	20±3.1	29±0.9

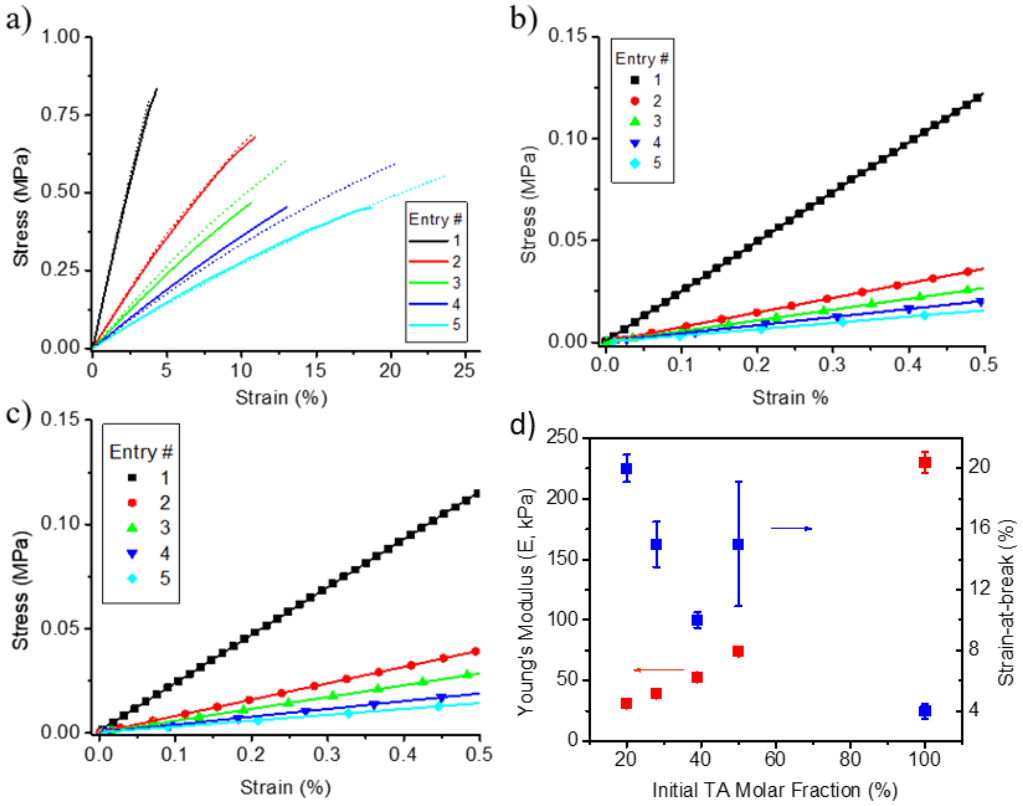

Figure 3.16. (a) Representative stress-strain curves of pristine (solid) and thermally mended (dashed) films under uniaxial tensile tests for polyaminal networks with varying crosslinker content (Entry 1-5, Table 3.2). (b) Expanded stress-strain curve reveals the linear response region from which the Young's moduli of pristine films were calculated from the slope in ε = 0 – 0.5 % range. (c) Expanded stress-strain curve to reveal the linear response region from which the Young's moduli of thermally mended films were calculated from the slope in ε = 0 – 0.5 % range. (d) The Young's modulus of the polyaminal thermosets increases with increasing crosslinking density. The strain-at-break is in the 4-20% range.

3.3.6 Activation energy of aminal exchange and dissociation constant of aminal bonds

To gain insight regarding the aminal bond exchange pathway, I conducted a kinetic study of the aminal bond exchange using aminal model compounds **1** and **2** as shown in Fig. 3.17a at different temperatures. These two monomers were chosen because there were no overlap peaks in ^{1}H-NMR. Upon mixing **1** and **2** in a stoichiometic ratio, the formation of **3** was observed to increase over time and to reach a steady concentration following a first-order rate law (Figure 3.17b). The aminal exchange rate increased with temperature as shown in Fig. 3.17c. Arrhenius (Figure 3.17d) and Eyring (Figure 3.17e) plot analysis of the rate constant at different temperatures

yielded an activation energy ($\Delta E^{\neq}$) of 109±5 kJ/mol, the activation enthalphy ($\Delta H^{\neq}$) of 106±5 kJ/mol and activation entropy ($\Delta S^{\neq}$) of 29±17 J/mol. The positive sign of $\Delta S^{\neq}$ suggests that the aminal exchange occurs by a dissociative pathway. The activation energy for aminal exchange is higher than the retro Diels-Alder value which is 88 kJ/mol.[51] The dependence of the rate of aminal exchange on temperature is not as sensitive as that for the retro DA reaction.

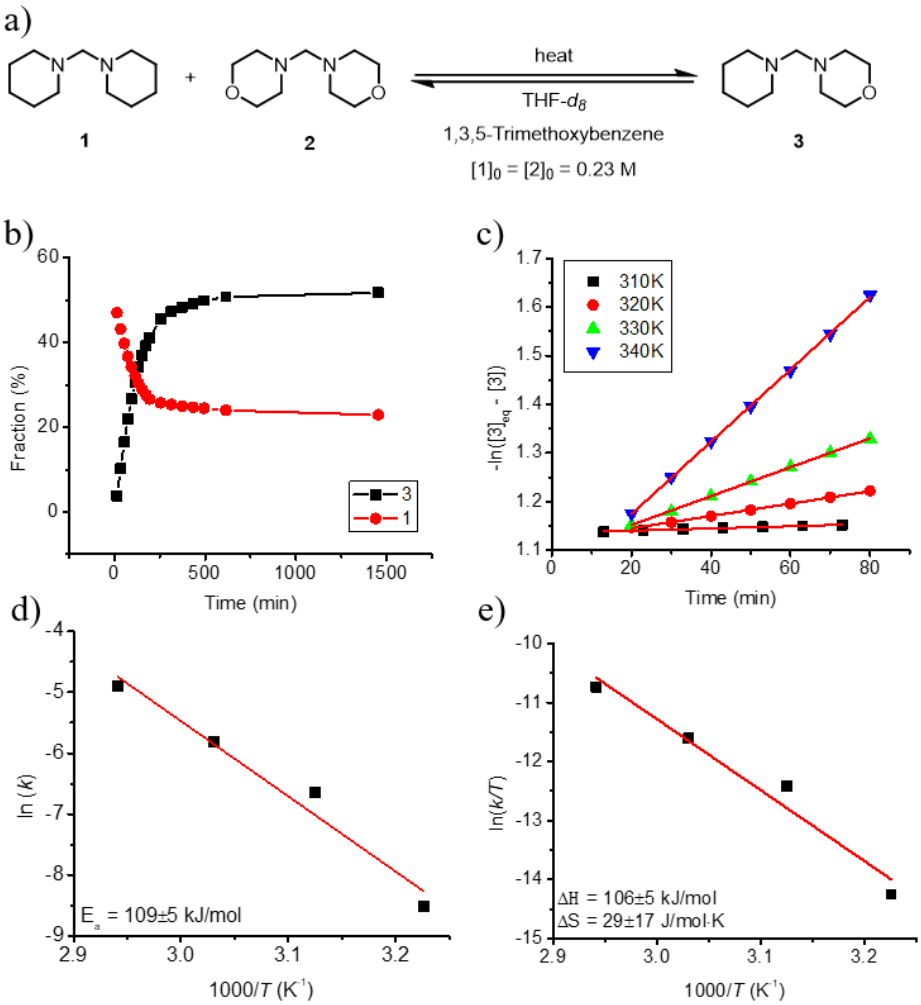

Figure 3.17. (a) Dynamic exchange reaction of equal molar model compounds **1** and **2** for kinetic study under N_2 atmosphere. [1,3,5-Trimethoxybenzene] = 0.23 M was used as an internal standard. (b) The formation of compound **3** and consumption of compound **1** were monitored for 1 day at 340K. (c) The formation of compound **3** followed a first order kinetic rate law at different temperatures. (d) Activation energy of aminal exchange was determined through Arrhenius plot analysis. (e) Eyring plot of aminal exchange reaction kinetics to determine the activation ΔH and ΔS.

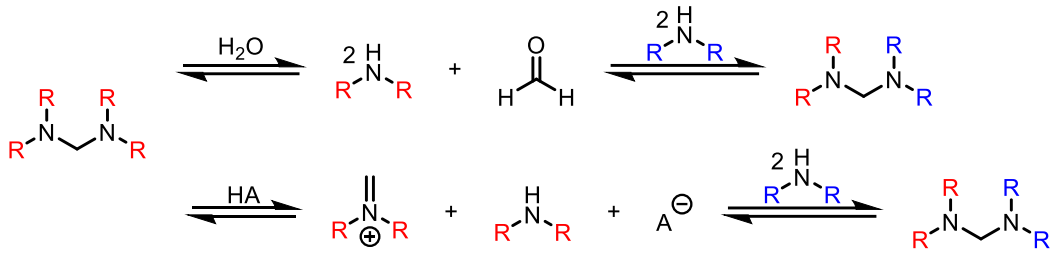

Scheme 3.5. Proposed dissociative mechanisms of dynamic aminal exchange through hydrolysis (top) or acid-catalyzed transaminalation (bottom).

As the aminal exchange has been shown to occur by a dissociative pathway, it can go through hydrolysis when water is present (Scheme 3.5-top). In the absence of water, I set out to quantify the equilibrium constant for the dissociation of aminal into iminium and secondary amine (Scheme 3.5-bottom) at different temperatures. Without any acid present, the dissociation is negligible. With addition of trifluoroacetic acid, dissociation becomes more pronounced, consistent with the hypothesis that the dissociation of aminals is promoted by acid (Figure 3.18a). The thermodynamic parameters for the aminal dissociation were obtained by Van't Hoff plot analysis of K_{eq} at different temperatures, yielding ΔH^o = 30.3 ± 2.5 kJ/mol and ΔS^o = 2.7 ± 0.83 J/mol respectively (Figure 3.18b). The aminal dissociation equilibrium constant was extracted from the linear fit equation (Figure 3.18c) to be 3.0 M at 120 ^{o}C, which is comparable to that of the retro-Diels-Alder reaction (1. 7 M),[48] indicating that the network can be readily depolymerized at this temperature in the presence of acid. By contrast, under pH neutral conditions, polyaminal polymers will be harder to depolymerize. The theoretical depolymerization (melting) temperature of each composition was calculated from dissociation constant plots that correspond to their gel points (Table 3.4). These theoretical values in neutral conditions were evidenced by the experimental observation that entries 1-4 maintained their topological structure while entry 5 turned into viscous fluid after 90 min at 110 °C. Upon cooling, this flowing fluid became solid and

behaved as a conventional thermoset. This material that followed the dissociative pathway has similar thermal behavior as described for vitrimers.

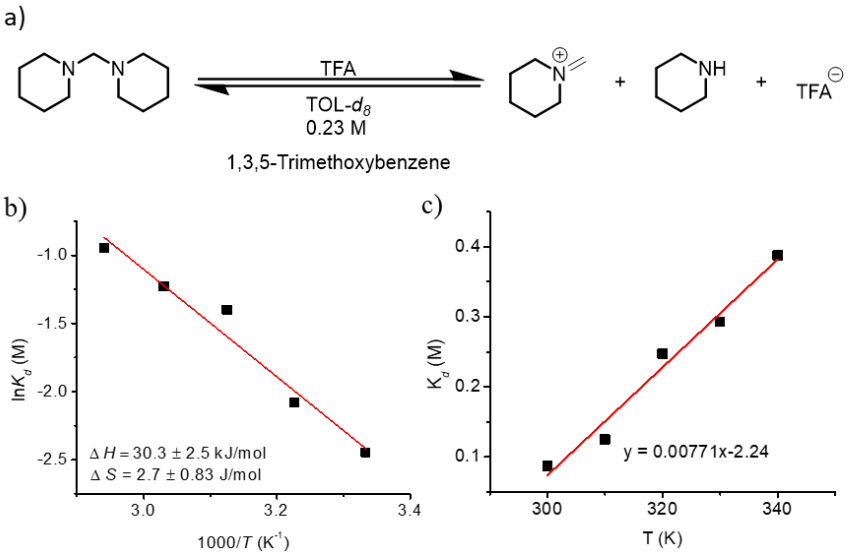

Figure 3.18. (a) Acid catalyzed dissociation constant. (b) Dissociation constant as a function of temperature. (c) Van't Hoff plot for the acid catalyzed aminal.

Table 3.4. Theoretical melting temperature of each composition in neutral and acidic conditions.

					In neutral condition	In acidic condition
Entry	Gel point	p	K_{eq}	K_d	Melting Temperature (°C)	Melting Temperature (°C)
1	83	0.83	24	4.20E-02	3698	23
2	91	0.91	102	9.78E-03	876	19
3	93	0.93	177	5.67E-03	515	18
4	96	0.96	576	1.74E-03	171	18
5	97	0.97	1045	9.57E-04	102	18

*Melting temperatures were extracted from the linear fit equations of dissociation constant as function of temperature plots.

3.3.7 Kinetics of aminal exchange reactions in the presence of different additives

To further confirm that transaminalation followed a dissociative mechanism, I decided to study aminal exchange with additives via ^{1}H-NMR. After mixing equal molar amounts of compounds **1** and **2** in dry TOL-d_8 inside a glovebox, the formation of compound **3** was monitored under neutral, acidic, and basic conditions at room temperature. The reaction with trifloroacedic acid (TFA) present was significantly faster than in neutral and basic conditions. An addition of a

small amount of piperidine had a negative effect on the exchange reaction rate as compared with that catalyzed by acid. For example, the addition of a base (e.g., DBU, 1 equiv.) at 80 min of the reaction time completely shut down the exchange reaction, evidenced by the compound **3** concentration remaining constant at ~20 % relative fraction (Figure 3.19) (Note: the equilibrium **3** concentration is 50% relative fraction as previously shown in Figure 17b). These results are consistent with the observation that the aminal exchange reaction occurs by a dissociative pathway where an iminium ion is produced as an intermediate followed by the addition of another secondary amine to yield new aminal linkages. Temperature dependent SRA results are also consistent with dissociative bond exchange (Figure 3.20). Transaminalation in neutral conditions is sluggish and is presumably catalyzed by the protic source on the glassware surface.

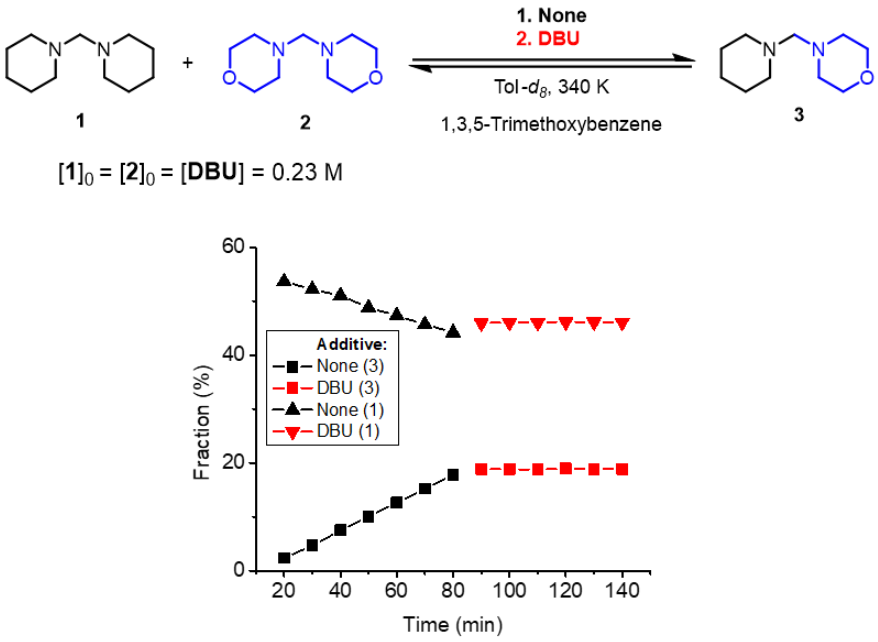

Figure 3.19. Change of the relative fraction of compounds **1** and **3** over time without and then with DBU (1 equiv.) presence at 340 K under N_2 atmosphere as monitored by ^{1}H NMR spectroscopy.

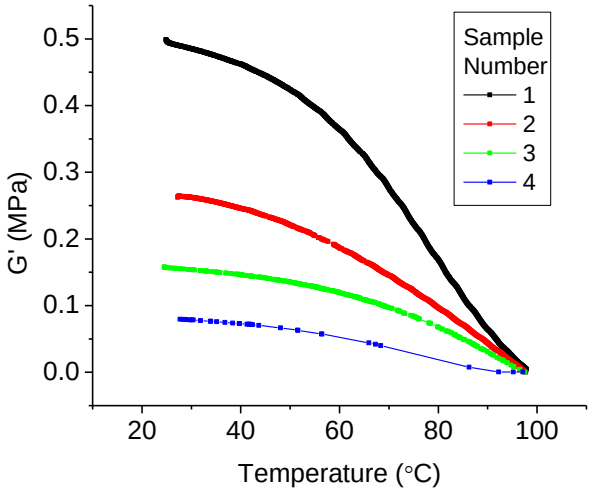

Figure 3.20. Temperature dependent stress relaxation analysis suggested aminal exchange followed a dissociative pathway.

3.4. Conclusion

It has been shown that the condensation of formaldehyde and secondary amine to form aminal bonds is thermodynamically favored in THF, allowing for the facile synthesis of polyaminal networks. Cross-linked polyaminals can be thermally reprocessed and recycled. Thermally mended polyaminal networks exhibited comparable tensile properties relative to the pristine polymers, indicating that the thermal healing by dynamic aminal bond exchange is effective. The aminal bond exchange in the network was found to occur by a dissociative pathway, catalyzed by the presence of protic acid. As the polyaminal networks in this study had low T_g and modulus, our future effort will be focused on the development of cross-linked polyaminals with enhanced mechanical properties via judicious choice of monomers.

3.5. Experimental information

3.5.1 Preliminary experimental procedure

Monomers **4** and **5** were synthesized by mixing tri-tosylate, 4-hydroxybenzaldehyde (3.5 equiv. relative to tri-tosylate) and K_2CO_3 (4 equiv. relative to tri-tosylate) reflux overnight in DMF

under N_2 (Scheme 3.2). Monomers **4** and **5** were diluted with water and extracted with ethyl acetate. The organic layer was washed with water 3 more times and the solvent was removed. Both monomers were purified with a chromatography column (7 hexane : 3 ethyl acetate). Monomer with a nitro group (**6**) was synthesized by mixing monomer **4** with 70 % HNO_3 (minimum 4 equiv. relative to monomer 4). After the mixture became homogeneous (turned yellow), the reaction was allowed to go for another 12 h. The solution was poured into distilled H_2O to precipitate out the product from the solution. The product was washed with water several times. Proton NMR in $CDCl_3$ as followed (Figure 3.21 – 3.23):

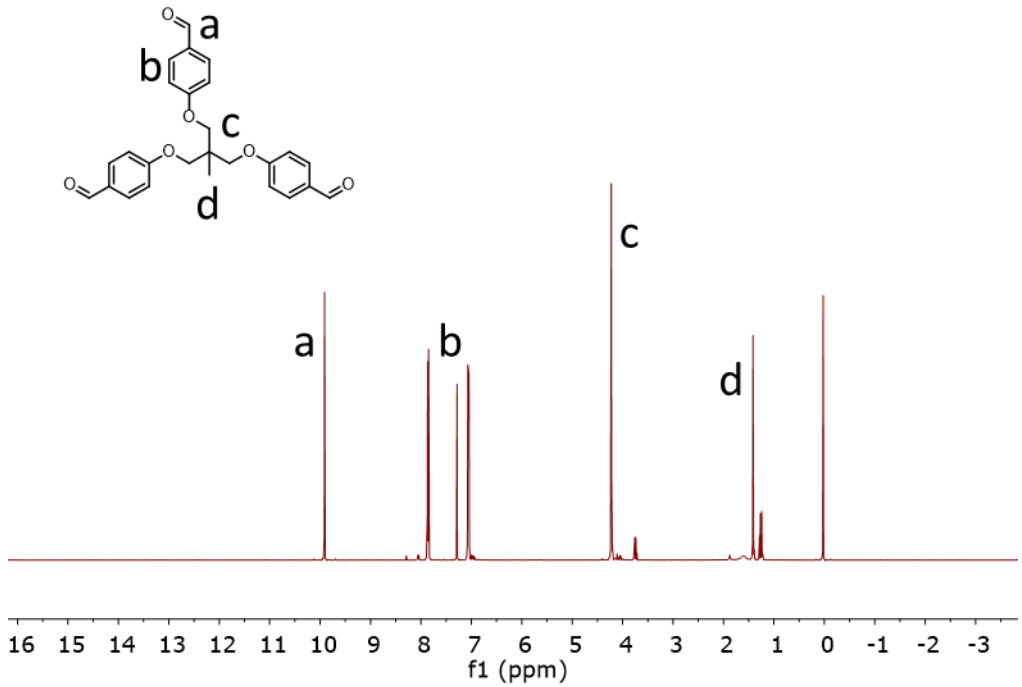

Figure 3.21. ^{1}H-NMR spectrum of trialdehyde 1 in $CDCl_3$.

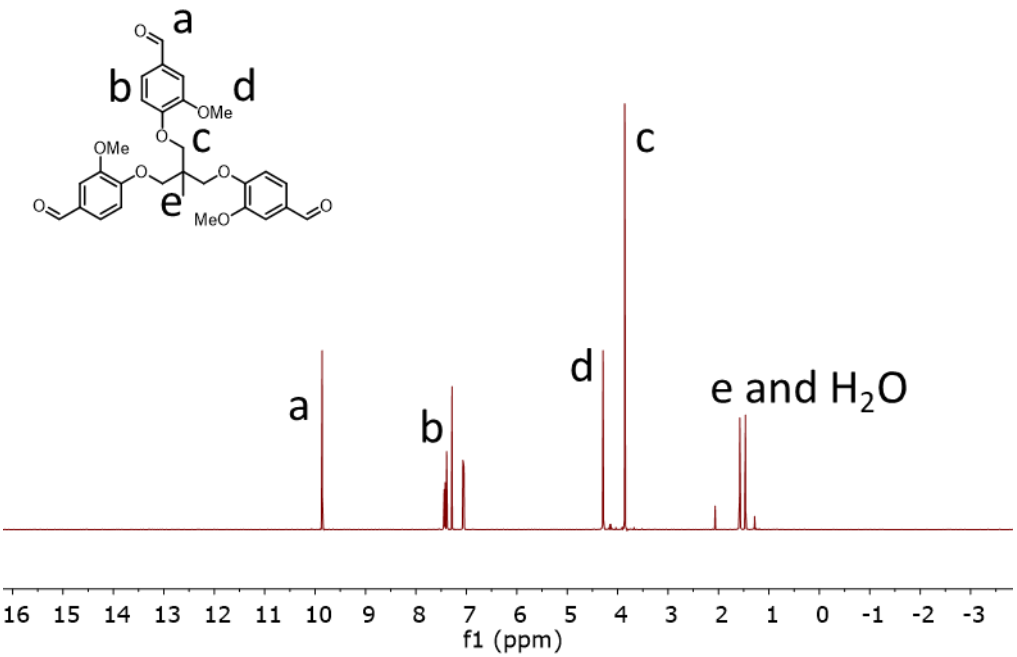

Figure 3.22. ^{1}H-NMR spectrum of trialdehyde 2 in $CDCl_3$.

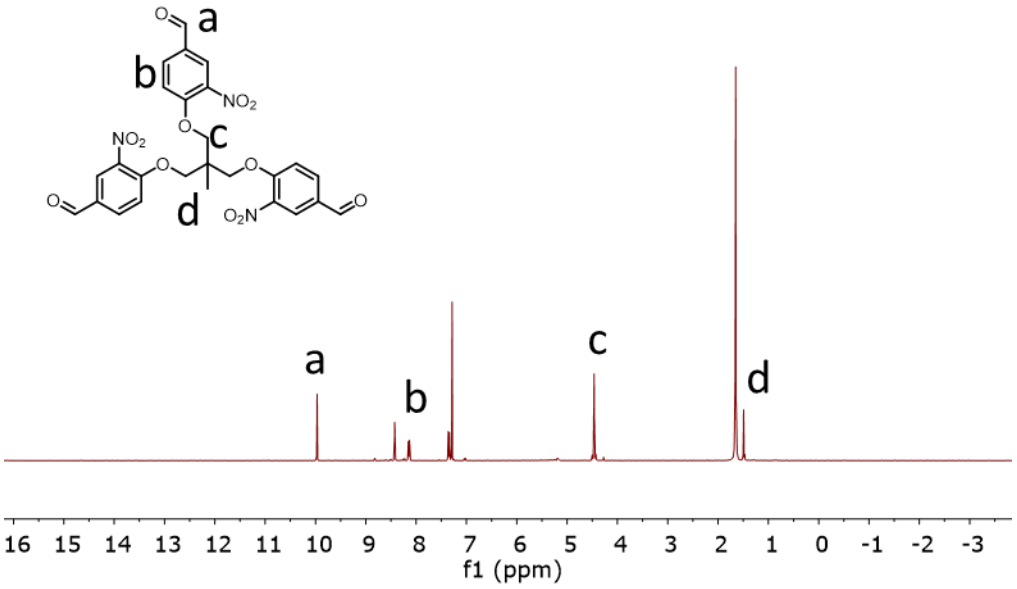

Figure 3.23. ^{1}H-NMR spectrum of trialdehyde 3 in $CDCl_3$.

Polyethylene glycol dipiperazine (protective) was synthesized from PEG ditosylate, ethyl 1-piperazine (3 equiv. relative to PEG ditosylate), and K_2CO_3 (6 equiv. relative to PEG ditosylate)

in acetonitrile at 80 °C. After 14 h, solvent was pumped off and the sample was then redissolved in DCM. The organic layer was washed with water two times and removed in vacuo accordingly. After solvent removal, the crude was redissolved in a small amount of DCM and recrystallized by adding ether and then stored at -20 °C. The ^{1}H-NMR spectrum of PEG dipiperazine (protective) is shown in Figure 3.24. Polyethylene glycol dipiperiazine was synthesized by dipiperazine (protective) and NaOH (15 equiv. relative to PEG dipiperazine (protective)) in water at 60 °C overnight. The product was extracted from the water layer with DCM and precipitated out from hexane (Scheme 3.6). The ^{1}H-NMR spectrum of PEG dipiperazine is shown in Figure 3.25.

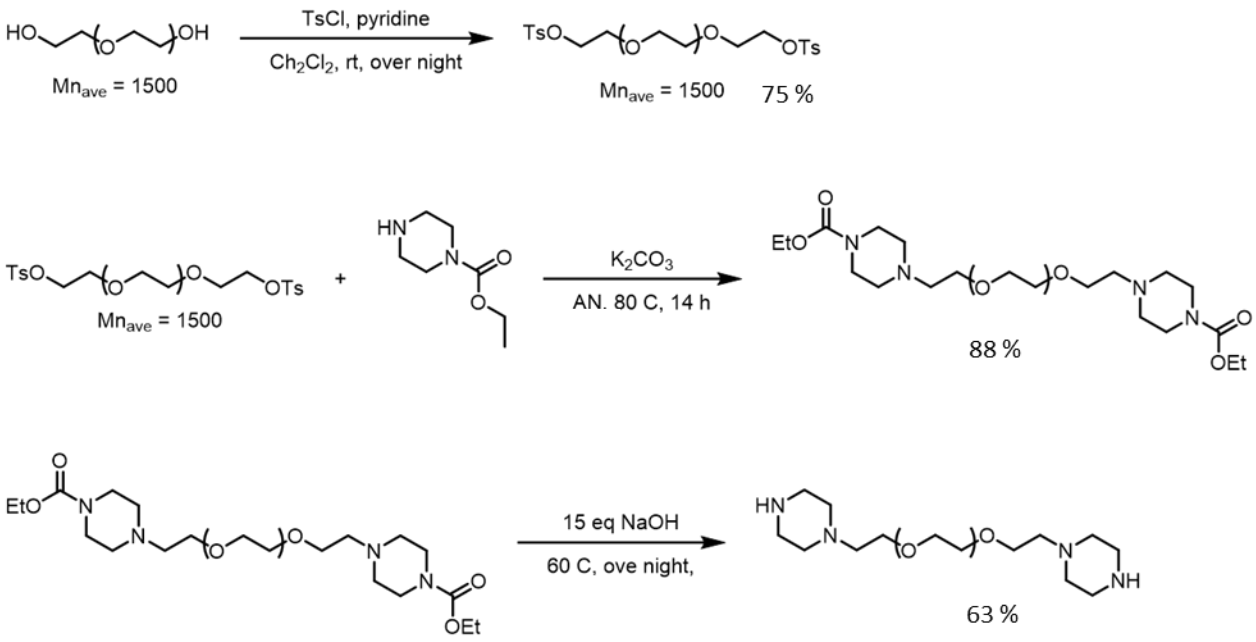

Scheme 3.6. Synthesis of poly (ethylene glycol)-1,2-bis(2-piperazin-1-yl).

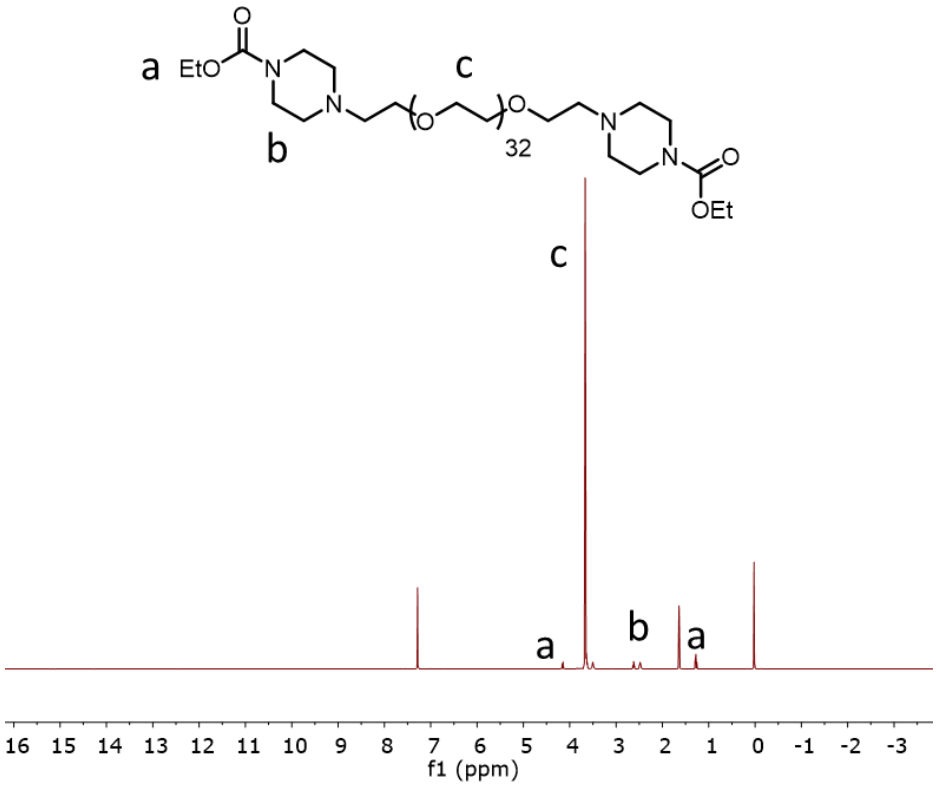

Figure 3.24. ^{1}H-NMR spectrum of PEG dipiperazine (protective) in $CDCl_3$.

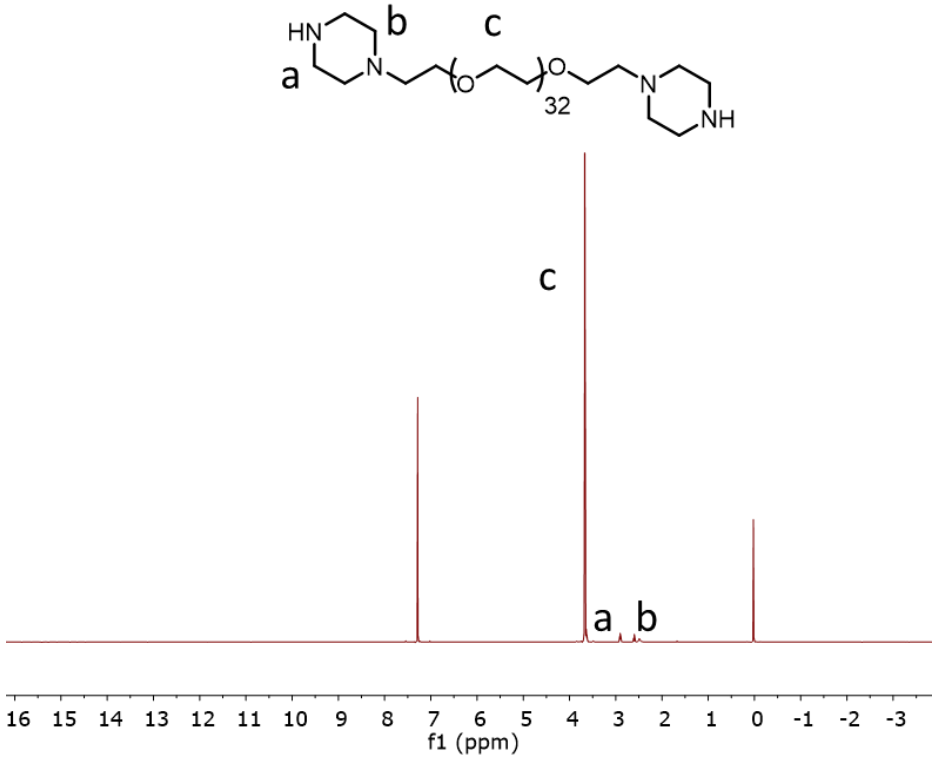

Figure 3.25. ^{1}H-NMR spectrum of PEG dipiperazine in $CDCl_3$.

3.5.2 General experimental procedures

General consideration. All chemicals were purchased from Sigma-Aldrich and used without further purification. Deuterated solvents, THF-d_8 and TOL-d_8 were purchased from Fisher Scientific. Model compounds **1**, **2** and those shown in Table 3.1 were prepared by previously reported procedures (Scheme 3.7)[72] and distilled and stored under nitrogen before use in the kinetic studies. Aluminum molding plates were made by the LSU mechanical shop. Deuterated THF was dried with molecular sieves overnight before use in the kinetic studies. Deuterated toluene was dried with calcium hydride and freeze pump thawed (3 cycles) followed by vacuum transfer.

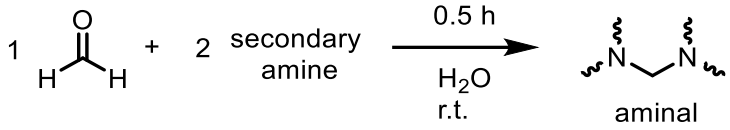

Scheme 3.7.

Preparation of monomer and polyaminals. Tris[2-(methylamino)ethyl]amine (TA, Scheme 3.8, Figure 3.26) was synthesized following a published procedure.[69] Linear polyaminal was prepared in NEAT by N,N′-dimethyl-1,6-hexanediamine (DA) and paraformaldehyde. The reaction was conducted at 70 °C under atmosphere pressure until the reaction became homogenous. Cross-linked polyaminals (entry 1-5) were prepared by mixing TA/DA and paraformaldehyde in 45 wt% THF. A representative procedure for the synthesis of a polyaminal network (Entry 2, Table 3.2) is given as follows. Triamine (0.5 g, 2.66 mmol), DA (0.575 g, 3.98 mmol) and paraformaldehyde (0.239 g, 7.97 mmol) were dissolved in THF in a closed vial. The heterogenous solutions were heated to 70 °C until all paraformaldehyde disappeared. The reaction was cooled to room temperature followed by heating in a vacuum oven at 70 °C overnight. Entries 1, 3, and 4 were also made in a similar manner except that the solvent was removed in vacuo for

entry 5 before placing in the vacuum oven. After removal from the vacuum oven, materials were molded in an aluminum mold.

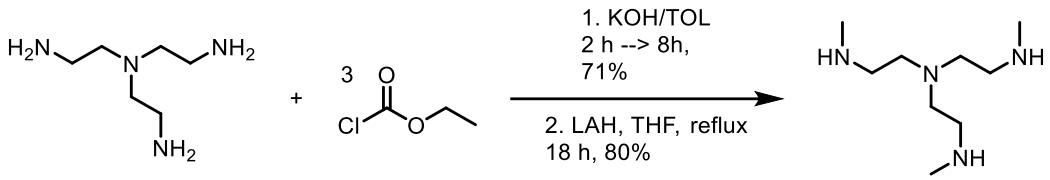

Scheme 3.8.

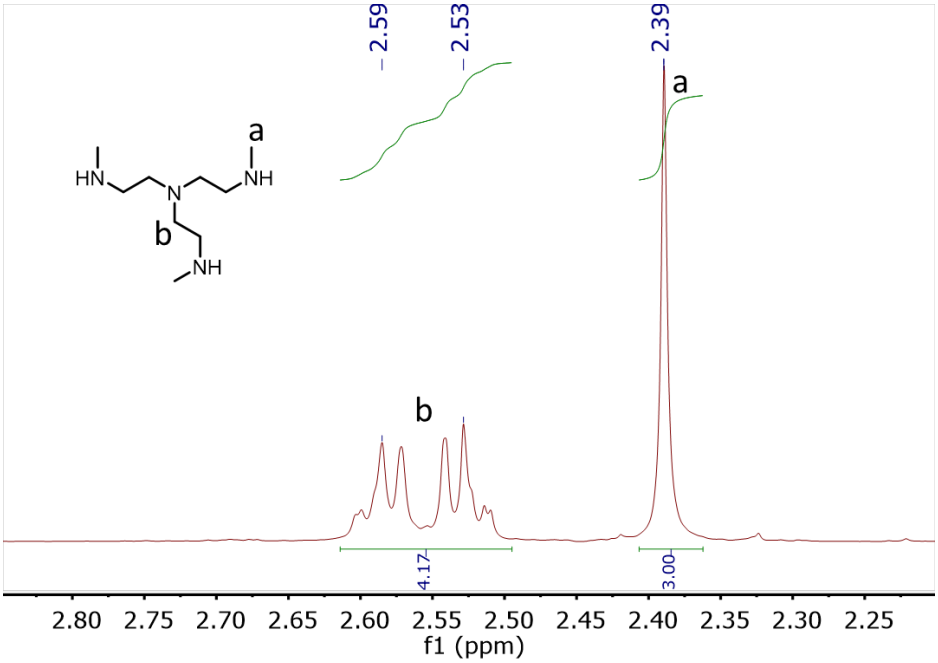

Figure 3.26. ^{1}H-NMR spectrum of triamine in $CDCl_3$.

IR spectroscopy measurement. The reaction progression and conversion were determined by monitoring the disappearance of N-H bending (700-800 cm^{-1}) over time using an ATR-FTIR spectrometer (Bruker Alpha). The FTIR spectrum of the TA/DA solution (entries 1-5) without paraformaldehyde was measured as a reference. After addition of paraformaldehyde, the mixtures were heated until homogenous. The FTIR spectrum of the THF gel was measured again. The aminal conversion was determined by the ratio of unreacted N-H to the initial N-H peak intensity.

Dynamic mechanical analysis (DMA). Tensile testing was conducted using dog bone shaped tensile bars (ca. 1 mm (T) × 5 mm (W) × 12 mm (L) and a gauge length of 14 mm). The samples were stored for at least 24 h at room temperature in a desiccator prior to testing. Stress-strain curve experiments were performed using TA instruments DMA Q800 under uniaxial tensile mode. The experiments were conducted with a controlled force, 0.500 N/min at room temperature with a preload force 0.001 N until the sample yielded. Young's moduli (E') were determined from the slope of the linear stress-strain curve in the 0 to 0.5 % strain range. Stress relaxation analysis (SRA) experiments were conducted in tensile mode with a controlled strain and a preload force 0.001 N at specified temperatures (50-75 °C). The samples were kept at isothermal conditions (50-75 °C) for 10 min. Subsequently, each sample was subjected to an instantaneous 1% strain. The stress relaxation was monitored, while maintaining a 1 % strain until the stress relaxation modulus had relaxed to at least 37% (1/e) of its initial value. The activation energy (Ea) was calculated using a reported method.[73] Fracture samples from the initial tensile test were placed into an aluminum dog-bone-shaped mold overnight under vacuum at 70 °C. Each reprocessed material was subjected to the tensile test. A triplicate to quintuplicate of each sample was subjected to the stress-strain tests or stress relaxation tests to determine the mean values of relevant parameters and standard deviations. Dynamic mechanical thermal analysis (DMTA) was performed on a TA instrument DMA Q800 under uniaxial tensile mode utilizing rectangular films (ca. 1 mm (T) × 5 mm (W) × 12 mm (L) and a gauge length of 14 mm). The axial force was adjusted to 0.001 N and a strain adjustment of 0.5%. A temperature ramp was then performed from room temperature to 100 °C at a rate of 2.5 °C/min.

Kinetics studies of aminal bond exchange. Proton NMR spectra were recorded on a Bruker AV-400 spectrometer, and the chemical shifts in parts per million (ppm) were referenced

relative to protio impurity in TOL-d_8. Internal standard 1,3,5-Trimethoxybenzene was used for the kinetic study. A representative procedure for kinetic study is given as follows. Inside the glovebox, di-(piperidin-1-yl)methane (21 mg, 0.115 mmol), dimorpholinomethane (21 mg, 0.115 mmol) and 1,3,5- trimethoxybenzene (19 mg, 0.115 mmol) were dissolved in TOL-d_8 (0.5 mL) in a dried vial. The mixture was then transferred into a J. Young NMR tube followed by the addition of a TOL-d_8 stock solution of TFA (23 μL, 500 mM, 0.1 eqv. relative to the total aminal content) at room temperature. Proton NMR spectra were collected immediately after the preparation of the reaction mixture. Each spectrum was collected with 10 scans and 2 s relaxation time at room temperature. All kinetic experiments were repeated twice to get the mean reaction rate.

Thermal analysis. Differential scanning calorimetry (DSC) analysis of the cross-linked polyaminal (Entry 1-5, Table 3.2) with DSC was conducted using a TA DSC 2920 instrument. The polymer (10 mg) was hermetically sealed in a standard aluminum pan. An empty pan was used as a reference. The sample was kept at -120 °C for 2 min and then heated to 100 °C at 10 °C·min^{-1}. Heat flow was recorded during the heating and cooling cycles, and normalized by the sample mass. Experiments with TGA were carried out on a TA 2950 TGA under a nitrogen atmosphere with a heating rate of 10 °C/min. The scanned temperature range was room temperature to 600 °C. Data were analyzed with Thermal Advantage Software.

Characterization of self-healing and recycling properties. Cross-linked polyaminals were cut into pieces with a razor blade and were remolded into a triangular shaped material in a mold at 80 °C in air. The red material was obtained by adding rhodamine B (0.05 wt%). Disc samples were cut with a razor blade and cross re-attached at the cut-interface followed by heating the material to 80 °C for 1 h in the mold. Merged bi-modulus samples were prepared in a similar manner.

MALDI-TOF MS. Experiments were conducted on a Bruker UltrafleXtreme tandem time-of-flight (TOF) mass spectrometer. The instrument was calibrated with Peptide Calibration Standard II consisting of standard peptides Angiotensin I, Angiotensin II, Substance P, Bombesin, ACTH clip 1-17, ACTH clip 18-39, and Somatoratin 28 (Bruker Daltonics, Billerica, MA) prior to experiment. A saturated methanol solution of α-cyano-4-hydroxycinnamic acid was used as a matrix. Samples were prepared by mixing a DCM solution of polymers (10 mg/mL) with matrix at 1:1 volume ratio, which were then deposited onto a 384-well ground-steel sample plate using the dry droplet method. Experiments were done in positive reflector mode. The data analysis was performed with flexAnalysis software.

Dissociation constant of model compound. Proton NMR spectra were recorded on a Bruker AV-500 spectrometer, and the chemical shifts in parts per million (ppm) were referenced relative to protio impurities in THF-d_8. Molecule 1,3,5-Trimethoxybenzene was used as internal standard. Spectra were collected at different temperatures to determine the equilibrium constant. Spectra were collected twice for each temperature (10 min between) to ensure integration stayed constant (equilibrium). A representative procedure for measuring the K_d of the aminal hydrolysis equilibrium is given as follows. Dimorpholinomethane (21 mg, 0.115 mmol) and 1,3,5-trimethoxybenzene (19 mg, 0.115 mmol) was dissolved in THF-d_8 (0.5 mL) followed by adding H_2O (5 mg) in a dried vial. The mixture was then transferred into a J. Young NMR tube at room temperature. Proton NMR spectra were collected immediately after the preparation of the reaction mixture. Each spectrum was collected with 8 scans and 2 s relaxation time. A series of dissociation studies were performed under a similar manner at different temperatures (300, 310, 320, 330, and 340 K, Figure 3.27). Dissociation equilibrium constant was calculated from Equation 1. All

dissociative experiments were repeated three times to get the average K_d. The enthalpy (ΔH_d) and entropy (ΔS_d) were extracted from Van't Hoff plot analysis (Figure 3.28).

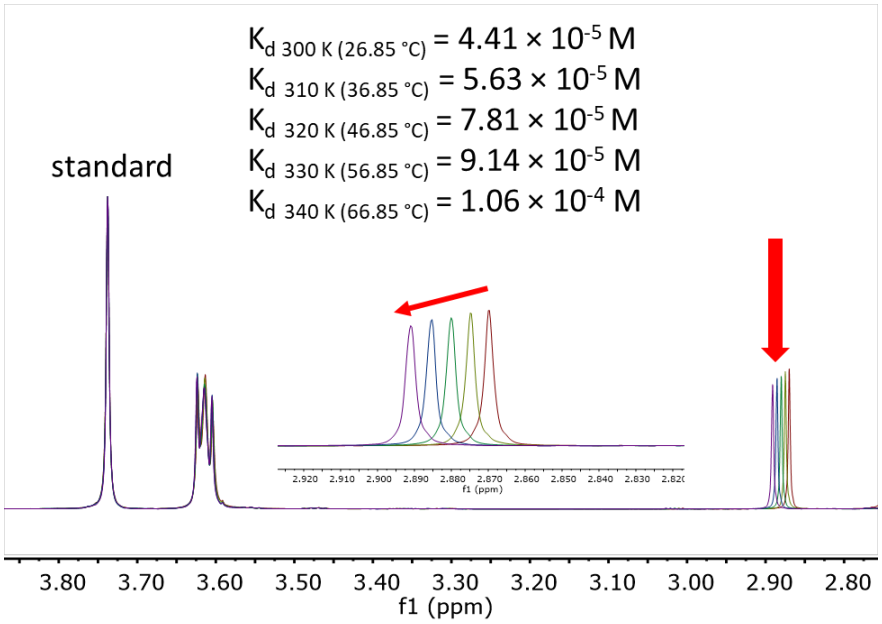

Figure 3.27. ^{1}H NMR of a series of dissociation constant were performed at 300, 310, 320, 330, and 340 K.

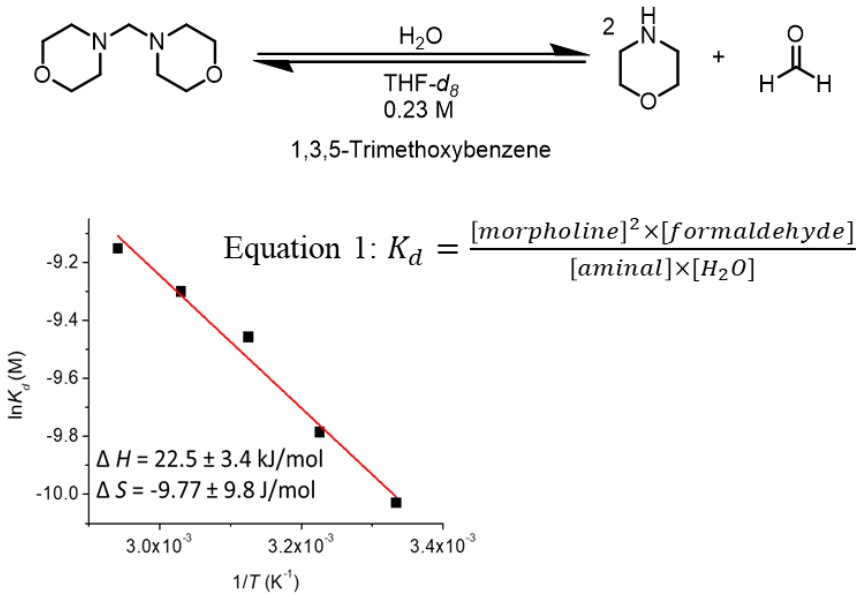

Figure 3.28. Dissociation constant and Van't Hoff plot for the hydrolysis of ring aminals.

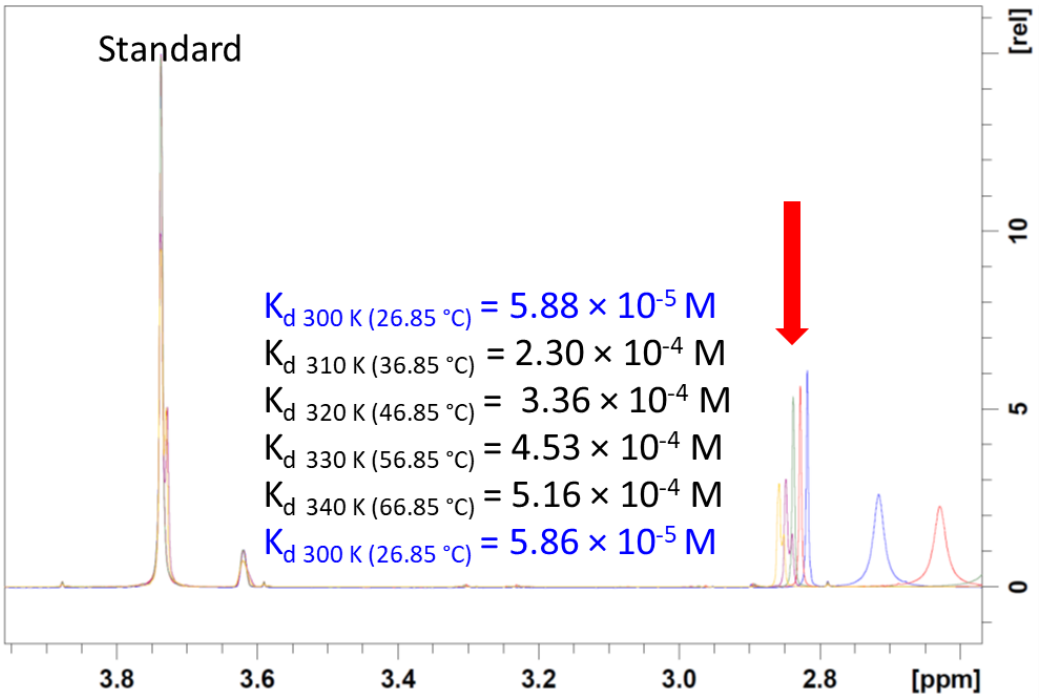

Figure 3.29. ^{1}H NMR of a series of dissociation constant were performed at 300, 310, 320, 330, and 340 K.

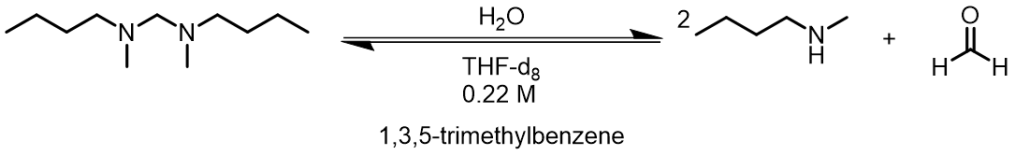

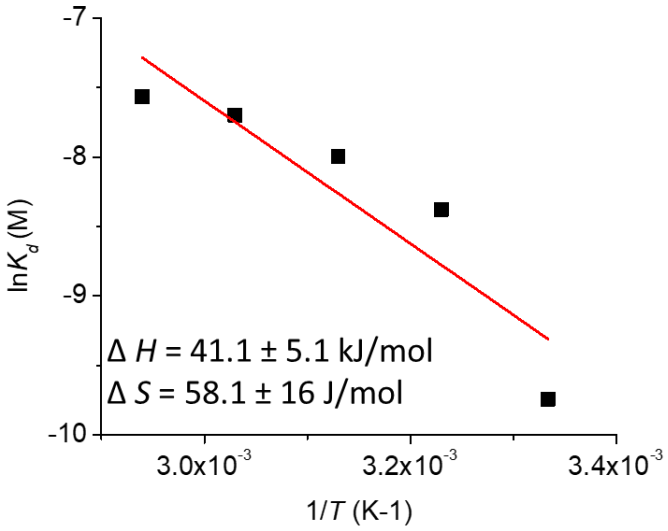

Figure 3.30. Dissociation constant and Van't Hoff plot for the hydrolysis of linear aminals.

A representative procedure to measure the K_d of aminal dissociation into iminium and secondary amine is given as follows. Di-(piperidin-1-yl)methane (21 mg, 0.115 mmol) and 1,3,5-trimethoxybenzene (19 mg, 0.115 mmol) was dissolved in TOL-d_8 (0.5 mL) followed by adding 1 equiv. TFA (13 mg, 9 µL) in a dried vial. The mixture was then transferred into a J. Young NMR tube at room temperature. Proton NMR spectra were collected immediately after preparation of the reaction mixture. Each spectrum was collected with 8 scans and 2 s relaxation time. A series of dissociation studies were performed under a similar manner at different temperatures (300, 310, 320, 330, and 340 K, Figure 3.31). Dissociation equilibrium constant was calculated from equation 2. All dissociative experiments were repeated three times to get the average K_d. The enthalpy (ΔH_d) and entropy (ΔS_d) were extracted from Van't Hoff plot (Figure 3.32).

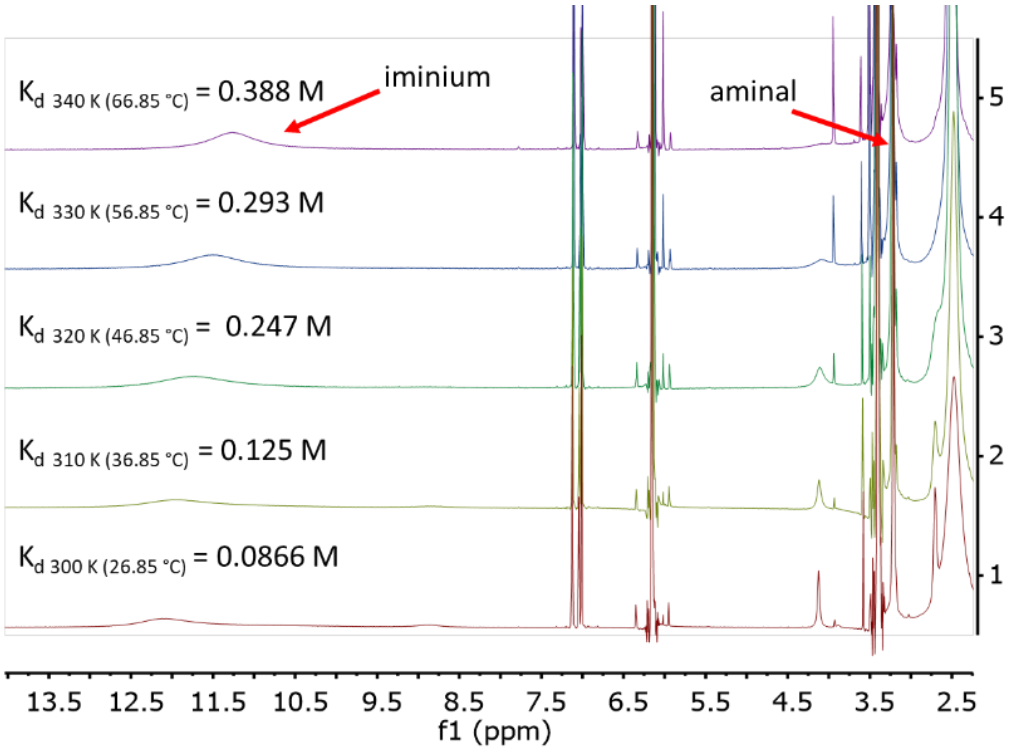

Figure 3.31. ^{1}H NMR of a series of dissociation constant were performed at 300, 310, 320, 330, and 340 K.

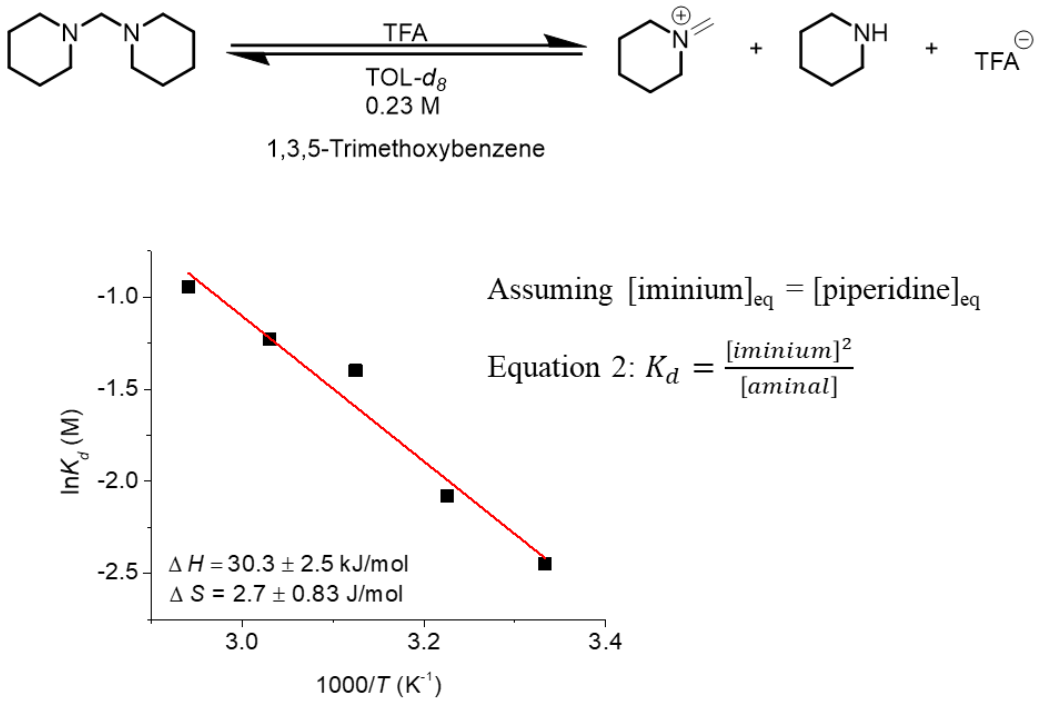

Figure 3.32. Van't Hoff plot for the acid catalyzed piperidine aminal.

Activation energy of the exchange reaction of aminal model compounds. Proton NMR spectra were recorded on a Bruker AV-500 spectrometer, and the chemical shifts in parts per million (ppm) were referenced relative to THF. A representative procedure is given as follows. The Bruker AV-500 was preheated to 310K before adding sample. Compound **1** (21 mg, 0.115 mmol), **2** (21 mg, 0.115 mmol) and internal standard 1,3,5-trimethoxybenzene (19 mg, 0.115 mmol) were dissolved in THF-d_8 (0.5 mL) under N_2 atmosphere. The mixture was transferred into a J. Young NMR tube at room temperature. Proton NMR spectra were collected immediately after preparation of the reaction mixture. Each spectrum was collected with 10 scans and 2 s relaxation time (~ 1 min per spectrum) for 120 times. A series of kinetic studies were performed under a similar manner at different temperatures (310, 320, 330, and 340 K). The equilibrium concentrations were reached at 340 K for 24 h. All kinetic experiments were repeated three times to get the average and standard deviation. The dissociation rate constant (k_d) and dissociation activation energy (ΔE_a) were determined utilizing the previously reported methods.[49]

Chapter 4 : Conclusion

This dissertation has focused on the development of thermosets consisting of dynamic covalent bonds, in particular imine or aminal bonds. Research effort has been focused on the design and synthesis of monomers, polymer networks and kinetic or thermodynamic studies using model compounds. In contrast to conventional thermosets consisting of permanent covalent bonds, polymer networks comprised of dynamic covalent bonds, also known as covalent adaptable networks (CANs), exhibit creep behavior under stress and stress relaxation behavior due to the dynamic bond exchange.

In Chapter 2, I investigated the synthesis of solvent swelled polymer networks comprised of dynamic imine linages by condensation of multifunctional aldehydes with primary diamines. Dynamic mechanical analysis revealed the irreversible deformation of these polyimine gels under a constant compressive stress, in sharp contrast to the polymer gel comprised of permanent covalent bond which exhibited minimal deformation upon removal of the stress. The degree of deformation was found to be solvent dependent. The polyimine gels also exhibited stress relaxation behavior when compressed under a constant strain, in contrast to polymer gel comprised of permanent covalent bonds which show no signs of stress relaxation over time. Kinetic studies of model imine compounds have revealed the imine bond exchange reaction to be solvent dependent. There is a correlation between the relative imine bond exchange kinetic with the relative stress relaxation rate of the polyimine gels, suggesting the former is likely the molecular basis for the macroscopic dynamic behavior of the gel network. Imine exchange can occur by either an associative or a dissociative pathway. The former requires the presence of a catalytic amount of primary amine, whereas the latter facilitates the imine exchange via hydrolysis of the imine back to the amine and aldehyde via equilibrium. Kinetic data suggest that the associative mechanism is

the main contribution to the imine bond exchange while the exchange by dissociative mechanism through hydrolysis has a minor contribution in the polyimine networks in this study.

Aminals can typically be synthesized by condensation reaction of an aldehyde or ketone with two equivalents of primary or secondary amines. While aminals have been known for a long time in organic chemistry, they have not been incorporated into the design of CANs. Step-growth polymerization to access polyaminal prefers the use of amine and aldehydes that are reactive towards condensation but with few or no other side reactions. In Chapter 3, condensation of formaldehyde with various secondary amines has been screened to identify suitable monomers. The results suggested that less steric hindered secondary amine produced aminals most cleanly. I therefore set out to investigate the synthesis of multifunctional secondary amine with less sterically hindered *N*-substitution and subsequent polymerization with formaldehyde to form polyaminal networks. Films of polyaminal networks exhibit stress relaxation behavior when pulled under a constant strain. The stress decay rate with temperature exhibited an Arrhenius relationship with activation energy of 51-81 kcal/mol depending on the crosslinking content in the network. Kinetic studies revealed that the aminal exchange occurs by a dissociative pathway that involves the formation of iminium intermediates in the presence of a catalytic protic source. The thermodynamics ($\Delta H°$, $\Delta S°$, K_d) of this dissociation reaction and hydrolysis of aminals to form secondary amine and aldehyde were also determined by variant-temperature NMR experiments. The analysis of these parameters suggests that polyaminal networks can be reprocessed at room temperature under a neutral condition as a viscoelastic solid (above gel point) rather than a viscoelastic liquid, consistent with the experimental observation.

Thermosets comprised of dynamic covalent bonds have several advantages over conventional thermosets. The former can be reprocessed, remended and recycled due to the

presence of reversible covalent bonds. Both polyimine gels and bulk materials in Chapter 2 showed that fractured polymer networks can be healed upon heating or rubbing with solvents at the fractured interface. The polyimine network can also be hydrolytically degraded in water for chemical recycling. In Chapter 3, the polyamine networks, upon thermal healing, exhibited comparable mechanical properties as the pristine samples, highlighting their unique potential as re-mendable thermosetting materials.

References

1. (a) Lovell, L. G.; Berchtold, K. A.; Elliott, J. E.; Lu, H.; Bowman, C. N., Understanding the kinetics and network formation of dimethacrylate dental resins. *Polymers for Advanced Technologies* **2001,** *12* (6), 335-345; (b) Lu, H.; Carioscia, J. A.; Stansbury, J. W.; Bowman, C. N., Investigations of step-growth thiol-ene polymerizations for novel dental restoratives. *Dental Materials* **2005,** *21* (12), 1129-1136.

2. McMahon, T. T.; Zadnik, K., Twenty-five Years of Contact Lenses: The Impact on the Cornea and Ophthalmic Practice. *Cornea* **2000,** *19* (5), 730-740.

3. (a) Harant, A. W.; Khire, V. S.; Thibodaux, M. S.; Bowman, C. N., Thiol−Ene Photopolymer Grafts on Functionalized Glass and Silicon Surfaces. *Macromolecules* **2006,** *39* (4), 1461-1466; (b) Khire, V. S.; Lee, T. Y.; Bowman, C. N., Surface Modification Using Thiol−Acrylate Conjugate Addition Reactions. *Macromolecules* **2007,** *40* (16), 5669-5677.

4. Bowman, C. N.; Kloxin, C. J., Toward an enhanced understanding and implementation of photopolymerization reactions. *AIChE Journal* **2008,** *54* (11), 2775-2795.

5. Xie, T., Recent advances in polymer shape memory. *Polymer* **2011,** *52* (22), 4985-5000.

6. (a) Botterhuis, N. E.; van Beek, D. J. M.; van Gemert, G. M. L.; Bosman, A. W.; Sijbesma, R. P., Self-assembly and morphology of polydimethylsiloxane supramolecular thermoplastic elastomers. *Journal of Polymer Science Part A: Polymer Chemistry* **2008,** *46* (12), 3877-3885; (b) Zhang, K.; Fahs, G. B.; Aiba, M.; Moore, R. B.; Long, T. E., Nucleobase-functionalized ABC triblock copolymers: self-assembly of supramolecular architectures. *Chemical Communications* **2014,** *50* (65), 9145-9148; (c) Koevoets, R. A.; Versteegen, R. M.; Kooijman, H.; Spek, A. L.; Sijbesma, R. P.; Meijer, E. W., Molecular Recognition in a Thermoplastic Elastomer. *Journal of the American Chemical Society* **2005,** *127* (9), 2999-3003.

7. Kolitz, M.; Cohen-Arazi, N.; Hagag, I.; Katzhendler, J.; Domb, A. J., Biodegradable Polyesters Derived from Amino Acids. *Macromolecules* **2009,** *42* (13), 4520-4530.

8. (a) Müller, C. M. O.; Laurindo, J. B.; Yamashita, F., Composites of thermoplastic starch and nanoclays produced by extrusion and thermopressing. *Carbohydrate Polymers* **2012,** *89* (2), 504-510; (b) Huang, M.; Yu, J., Structure and properties of thermoplastic corn starch/montmorillonite biodegradable composites. *Journal of Applied Polymer Science* **2006,** *99* (1), 170-176.

9. Bishop, J. P.; Register, R. A., Thermoplastic Elastomers with Composite Crystalline−Glassy Hard Domains and Single-Phase Melts. *Macromolecules* **2010,** *43* (11), 4954-4960.

10. (a) Lehn, J.-M., From supramolecular chemistry towards constitutional dynamic chemistry and adaptive chemistry. *Chemical Society Reviews* **2007,** *36* (2), 151-160; (b) Rowan, S. J.; Cantrill, S. J.; Cousins, G. R. L.; Sanders, J. K. M.; Stoddart, J. F., Dynamic Covalent Chemistry.

Angewandte Chemie International Edition **2002,** *41* (6), 898-952; (c) Jin, Y.; Yu, C.; Denman, R. J.; Zhang, W., Recent advances in dynamic covalent chemistry. *Chem. Soc. Rev.* **2013,** *42* (16), 6634.

11. Aida, T.; Meijer, E. W.; Stupp, S. I., Functional Supramolecular Polymers. *Science* **2012,** *335* (6070), 813-817.

12. Jin, Y.; Yu, C.; Denman, R. J.; Zhang, W., Recent advances in dynamic covalent chemistry. *Chemical Society Reviews* **2013,** *42* (16), 6634-6654.

13. (a) Kricheldorf, H. R., Macrocycles. 21. Role of Ring−Ring Equilibria in Thermodynamically Controlled Polycondensations. *Macromolecules* **2003,** *36* (7), 2302-2308; (b) Xie, J.; Hsieh, Y.-L., Enzyme-catalyzed transesterification of vinyl esters on cellulose solids. *Journal of Polymer Science Part A: Polymer Chemistry* **2001,** *39* (11), 1931-1939; (c) Berkane, C.; Mezoul, G.; Lalot, T.; Brigodiot, M.; Maréchal, E., Lipase-Catalyzed Polyester Synthesis in Organic Medium. Study of Ring−Chain Equilibrium. *Macromolecules* **1997,** *30* (25), 7729-7734.

14. (a) Chen, X.; Dam, M. A.; Ono, K.; Mal, A.; Shen, H.; Nutt, S. R.; Sheran, K.; Wudl, F., A Thermally Re-mendable Cross-Linked Polymeric Material. *Science* **2002,** *295* (5560), 1698-1702; (b) Shao, C.; Wang, M.; Chang, H.; Xu, F.; Yang, J., A Self-Healing Cellulose Nanocrystal-Poly(ethylene glycol) Nanocomposite Hydrogel via Diels–Alder Click Reaction. *ACS Sustainable Chemistry & Engineering* **2017,** *5* (7), 6167-6174.

15. Banerjee, S.; Tripathy, R.; Cozzens, D.; Nagy, T.; Keki, S.; Zsuga, M.; Faust, R., Photoinduced Smart, Self-Healing Polymer Sealant for Photovoltaics. *ACS Applied Materials & Interfaces* **2015,** *7* (3), 2064-2072.

16. (a) Yoon, J. A.; Kamada, J.; Koynov, K.; Mohin, J.; Nicolaÿ, R.; Zhang, Y.; Balazs, A. C.; Kowalewski, T.; Matyjaszewski, K., Self-Healing Polymer Films Based on Thiol–Disulfide Exchange Reactions and Self-Healing Kinetics Measured Using Atomic Force Microscopy. *Macromolecules* **2012,** *45* (1), 142-149; (b) Lei, Z. Q.; Xiang, H. P.; Yuan, Y. J.; Rong, M. Z.; Zhang, M. Q., Room-Temperature Self-Healable and Remoldable Cross-linked Polymer Based on the Dynamic Exchange of Disulfide Bonds. *Chemistry of Materials* **2014,** *26* (6), 2038-2046.

17. (a) Nakazawa, I.; Suda, S.; Masuda, M.; Asai, M.; Shimizu, T., pH-dependent reversible polymers formed from cyclic sugar- and aromatic boronic acid-based bolaamphiphiles. *Chemical Communications* **2000,** (10), 881-882; (b) Cash, J. J.; Kubo, T.; Bapat, A. P.; Sumerlin, B. S., Room-Temperature Self-Healing Polymers Based on Dynamic-Covalent Boronic Esters. *Macromolecules* **2015,** *48* (7), 2098-2106.

18. Kloxin, C. J.; Scott, T. F.; Adzima, B. J.; Bowman, C. N., Covalent Adaptable Networks (CANs): A Unique Paradigm in Crosslinked Polymers. *Macromolecules* **2010,** *43* (6), 2643-2653.

19. Kloxin, C. J.; Scott, T. F.; Adzima, B. J.; Bowman, C. N., Covalent Adaptable Networks (CANs): A Unique Paradigm in Cross-Linked Polymers. *Macromolecules* **2010,** *43* (6), 2643-2653.

20. (a) Amamoto, Y.; Kamada, J.; Otsuka, H.; Takahara, A.; Matyjaszewski, K., Repeatable Photoinduced Self-Healing of Covalently Cross-Linked Polymers through Reshuffling of Trithiocarbonate Units. *Angewandte Chemie International Edition* **2011,** *50* (7), 1660-1663; (b) Ying, H.; Zhang, Y.; Cheng, J., Dynamic urea bond for the design of reversible and self-healing polymers. *Nat. Commun.* **2014,** *5*, 3218.

21. (a) Cox, L. M.; Li, Z.; Sowan, N.; Nair, D.; Xiao, J.; Bowman, C. N.; Ding, Y., Reconfigurable surface patterns on covalent adaptive network polymers using nanoimprint lithography. *Polymer* **2014,** *55* (23), 5933-5937; (b) Thongsomboon, W.; Sherwood, M.; Arellano, N.; Nelson, A., Thermally Induced Nanoimprinting of Biodegradable Polycarbonates Using Dynamic Covalent Cross-Links. *ACS Macro Letters* **2013,** *2* (1), 19-22.

22. McKinnon, D. D.; Domaille, D. W.; Cha, J. N.; Anseth, K. S., Biophysically Defined and Cytocompatible Covalently Adaptable Networks as Viscoelastic 3D Cell Culture Systems. *Advanced Materials* **2014,** *26* (6), 865-872.

23. Adzima, B. J.; Kloxin, C. J.; Bowman, C. N., Externally Triggered Healing of a Thermoreversible Covalent Network via Self-Limited Hysteresis Heating. *Advanced Materials* **2010,** *22* (25), 2784-2787.

24. Goussé, C.; Gandini, A.; Hodge, P., Application of the Diels−Alder Reaction to Polymers Bearing Furan Moieties. 2. Diels−Alder and Retro-Diels−Alder Reactions Involving Furan Rings in Some Styrene Copolymers. *Macromolecules* **1998,** *31* (2), 314-321.

25. (a) Chen, X.; Wudl, F.; Mal, A. K.; Shen, H.; Nutt, S. R., New Thermally Remendable Highly Cross-Linked Polymeric Materials. *Macromolecules* **2003,** *36* (6), 1802-1807; (b) Imai, Y.; Itoh, H.; Naka, K.; Chujo, Y., Thermally Reversible IPN Organic−Inorganic Polymer Hybrids Utilizing the Diels−Alder Reaction. *Macromolecules* **2000,** *33* (12), 4343-4346.

26. Chujo, Y.; Sada, K.; Saegusa, T., Reversible gelation of polyoxazoline by means of Diels-Alder reaction. *Macromolecules* **1990,** *23* (10), 2636-2641.

27. Polaske, N. W.; McGrath, D. V.; McElhanon, J. R., Thermally Reversible Dendronized Linear AB Step-Polymers via "Click" Chemistry. *Macromolecules* **2011,** *44* (9), 3203-3210.

28. (a) Seoane Rivero, R.; Navarro, R.; Bilbao Solaguren, P.; Gondra Zubieta, K.; Cuevas, J. M.; Marcos-Fernández, A., Synthesis and characterization of photo-crosslinkable linear segmented polyurethanes based on coumarin. *European Polymer Journal* **2017,** *92* (Supplement C), 263-274; (b) Ren, B.; Zhao, D.; Liu, S.; Liu, X.; Tong, Z., Synthesis and Characterization of Poly(ferrocenylsilanes) with Coumarin Side Groups and Their Photochemical Reactivity and Electrochemical Behavior. *Macromolecules* **2007,** *40* (13), 4501-4508; (c) Trenor, S. R.; Shultz, A. R.; Love, B. J.; Long, T. E., Coumarins in Polymers: From Light Harvesting to Photo-Cross-Linkable Tissue Scaffolds. *Chemical Reviews* **2004,** *104* (6), 3059-3078.

29. (a) Lendlein, A.; Jiang, H.; Junger, O.; Langer, R., Light-induced shape-memory polymers. *Nature* **2005,** *434* (7035), 879-882; (b) Gattás-Asfura, K. M.; Weisman, E.; Andreopoulos, F. M.;

Micic, M.; Muller, B.; Sirpal, S.; Pham, S. M.; Leblanc, R. M., Nitrocinnamate-Functionalized Gelatin: Synthesis and "Smart" Hydrogel Formation via Photo-Cross-Linking. *Biomacromolecules* **2005,** *6* (3), 1503-1509; (c) Zheng, Y.; Micic, M.; Mello, S. V.; Mabrouki, M.; Andreopoulos, F. M.; Konka, V.; Pham, S. M.; Leblanc, R. M., PEG-Based Hydrogel Synthesis via the Photodimerization of Anthracene Groups. *Macromolecules* **2002,** *35* (13), 5228-5234.

30. (a) Connal, L. A.; Vestberg, R.; Hawker, C. J.; Qiao, G. G., Fabrication of Reversibly Crosslinkable, 3-Dimensionally Conformal Polymeric Microstructures. *Advanced Functional Materials* **2008,** *18* (20), 3315-3322; (b) Jun, M.; Yoshifumi, O.; Katsuyuki, T., Photodimerization of Anthryl Moieties in a Poly(methacrylic acid) Derivative as Reversible Cross-linking Step in Molecular Imprinting. *Chemistry Letters* **2006,** *35* (1), 80-81.

31. Imai, Y.; Ogoshi, T.; Naka, K.; Chujo, Y., Formation of IPN organic-inorganic polymer hybrids utilizing the photodimerization of thymine. *Polymer Bulletin* **2000,** *45* (1), 9-16.

32. Higaki, Y.; Otsuka, H.; Takahara, A., Dynamic Formation of Graft Polymers via Radical Crossover Reaction of Alkoxyamines. *Macromolecules* **2004,** *37* (5), 1696-1701.

33. Higaki, Y.; Otsuka, H.; Takahara, A., A Thermodynamic Polymer Cross-Linking System Based on Radically Exchangeable Covalent Bonds. *Macromolecules* **2006,** *39* (6), 2121-2125.

34. (a) Scott, T. F.; Schneider, A. D.; Cook, W. D.; Bowman, C. N., Photoinduced Plasticity in Cross-Linked Polymers. *Science* **2005,** *308* (5728), 1615-1617; (b) Kloxin, C. J.; Scott, T. F.; Park, H. Y.; Bowman, C. N., Mechanophotopatterning on a Photoresponsive Elastomer. *Advanced Materials* **2011,** *23* (17), 1977-1981.

35. Amamoto, Y.; Otsuka, H.; Takahara, A.; Matyjaszewski, K., Self-Healing of Covalently Cross-Linked Polymers by Reshuffling Thiuram Disulfide Moieties in Air under Visible Light. *Advanced Materials* **2012,** *24* (29), 3975-3980.

36. Montarnal, D.; Capelot, M.; Tournilhac, F.; Leibler, L., Silica-Like Malleable Materials from Permanent Organic Networks. *Science* **2011,** *334* (6058), 965-968.

37. Angell, C. A., Formation of Glasses from Liquids and Biopolymers. *Science* **1995,** *267* (5206), 1924-1935.

38. Williams, M. L.; Landel, R. F.; Ferry, J. D., The Temperature Dependence of Relaxation Mechanisms in Amorphous Polymers and Other Glass-forming Liquids. *Journal of the American Chemical Society* **1955,** *77* (14), 3701-3707.

39. Dyre, J. C., Colloquium. *Reviews of Modern Physics* **2006,** *78* (3), 953-972.

40. Denissen, W.; Winne, J. M.; Du Prez, F. E., Vitrimers: permanent organic networks with glass-like fluidity. *Chemical Science* **2016,** *7* (1), 30-38.

41. Rabenstein, D. L.; Weaver, K. H., Kinetics and Equilibria of the Thiol/Disulfide Exchange Reactions of Somatostatin with Glutathione. *The Journal of Organic Chemistry* **1996,** *61* (21), 7391-7397.

42. (a) Tsarevsky, N. V.; Matyjaszewski, K., Reversible Redox Cleavage/Coupling of Polystyrene with Disulfide or Thiol Groups Prepared by Atom Transfer Radical Polymerization. *Macromolecules* **2002,** *35* (24), 9009-9014; (b) Tesoro, G. C.; Sastri, V., Reversible crosslinking in epoxy resins. I. Feasibility studies. *Journal of Applied Polymer Science* **1990,** *39* (7), 1425-1437.

43. Michal, B. T.; Jaye, C. A.; Spencer, E. J.; Rowan, S. J., Inherently Photohealable and Thermal Shape-Memory Polydisulfide Networks. *ACS Macro Letters* **2013,** *2* (8), 694-699.

44. (a) Canadell, J.; Goossens, H.; Klumperman, B., Self-Healing Materials Based on Disulfide Links. *Macromolecules* **2011,** *44* (8), 2536-2541; (b) Pepels, M.; Filot, I.; Klumperman, B.; Goossens, H., Self-healing systems based on disulfide-thiol exchange reactions. *Polymer Chemistry* **2013,** *4* (18), 4955-4965.

45. (a) Pack, J. W.; Kim, S. H.; Park, S. Y.; Lee, Y.-W.; Kim, Y. H., Kinetic and Mechanistic Studies of l-Lactide Polymerization in Supercritical Chlorodifluoromethane. *Macromolecules* **2003,** *36* (24), 8923-8930; (b) Robert, J. L.; Aubrecht, K. B., Ring-Opening Polymerization of Lactide To Form a Biodegradable Polymer. *Journal of Chemical Education* **2008,** *85* (2), 258.

46. Zeng, J.; Wang, X.; Zhao, B.; Sun, J.; Wang, Y., Rapid In Situ Transesterification of Sunflower Oil. *Industrial & Engineering Chemistry Research* **2009,** *48* (2), 850-856.

47. Capelot, M.; Montarnal, D.; Tournilhac, F.; Leibler, L., Metal-Catalyzed Transesterification for Healing and Assembling of Thermosets. *Journal of the American Chemical Society* **2012,** *134* (18), 7664-7667.

48. Adzima, B. J.; Aguirre, H. A.; Kloxin, C. J.; Scott, T. F.; Bowman, C. N., Rheological and chemical analysis of reverse gelation in a covalently crosslinked Diels-Alder polymer network. *Macromolecules* **2008,** *41* (23), 9112-9117.

49. Liu, W.-X.; Zhang, C.; Zhang, H.; Zhao, N.; Yu, Z.-X.; Xu, J., Oxime-Based and Catalyst-Free Dynamic Covalent Polyurethanes. *Journal of the American Chemical Society* **2017,** *139* (25), 8678-8684.

50. Schiff, H., Mittheilungen aus dem Universitätslaboratorium in Pisa: Eine neue Reihe organischer Basen. *Justus Liebigs Annalen der Chemie* **1864,** *131* (1), 118-119.

51. Ciaccia, M.; Cacciapaglia, R.; Mencarelli, P.; Mandolini, L.; Di Stefano, S., Fast transimination in organic solvents in the absence of proton and metal catalysts. A key to imine metathesis catalyzed by primary amines under mild conditions. *Chemical Science* **2013,** *4* (5), 2253-2261.

52. (a) Deng, G.; Li, F.; Yu, H.; Liu, F.; Liu, C.; Sun, W.; Jiang, H.; Chen, Y., Dynamic Hydrogels with an Environmental Adaptive Self-Healing Ability and Dual Responsive Sol–Gel Transitions. *ACS Macro Letters* **2012,** *1* (2), 275-279; (b) Deng, G.; Tang, C.; Li, F.; Jiang, H.; Chen, Y., Covalent Cross-Linked Polymer Gels with Reversible Sol−Gel Transition and Self-Healing Properties. *Macromolecules* **2010,** *43* (3), 1191-1194; (c) Yang, B.; Zhang, Y.; Zhang, X.; Tao, L.; Li, S.; Wei, Y., Facilely prepared inexpensive and biocompatible self-healing hydrogel: a new injectable cell therapy carrier. *Polymer Chemistry* **2012,** *3* (12), 3235-3238.

53. Belowich, M. E.; Stoddart, J. F., Dynamic imine chemistry. *Chemical Society Reviews* **2012,** *41* (6), 2003-2024.

54. Kovaříček, P.; Lehn, J.-M., Merging Constitutional and Motional Covalent Dynamics in Reversible Imine Formation and Exchange Processes. *Journal of the American Chemical Society* **2012,** *134* (22), 9446-9455.

55. Jin, Y.; Wang, Q.; Taynton, P.; Zhang, W., Dynamic Covalent Chemistry Approaches Toward Macrocycles, Molecular Cages, and Polymers. *Accounts of Chemical Research* **2014,** *47* (5), 1575-1586.

56. Taynton, P.; Yu, K.; Shoemaker, R. K.; Jin, Y.; Qi, H. J.; Zhang, W., Heat- or Water-Driven Malleability in a Highly Recyclable Covalent Network Polymer. *Advanced Materials* **2014,** *26* (23), 3938-3942.

57. Whiteley, J. M.; Taynton, P.; Zhang, W.; Lee, S.-H., Ultra-thin Solid-State Li-Ion Electrolyte Membrane Facilitated by a Self-Healing Polymer Matrix. *Advanced Materials* **2015,** *27* (43), 6922-6927.

58. Taynton, P.; Ni, H.; Zhu, C.; Yu, K.; Loob, S.; Jin, Y.; Qi, H. J.; Zhang, W., Repairable Woven Carbon Fiber Composites with Full Recyclability Enabled by Malleable Polyimine Networks. *Advanced Materials* **2016,** *28* (15), 2904-2909.

59. Ciaccia, M.; Di Stefano, S., Mechanisms of imine exchange reactions in organic solvents. *Organic & Biomolecular Chemistry* **2015,** *13* (3), 646-654.

60. Paul C. Hiemenz, T. P. L., *Polymer Chemistry, Second Edition*. 2007.

61. Shimada, K.; Kato, H.; Saito, T.; Matsuyama, S.; Kinugasa, S., Precise measurement of the self-diffusion coefficient for poly(ethylene glycol) in aqueous solution using uniform oligomers. *The Journal of Chemical Physics* **2005,** *122* (24), 244914.

62. Cantrell, G. K.; Meyer, T. Y., Transition-Metal-Catalyzed Imine Metathesis. *Organometallics* **1997,** *16* (25), 5381-5383.

63. Hayes, J. F.; Hayler, J. D.; Walsgrove, T. C.; Wicks, C., Synthesis of new azepino[3,4,5-cd]indole derivatives. *Journal of Heterocyclic Chemistry* **1996,** *33* (1), 209-212.

64. Garber, L.; Chen, C.; Kilchrist, K. V.; Bounds, C.; Pojman, J. A.; Hayes, D., Thiol-acrylate nanocomposite foams for critical size bone defect repair: A novel biomaterial. *Journal of Biomedical Materials Research Part A* **2013,** *101* (12), 3531-3541.

65. Pandey, P.; Katsoulidis, A. P.; Eryazici, I.; Wu, Y.; Kanatzidis, M. G.; Nguyen, S. T., Imine-Linked Microporous Polymer Organic Frameworks. *Chemistry of Materials* **2010,** *22* (17), 4974-4979.

66. (a) García, J. M.; Jones, G. O.; Virwani, K.; McCloskey, B. D.; Boday, D. J.; ter Huurne, G. M.; Horn, H. W.; Coady, D. J.; Bintaleb, A. M.; Alabdulrahman, A. M. S.; Alsewailem, F.; Almegren, H. A. A.; Hedrick, J. L., Recyclable, Strong Thermosets and Organogels via Paraformaldehyde Condensation with Diamines. *Science* **2014,** *344* (6185), 732-735; (b) Fox, C. H.; ter Hurrne, G. M.; Wojtecki, R. J.; Jones, G. O.; Horn, H. W.; Meijer, E. W.; Frank, C. W.; Hedrick, J. L.; García, J. M., Supramolecular motifs in dynamic covalent PEG-hemiaminal organogels. **2015,** *6*, 7417.

67. (a) H. Billman, J.; Yu Chen Ho, J.; R. Caswell, L., *The Formation of Solid Derivatives of Aldehydes. I. 2-Substituted-1,3Bis(p-Methoxybenzyl)-Tetrahydroimidazoles*. 1952; Vol. 17, p 1375-1378; (b) Jurčík, V.; Wilhelm, R., Preparation of aminals in water. *Tetrahedron* **2004,** *60* (14), 3205-3210; (c) Hine, J.; Narducy, K. W., Imines, imidazolidines, and imidazolidinium ions from the reactions of ethylenediamine derivatives with isobutyraldehyde and acetone. *Journal of the American Chemical Society* **1973,** *95* (10), 3362-3368; (d) Buchs, B.; Godin, G.; Trachsel, A.; de Saint Laumer, J.-Y.; Lehn, J.-M.; Herrmann, A., Reversible Aminal Formation: Controlling the Evaporation of Bioactive Volatiles by Dynamic Combinatorial/Covalent Chemistry. *European Journal of Organic Chemistry* **2011,** *2011* (4), 681-695.

68. Katritzky, A. R.; Yannakopoulou, K.; Lang, H., Aminal exchange. *Journal of the Chemical Society, Perkin Transactions 2* **1994,** (8), 1867-1870.

69. Comby, S.; Imbert, D.; Vandevyver, C.; Bünzli, J.-C. G., A Novel Strategy for the Design of 8-Hydroxyquinolinate-Based Lanthanide Bioprobes That Emit in the Near Infrared Range. *Chemistry – A European Journal* **2007,** *13* (3), 936-944.

70. Kloxin, C. J.; Bowman, C. N., Covalent adaptable networks: smart, reconfigurable and responsive network systems. *Chemical Society Reviews* **2013,** *42* (17), 7161-7173.

71. (a) Zhang, Y.; Ying, H.; Hart, K. R.; Wu, Y.; Hsu, A. J.; Coppola, A. M.; Kim, T. A.; Yang, K.; Sottos, N. R.; White, S. R.; Cheng, J., Malleable and Recyclable Poly(urea-urethane) Thermosets bearing Hindered Urea Bonds. *Advanced Materials* **2016,** *28* (35), 7646-7651; (b) Fortman, D. J.; Brutman, J. P.; Cramer, C. J.; Hillmyer, M. A.; Dichtel, W. R., Mechanically Activated, Catalyst-Free Polyhydroxyurethane Vitrimers. *Journal of the American Chemical Society* **2015,** *137* (44), 14019-14022; (c) Yu, K.; Taynton, P.; Zhang, W.; Dunn, M. L.; Qi, H. J., Influence of stoichiometry on the glass transition and bond exchange reactions in epoxy thermoset polymers. *RSC Advances* **2014,** *4* (89), 48682-48690; (d) Denissen, W.; Droesbeke, M.; Nicolaÿ, R.; Leibler, L.; Winne, J. M.; Du Prez, F. E., Chemical control of the viscoelastic properties of vinylogous urethane vitrimers. **2017,** *8*, 14857.

72. Heaney, H.; Papageorgiou, G.; Wilkins, R. F., The generation of iminium ions using chlorosilanes and their reactions with electron rich aromatic heterocycles. *Tetrahedron* **1997,** *53* (8), 2941-2958.

73. Brutman, J. P.; Delgado, P. A.; Hillmyer, M. A., Polylactide Vitrimers. *ACS Macro Letters* **2014,** *3* (7), 607-610.

Appendix. Copyright Permissions

Covalent adaptable networks: smart, reconfigurable and responsive network systems

C. J. Kloxin and C. N. Bowman, Chem. Soc. Rev., 2013, **42**, 7161

DOI: 10.1039/C3CS60046G

Title:	Readily Prepared Dynamic Hydrogels by Combining Phenyl Boronic Acid- and Maltose-Modified Anionic Polysaccharides at Neutral pH
Author:	Dominte Tarus,Emilie Hachet,Léa Messager,Bogdan Catargi,Valérie Ravaine,Rachel Auzély-Velty
Publication:	Macromolecular Rapid Communications
Publisher:	John Wiley and Sons
Date:	Nov 10, 2014

Quick Price Estimate

Please review the credit line for the requested figure/table.
If the figure/table you wish to reproduce is credited to a source other than the author of the publication (i.e third party material) you will need to obtain permission from that copyright holder, book or journal before making any use of the material. For the avoidance of doubt – any and all third party content is expressly excluded from this permission.
Otherwise please proceed with your order.

John Wiley and Sons grants a license for all orders, including $0 orders. Please select the Continue button and place an order for this reuse.

This license allows only minor adaptations as required by the new publication format (with no additions, deletions or modifications to the text that materially alter the meaning of what the author has written). If you wish to make more significant changes to the work please select “I don’t see my intended use” and provide full details of your proposed adaptation for review by John Wiley and Sons.

Title:	Design of multi-phase dynamic chemical networks
Author:	Chenrui Chen, Junjun Tan, Ming-Chien Hsieh, Ting Pan, Jay T. Goodwin, Anil K. Mehta
Publication:	Nature Chemistry
Publisher:	Nature Publishing Group
Date:	Feb 27, 2017

Quick Price Estimate

This reuse request is free of charge although you are required to obtain a license through Rightslink and comply with the license terms and conditions. You will not be charged for this order. Please select the Continue button and place an order for this reuse.

Adaptations/modifications - Springer Nature allows adaptation of figures for style and formatting purposes under this license under the condition that this does not alter the meaning of the content".

Selection of academic/educational signifies you will reuse content in a not-for-profit setting. Reuse not permitted in for-profit settings including, but not limited to: textbook publishing, medical communication companies, or pharmaceutical organizations.

Vitrimers: permanent organic networks with glass-like fluidity

W. Denissen, J. M. Winne and F. E. Du Prez, Chem. Sci., 2016, **7**, 30

DOI: 10.1039/C5SC02223A

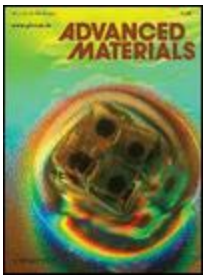

Title:	Self-Healing of Covalently Cross-Linked Polymers by Reshuffling Thiuram Disulfide Moieties in Air under Visible Light
Author:	Yoshifumi Amamoto,Hideyuki Otsuka,Atsushi Takahara,Krzysztof Matyjaszewski
Publication:	Advanced Materials
Publisher:	John Wiley and Sons
Date:	Jun 22, 2012

Quick Price Estimate

Please review the credit line for the requested figure/table.
If the figure/table you wish to reproduce is credited to a source other than the author of the publication (i.e third party material) you will need to obtain permission from that copyright holder, book or journal before making any use of the material. For the avoidance of doubt – any and all third party content is expressly excluded from this permission.
Otherwise please proceed with your order.

John Wiley and Sons grants a license for all orders, including $0 orders. Please select the Continue button and place an order for this reuse.

This license allows only minor adaptations as required by the new publication format (with no additions, deletions or modifications to the text that materially alter the meaning of what the author has written). If you wish to make more significant changes to the work please select “I don’t see my intended use” and provide full details of your proposed adaptation for review by John Wiley and Sons.

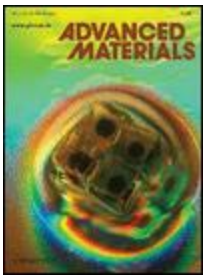

Title:	Heat- or Water-Driven Malleability in a Highly Recyclable Covalent Network Polymer
Author:	Philip Taynton,Kai Yu,Richard K. Shoemaker,Yinghua Jin,H. Jerry Qi,Wei Zhang
Publication:	Advanced Materials
Publisher:	John Wiley and Sons
Date:	Mar 27, 2014

Quick Price Estimate

Please review the credit line for the requested figure/table.
If the figure/table you wish to reproduce is credited to a source other than the author of the publication (i.e third party material) you will need to obtain permission from that copyright holder, book or journal before making any use of the material. For the avoidance of doubt – any and all third party content is expressly excluded from this permission.
Otherwise please proceed with your order.

John Wiley and Sons grants a license for all orders, including $0 orders. Please select the Continue button and place an order for this reuse.

This license allows only minor adaptations as required by the new publication format (with no additions, deletions or modifications to the text that materially alter the meaning of what the author has written). If you wish to make more significant changes to the work please select “I don’t see my intended use” and provide full details of your proposed adaptation for review by John Wiley and Sons.

Title: Dynamic Covalent Polymer Networks

	Based on Degenerative Imine Bond Exchange: Tuning the Malleability and Self-Healing Properties by Solvent	**If you're a copyright.com user,** you can login to RightsLink using your copyright.com credentials.
Author:	Albert Chao, Ioan Negulescu, Donghui Zhang	Already **a RightsLink user** or want to learn more?
Publication:	Macromolecules	
Publisher:	American Chemical Society	
Date:	Sep 1, 2016	
Copyright © 2016, American Chemical Society		

PERMISSION/LICENSE IS GRANTED FOR YOUR ORDER AT NO CHARGE

This type of permission/license, instead of the standard Terms & Conditions, is sent to you because no fee is being charged for your order. Please note the following:

- Permission is granted for your request in both print and electronic formats, and translations.
- If figures and/or tables were requested, they may be adapted or used in part.
- Please print this page for your records and send a copy of it to your publisher/graduate school.
- Appropriate credit for the requested material should be given as follows: "Reprinted (adapted) with permission from (COMPLETE REFERENCE CITATION). Copyright (YEAR) American Chemical Society." Insert appropriate information in place of the capitalized words.
- One-time permission is granted only for the use specified in your request. No additional uses are granted (such as derivative works or other editions). For any other uses, please submit a new request.

Vita

Albert Chao was born in Taipei, Taiwan. He attended University of Cincinnati, Ohio, USA, and received a B.S. degree in Chemistry in 2007. He then joined the graduate program in the Department of Chemistry at Louisiana State University in Louisiana in August, 2012. He conducted graduate research under the supervision of Professor Donghui Zhang.